Energy Efficiency Optimization in Millimeter Wave Backhaul Heterogeneous Networks

by

©Sylvester Boadi Aboagye

A Dissertation submitted to the School of Graduate Studies in partial fulfillment of the requirements for the degree of

Master of Electrical Engineering

Faculty of Engineering and Applied Science

Memorial University of Newfoundland

October 2018

St. John's Newfoundland

Abstract

Within the last few years, there has been a massive growth in the number of wireless devices and internet connections. This is expected to continue during the next few years. To satisfy the resulting high data traffic demands, dramatic expansion of network infrastructures as well as fast escalation of energy demands are expected. Meanwhile, there has been a growing concern about the energy consumption of wireless communication systems and their global carbon footprint. To that end, future wireless systems must satisfy three main requirements. Firstly, they must provide users with very high throughput. Secondly, they must be able to provide seamless connectivity as well as ubiquitous access to the expected enormous number of users. Finally, they must achieve the first two points with less energy consumption. The requirements can be summarized into the joint optimization of energy efficiency (EE), user association and backhaul (BH) flow assignment, which remains a fundamental objective in the design of next generation networks.

This thesis consists of two studies on EE maximization in heterogeneous networks (HetNets). In the first study, it is assumed that each user has already been associated to a single base station (BS). Under this setting, We consider enforcing a strict throughput demand on all user equipment (UEs), called joint EE, power, and flow control (JEEPF), versus allowing an acceptable range of demands for each, called joint EE, power, flow control, and throughput (JEEPFT). This minor change causes a dras-

tic difference in the formulation of both problems. JEEPF is convex while JEEPFT is quasiconvex, for which we propose a bisection method-based approach. In the second study, the problem of user association is added to the joint optimization of EE, power and BH flow control, and an energy efficient user association, power and flow control (EEUAPF) algorithm is proposed. The original EEUAPF optimization problem is a non-convex mixed integer programming problem, and therefore NP-hard. We show how this non-convex problem can be tailored into a form that can be approached using a classical mathematical programming technique called column generation and convex programming to derive the optimal solution with a low complexity.

Simulation results are used to demonstrate the EE gains of the proposed approaches in both studies.

"The only easy day was yesterday"

Acknowledgements

My gratitude goes to the Almighty God for the grace and wisdom that has seen me through my Master's program.

No amount of words can express how grateful I am to my supervisor, Dr. Telex M. N. Ngatched for the opportunity he gave me and for his unrelenting support, motivation, dedication and guidance throughout my Master's program at Memorial University of Newfoundland. I still keep to heart your words; *"...anything worth doing takes time."* Without our weekly meetings, together with Dr. Ahmed Ibrahim, this research would not have been successful. I am thankful for the time you devoted to me during my research program. Your valuable supervision not only made this research a success, but also made this journey a pleasant and unforgettable one.

I am highly indebted to Dr. Ahmed Ibrahim for being so kind and supportive throughout this journey. You were always willing to share your vast knowledge and experience with me. Your incessant support and advice were among the key determinants for the completion of this research. Thank you for the encouragement and emotional support as well.

This research was funded by the Natural Sciences and Engineering Research Council (NSERC), through their Discovery program. I am profoundly grateful to them for their assistance.

I would like to express my sincere appreciation to all my colleagues, friends, as

well as the academic staff in the Electrical and Computer Engineering Department. You all made my stay in St. John's enjoyable.

As the popular saying goes, *"save the best for the last"*, my deepest gratitude goes to my parents for their endless love and support, and to my siblings for making me smile through it all.

Table of Contents

List of Tables

List of Figures

List of Abbreviations

FCC	federal communications commission
WLAN	wireless local area network
IoT	internet of things
D2D	device to device
FinTech	financial technology
AWGN	additive white Gaussian noise
LTE-A	long-term evolution advance
SE	spectrum efficiency
EE	energy efficiency
$\overline{EE}$	inverse energy efficiency
OPEX	operational expenditure
5G	fifth generation
mmWave	millimeter wave
BS	base station
BH	backhaul
CN	core network
AN	access network
QoS	quality of service

3G	third generation
4G	fourth generation
3GPP LTE	third generation partnership project long-term evolution
CAPEX	capital expenditure
LPN	low power node
HetNets	heterogeneous networks
eNB	enhanced node B
PBS	pico base station
FBS	femto base stations
RSRP	reference signal received power
DL	downlink
SNR	signal-to-noise ratio
RE	range expansion
LoS	line of sight
NLoS	non line-of-sight
UL	uplink
CSG	closed subscriber group
FUE	femto UE
MUE	MBS UE
PUE	pico UE
CO_2	carbon dioxide
2G	second generation
UE	user equipment
NP	non polynomial
MBS	macro base station

CMOS	complementary metal-oxide semiconductor
RF	radio frequency
$FSPL$	free space path loss
PL	propagation loss
dB	decibels
TPL	total pathloss
SINR	signal-to-interference-and-noise ratio
CRE	cell range expansion
MIMO	multiple-input multiple-output
JEEPF	joint energy efficiency power and flow control
JEEPFT	joint EE, power allocation, flow control and throughput
OFDMA	orthogonal frequency-division multiple access
MTP	maximum transmit power
$EIRP$	equivalent isotropically radiated power
EPA	equal power allocation
RA	random allocation
LP	linear programming
MILP	mixed-integer linear programming
IP	integer programming
RE	range expansion
MPL	minimum pathloss
EEUAPF	energy efficient user association, power and flow control

Co-authorship Statement

I, Sylvester Boadi Aboagye, have the principal authorship status for all the manuscripts included in this thesis. However, all the manuscripts resulting from this work are co-authored by my supervisors Dr. Telex M. N. Ngatched and Dr. Ahmed Ibrahim. The list of manuscripts resulting from this thesis are cited below:

1. **Sylvester B. Aboagye**, Ahmed Ibrahim and Telex M. N. Ngatched, "Energy efficient power and flow control in millimeter wave backhaul heterogeneous networks," accepted *IEEE Global Telecommunications Conference (GLOBECOM 2018)*"

2. **Sylvester B. Aboagye**, Ahmed Ibrahim and Telex M. N. Ngatched, "Joint user association, power and flow control in millimeter wave backhaul heterogeneous networks: A column generation approach.," under review for publication in *IEEE Trans. Veh. Technol.*"

Chapter 1

Introduction

1.1 Motivation

The number of mobile devices and data connections grew from 7.6 billion in 2015 to 8.0 billion in 2016 [1]. This shows that close to half a billion new mobile devices and connections were added in 2016 as compared to the world average population growth rate of 83 million people per year. Thus, the growth rate of new mobile devices is approximately 6 times that of the world population growth. It is estimated that there will be 11.6 billion mobile-connected devices by the year 2021. This rapid growth in the number of mobile devices and data connections has been mainly driven by the existence of data hungry applications and the continuous increase of captivating wireless mobile applications. Particularly, technologies like augmented reality, Internet of Things (IoT), Device to Device (D2D) communications, e-health care and Financial Technology (FinTech) are a few of these emerging applications. Undeniably, this increase in the number of devices and the requirement for seamless connectivity as well as ubiquitous access can lead to the expansion of network infrastructures and increase in energy consumption. The escalation of energy consumption in cellular networks

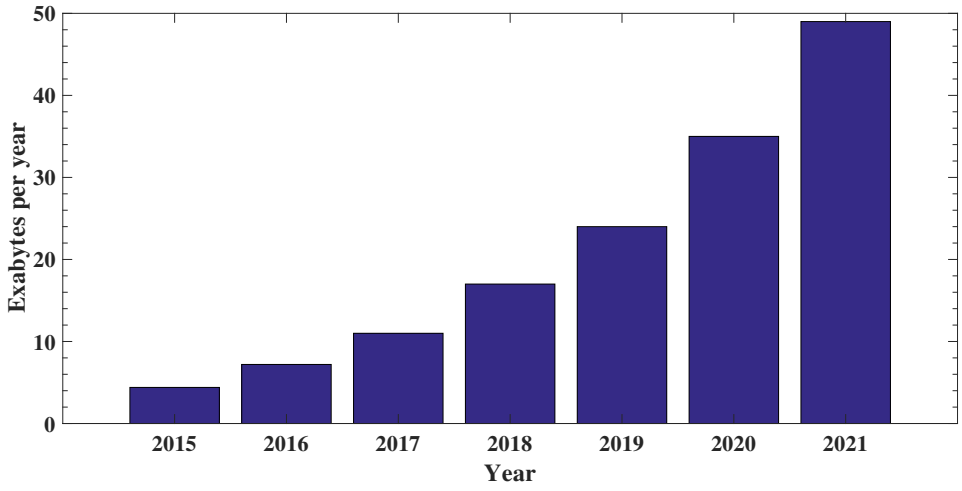

Figure 1.1: Global mobile data traffic forecast, 2015 to 2021.

is accompanied by an increase in the global carbon footprint which is deemed as a threat to global security and humanity [2].

Coupled with the rise in number of mobile devices, data traffic in cellular networks continues to grow dramatically and this trend is expected to continue in the foreseeable future. The global mobile data traffic forecast up to the year 2021 is as shown in Figure 1.1. From Shannon's capacity formula for an additive white Gaussian noise (AWGN) channel, the capacity of a channel is dependent on resources like the channel bandwidth, W, and the signal power, S (i.e. all other parameters being equal).

$$C = W \log_2 \left(1 + \frac{S}{I+N}\right). \tag{1.1}$$

In (1.1), I and N represent interference and noise power, respectively. However, it is important to note that the increase in capacity as a function of power is logarithmic and slow. Constrained by the cost of electricity and environmental regulations, increasing network capacity by scaling up the transmit power is not suitable and seems unrealistic in future networks. Again, the capacity of a channel can be increased by utilizing additional bandwidth. Currently, almost all wireless communication devices

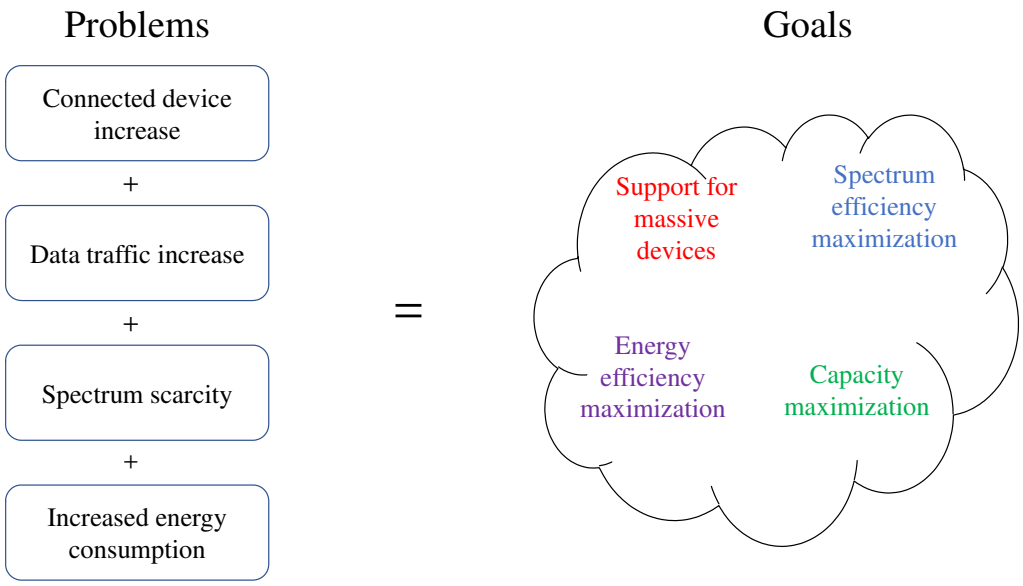

Figure 1.2: Goals of future wireless networks.

make use of the spectrum in the 300 MHz to 3 GHz, referred to as "sweet spot" because of its favorable propagation characteristics for wireless applications. This has resulted in the sub 3 GHz spectrum becoming nearly fully occupied.

Since the conception of wireless communications, several technologies have evolved over the years with the most recent being the Long-Term Evolution Advance (LTE-A). Unfortunately, the deployment of LTE-A is reaching maturity where little improvements in terms of capacity, spectrum efficiency (SE) and energy efficiency (EE) can be achieved. Hence, it will be highly impossible to satisfy future data demand either by increasing signal power or additional spectrum with the present cellular communication network technologies. In order to meet such an exponential increase in data demand and user, in a sustainable way, while simultaneously limiting the operational expenditure (OPEX), researchers in academia and the industry should focus on energy efficient future cellular networks.

The combined effect of the challenges discussed above has already triggered the

next major evolution in wireless communications – the fifth generation mobile network (5G). 5G has been envisioned to provide magnitudes of increase in data rates and bandwidth, ubiquitous coverage and connectivity, together with offering an enormous reduction in energy consumption [3] [4]. Specifically, 5G technology aims at achieving the goals of future wireless networks as shown in Figure 1.2.

Recent works on 5G mention heterogeneous networks (HetNets) and millimeter wave (mmWave) communications among its key enabling technologies [3] [5]. HetNets involve the deployment of base stations (BSs) with considerably different transmit power, coverage area, carrier frequencies and backhaul (BH) connection types [6]. While this heterogeneity in network architecture offers strong potential for coping with the explosive growth in data traffic [7], it also introduces the new challenges of (i) reducing overall network energy consumption, (ii) connecting all the BSs to a core network (CN) through high-capacity BH links since not all of the BSs will not have a direct connection to the CN, and (iii) associating users to BSs [8] [9] [10]. With the 3 GHz band fully occupied, it has become necessary to move toward and into the mmWave spectrum so as to make use of most of its relatively idle spectrum as shown in Figure 1.3. In addition, mmWave frequencies have high bandwidth enabling them to provide the BH link capacity on the order of Gbps which is adequately suitable to handle the BH traffic in 5G [11]. With the rapid pace of research development in the field of semiconductors, the dominant perception that mmWave spectrum is unsuitable for cellular communications due to the strong pathloss and attenuation effects (by water vapor, oxygen and rain) are now considered progressively more surmountable [12] [13]. The integration of these technologies to enable the realization of the goals of 5G cellular networks still faces many technical challenges, and as such calls for further investigations.

Motivated by the need to improve on the EE of cellular networks, this dissertation

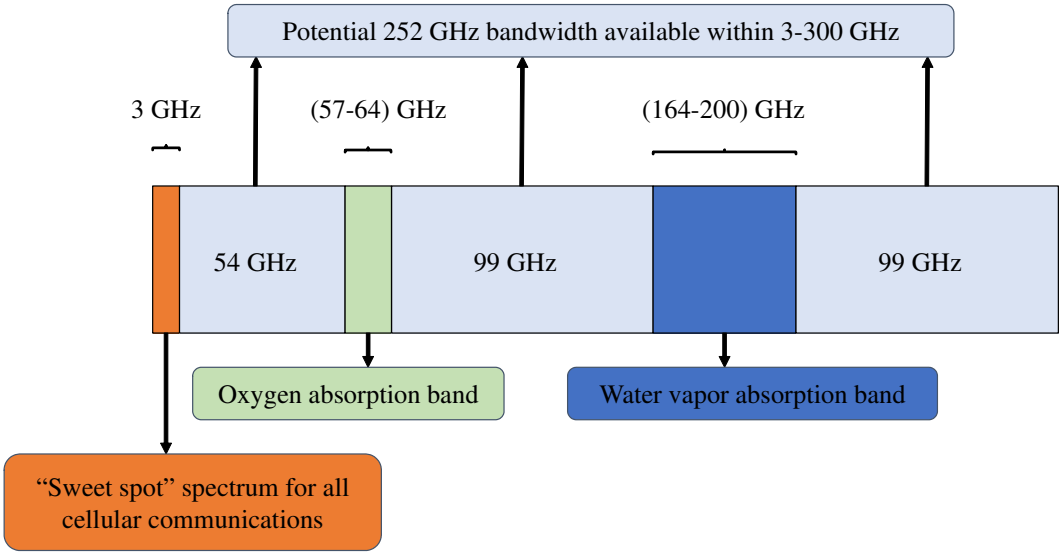

Figure 1.3: mmWave spectrum availability.

provides a contribution to the field of EE maximization in mmWave BH HetNets. Using a cross-layer optimization approach, this dissertation investigates how the optimization of user association, throughput demand and power control (all in the physical layer), and flow control (in the network layer) provides the ability to obtain global optimum user association, flow and power allocation under the common objective of maximizing EE. Cross-layer optimization, which in wireless networks refers to the joint optimization of multiple wireless network layers, has been deemed as an effective approach in wireless networks design. This design method has been shown to yield better results than considering each layer separately [14].

Specifically, this dissertation focuses on improving the AN and BH network throughput and SE, optimizing flow allocation on the numerous BH links resulting from the dense deployment of BSs, as well as reducing the energy consumption of future cellular networks. The improvement in the AN throughput is achieved by proposing a novel variable-rate joint throughput, power and BH flow optimization algorithm. The

BH link throughput improvement is achieved by implementing a mix of backhauling candidate solutions. The reduction in energy consumption is achieved in two folds: (i) by associating UEs to BSs that minimizes their AN and BH power consumption, and (ii) by optimizing power allocation to UEs already associated to BSs and the BH link power consumption. The QoS requirement of UEs are guaranteed in both cases.

Novel algorithms that jointly perform the tasks mentioned above are proposed. This will fill the void in literature on energy efficient algorithm design that jointly maximizes AN throughput, assigns flow on BH links and minimizes power consumption as well as well as providing a user association approach that maximizes EE while optimizing power and BH flow assignment without compromising UE QoS requirement.

Furthermore, the use of different mmWave frequency bands in the BH network design promises high capacity BH networks thereby eliminating the possibility of BH links becoming a bottleneck to the flow of BH traffic.

1.1.1 Thesis Objectives

The objectives of this dissertation are stated below:

- The use of two mmWave frequency bands in multiple BH link connections and a multi-hop BH network is investigated to know if the BH network can constitute to capacity or energy bottleneck in future HetNets.
- A fixed UE demand rate joint power allocation and BH flow assignment for EE maximization approach is developed in this dissertation.
- A bisection based method algorithm is proposed for the joint optimization of EE, power allocation, BH flow assignment and throughput demand maximization. It is also shown how the original non-linear and non-convex optimization problem

can be reformulated as a quasiconvex optimization problem and solved for the global optimum.

- A column generation based energy efficient user association, power allocation and BH flow control approach is proposed. It is shown how the original optimization problem, that aims at associating UEs to BSs that minimize power consumption in the AN and BH network while jointly performing BH flow assignment, which is a non-convex problem can be tailored into a form suitable for the application of column generation to derive the optimum solution.

- Simulation results are carried out for the proposed algorithms and novel approaches to validate their effectiveness.

1.1.2 Research Contributions

Motivated by the need to improve the EE and resource utilization in HetNets, the following research contributions are made:

1. The role of mmWave frequency bands in a multi-hop, multiple BH link connections in a heterogeneous network is studied. This is done to determine if mmWave BH links would or would not constitute energy or capacity bottleneck for HetNets. In particular, two mmWave frequency bands (60 GHz and 73 GHz) are used in the BH network. It is proved that mmWave frequency bands can provide very high data rates for BH traffic and as such would not be a capacity bottleneck for future HetNets under the right conditions (like BH link length on order of 200m).

2. The problem of joint EE, power allocation and BH flow control is studied aiming at the maximization of EE. This is studied for two setups. In the first setup, the

joint EE, power allocation and BH flow control optimization problem was studied for fixed UE throughput demands. This optimization problem was shown to be a convex optimization problem and, thus, can be solved efficiently using convex optimization techniques.

In the second set up, the throughput demands of UEs were chosen to be a variable that can take any value between the minimum QoS throughput and the maximum achievable throughput. This is aimed at improving the overall network throughput as some UEs can receive higher throughput depending on their channel conditions. This variable-rate joint EE, power allocation and BH flow control problem is formulated as a fractional and non-convex optimization, which is NP-hard and difficult to obtain the global optimal solution. The original fractional and non-convex optimization problem is reformulated into a quasi-convex optimization problem, and a bisection-based algorithm that obtains the global optimal solution is proposed. Simulation results are used to demonstrate the superiority of the variable-rate EE maximization algorithm over the fixed-rate EE maximization algorithm and other simple benchmark schemes in terms of EE, total network throughput, total network power consumption, and BH links load balancing.

3. The user association problem aimed at optimizing power allocation in the AN and BH networks as well as BH flow assignment jointly without compromising UEs quality of service (QoS) requirements is studied in this dissertation. The energy efficient user association scheme that optimizes power allocation in the AN and BH networks as well as BH flow assignment is formulated as a non-convex mixed integer programming problem, which is NP-hard. It is shown how this non-convex problem can be tailored into a form that can be tackled using a classical mathematical programming technique called column generation

to derive the optimal solution, with a low complexity. To that end, a column generation based energy efficient user association, power and BH flow control algorithm is proposed. In the provided results, the proposed algorithm is shown to achieve significant EE gains than conventional user association schemes. It is noticed from the results that, the type of user association scheme employed in HetNets affects the energy consumption in the AN and BH, and by using the right user association scheme, the EE gains can be significantly improved.

1.1.3 Thesis Outline

This dissertation studies EE maximization in heterogeneous cellular networks. More specifically, optimal user association techniques, AN and BH power allocation, BH flow assignment and user-throughput demand allocation based on channel conditions techniques are investigated.

Chapter 1 provides the motivation, objectives, research contribution and the outline of the dissertation.

Chapter 2 presents the concepts of homogeneous and heterogeneous cellular networks, and also describes the major technical challenges associated with heterogeneous network architecture. This chapter also presents the state-of-the-art works on millimeter wave communications and EE in HetNets.

Chapter 3 presents two EE maximization optimization frameworks: a fixed-UE rate joint energy efficient, power and flow control optimization scheme and a variable-rate energy efficient, power and flow control optimization scheme. A bisection method-based joint EE, power and BH flow control algorithm is proposed for the latter scheme. Simulation results show that the variable-rate EE algorithm performs better than the fixed-rate EE algorithm and other benchmark schemes.

Chapter 4 extends our system model in Chapter 3 to include user association.

However, the binary nature of the user association variables significantly increases the complexity of the joint energy efficient user association, power and BH link flow control optimization problem. A column generation based approach is proposed to derive the optimal user association, power and flow control with a lower complexity. Simulation results are used to demonstrate the effectiveness of the proposed approach.

Chapter 5 gives concluding remarks and mentions future works.

Bibliography

[1] Cisco, "Visual networking index: Global mobile data traffic forecast and methodology, 2016-2021," Mar. 2017.

[2] A. Fehske, G. Fettweis, J. Malmodin, and G. Biczok, "The global footprint of mobile communications: The ecological and economic perspective," *IEEE Commun. Mag.*, vol. 49, no. 8, pp. 55–62, Aug. 2011.

[3] J. G. Andrews, S. Buzzi, W. Choi, S. V. Hanly, A. Lozano, A. C. K. Soong, and J. C. Zhang, "What will 5g be?" *IEEE J. Sel. Areas Commun.*, vol. 32, no. 6, pp. 1065–1082, Jun. 2014.

[4] M. Agiwal, A. Roy, and N. Saxena, "Next generation 5g wireless networks: A comprehensive survey," *IEEE Commun. Surveys Tuts.*, vol. 18, no. 3, pp. 1617–1655, 3rd Quart. 2016.

[5] F. Boccardi, R. W. Heath, A. Lozano, T. L. Marzetta, and P. Popovski, "Five disruptive technology directions for 5g," *IEEE Commun. Mag.*, vol. 52, no. 2, pp. 74–80, Feb. 2014.

[6] A. Mesodiakaki, F. Adelantado, L. Alonso, and C. Verikoukis, "Energy-efficient user association in cognitive heterogeneous networks," *IEEE Commun. Mag.*, vol. 52, no. 7, pp. 22–29, Jul. 2014.

[7] A. Ghosh, N. Mangalvedhe, R. Ratasuk, B. Mondal, M. Cudak, E. Visotsky, T. A. Thomas, J. G. Andrews, P. Xia, H. S. Jo, H. S. Dhillon, and T. D. Novlan, "Heterogeneous cellular networks: From theory to practice," *IEEE Commun. Mag.*, vol. 50, no. 6, pp. 54–64, Jun. 2012.

[8] M. Jaber, M. A. Imran, R. Tafazolli, and A. Tukmanov, "5g backhaul challenges and emerging research directions: A survey," *IEEE Access*, vol. 4, pp. 1743–1766, Apr. 2016.

[9] D. C. Chen, T. Q. S. Quek, and M. Kountouris, "Backhauling in heterogeneous cellular networks: Modeling and tradeoffs," *IEEE Trans. Wireless Commun.*, vol. 14, no. 6, pp. 3194–3206, Jun. 2015.

[10] C. Dehos, J. L. González, A. D. Domenico, D. Kténas, and L. Dussopt, "Millimeter-wave access and backhauling: the solution to the exponential data traffic increase in 5g mobile communications systems?" *IEEE Commun. Mag.*, vol. 52, no. 9, pp. 88–95, Sep. 2014.

[11] L. Wei, R. Q. Hu, Y. Qian, and G. Wu, "Key elements to enable millimeter wave communications for 5g wireless systems," *IEEE Wireless Commun.*, vol. 21, no. 6, pp. 136–143, Dec. 2014.

[12] A. V. Alejos, M. G. Sanchez, and I. Cuinas, "Measurement and analysis of propagation mechanisms at 40 ghz: Viability of site shielding forced by obstacles," *IEEE Trans. Veh. Technol.*, vol. 57, no. 6, pp. 3369–3380, Nov. 2008.

[13] Z. Pi and F. Khan, "An introduction to millimeter-wave mobile broadband systems," *IEEE Commun. Mag.*, vol. 49, no. 6, pp. 101–107, Jun. 2011.

[14] X. Lin, N. B. Shroff, and R. Srikant, "A tutorial on cross-layer optimization in wireless networks," *IEEE J. Sel. Areas Commun.*, vol. 24, no. 8, pp. 1452–1463, Aug. 2006.

Chapter 2

Background and Literature Review

2.1 Homogeneous Cellular Networks

A homogeneous cellular network architecture consists of the deployment of macro base stations (MBSs) of the same transmit power levels, antenna patterns, receiver noise floors and backhaul connectivity to the core network. The deployment of a homogeneous cellular network involves a macro-centric network planning process as depicted in Figure 2.2a, in which the locations of MBSs are carefully chosen, in order to maximize the coverage and minimize the interference between the MBSs. Untill the past few years, homogeneous cellular technologies such as 3G, 4G and most importantly the legacy 3rd Generation Partnership Project Long-Term Evolution (3GPP LTE) managed to support the different QoS requirements of users while guaranteeing a seamless connectivity for all users in the network. However, (i) the exponential increase in the number of connected devices, (ii) the continuous demand for higher data rates and (iii) the rapid growth of data traffic call for increasing the network capacity and coverage. One way of achieving this can be to densify the MBSs in the cellular network as shown in Figure 2.1. MBS densification can take the form of adding more

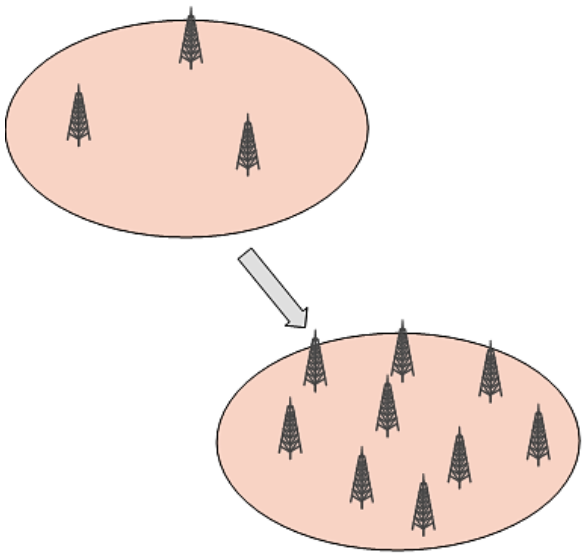

Figure 2.1: Densification of homogeneous cellular network.

sectors per MBS site or by deploying more MBSs. The deployment of additional MBSs can reduce the distance between a BS and a user thereby improving pathloss conditions, increasing frequency reuse and also enabling cell splitting gains. Unfortunately, this approach is highly complex in homogeneous cellular networks. Detailed network planning are required prior to the installation of the additional MBSs. Moreover, site acquisition for cell towers and BSs can become difficult and prohibitively expensive especially in densely populated areas. Also, MBSs do require an air conditioning unit for the power amplifier and a shelter to house the base transceiver station/node B (in 3G networks). Furthermore, fiber optic BH connections will be needed for most MBSs to connect the AN to the CN. In a nutshell, reducing the cell size using additional MBSs will incur more cost (capital expenditure (CAPEX) and operational expenditure (OPEX)) and energy usage since each MBS's transmit power varies between 5 and 40 W [1].

The above mentioned challenges associated with the dense deployment of traditional MBSs can be overcome by utilizing BSs with lower transmit power, on the

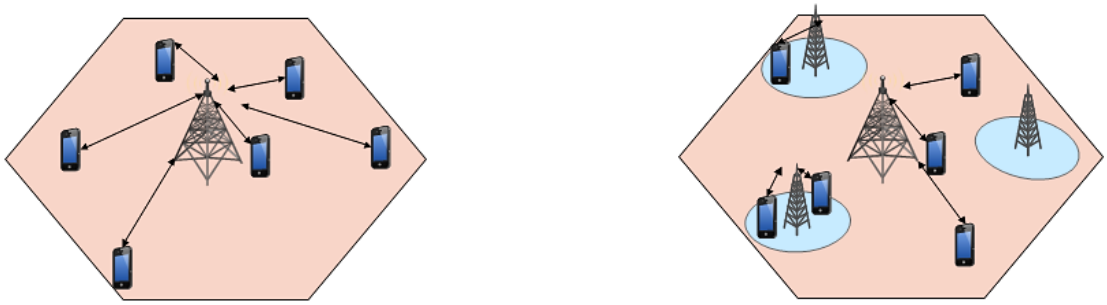

(a) Homogeneous cellular network

(b) Heterogeneous cellular network

Figure 2.2: Homogeneous vs Heterogeneous AN.

average 250 mW to 2 W (i.e. low power nodes), and different BH connection types over-laid in a MBS's coverage area as illustrated in Figure 2.2b. Thus, future cellular networks will be heterogeneous in nature.

2.2 Heterogeneous Networks

The migration from a homogeneous cellular network to a heterogeneous cellular network is perceived as a sustainable way to support a broad range of connectivity and to deliver unprecedented user experience in future cellular networks. As such, this area has received significant attention in the wireless industry and the academic research communities. A network that consists of a mix of MBSs and low power nodes, where some may be configured with restricted access and some may lack wired BH, is referred to as a heterogeneous network and is illustrated in Figure 2.3. Each class of BS is referred to as a tier and the low power nodes include micro, pico and femto BSs. MBSs refer to the conventional operator-installed BSs that provide open public access for wide coverage area distances of up to a few kilometers. They are referred to as enhanced NodeBs (eNBs) in LTE. Generally, MBSs can emit up to 46 dBm transmit power and can serve thousands of customers using a dedicated BH connection.

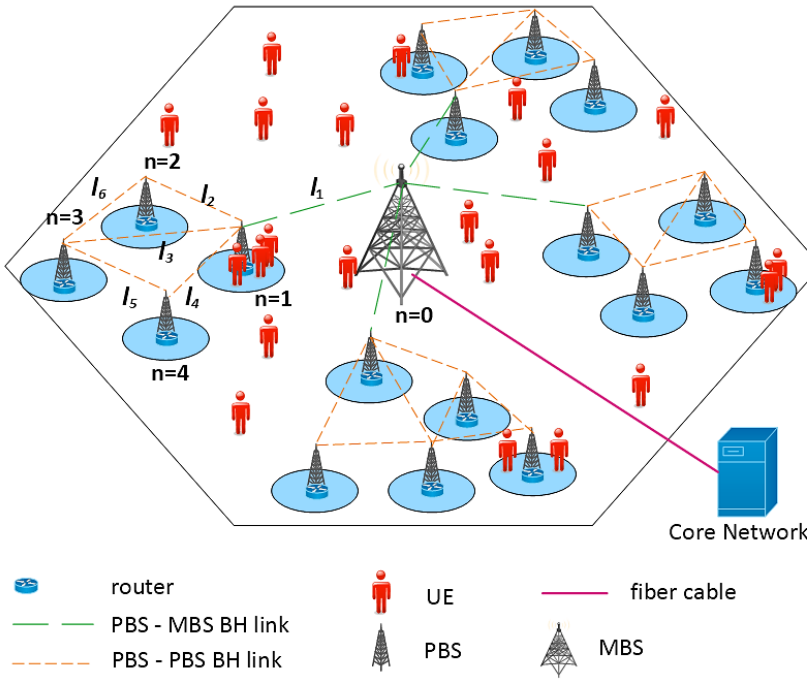

Figure 2.3: A two-tier heterogeneous network topology utilizing a mix of MBS and PBSs.

Pico BSs (PBSs) are low-powered operator-installed BSs with similar BH and access features as MBSs. They usually provide coverage over a radio range of 300 m or less for a few tens of UEs. Their transmit power ranges from 23 to 30 dBm. PBSs are mainly deployed for capacity enhancement, especially in areas with insufficient MBS penetration. Femto BSs (FBSs), with coverage range of less than 50 m, are low cost, low power, user-deployed access points for data traffic offloading using consumers' broadband connection. FBSs are also referred to as home BSs or home eNBs and have typical transmit power of less than 23 dBm. They can operate in either an open access or a restricted (closed subscriber group) access.

Since LTE Release 10, the deployment of HetNets has been an important evolution direction in 3GPP in providing the necessary means to accomodate the anticipated huge traffic growth [2]. In Figure 2.3, the MBS connects to the CN through a fiber cable. The PBSs connect with themselves or the MBS through a wireless BH connec-

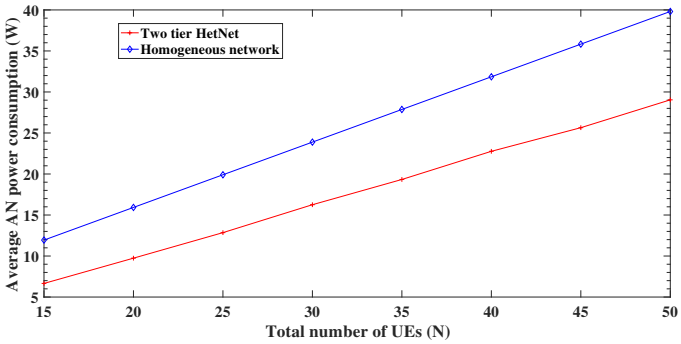

Figure 2.4: Comparison of the average AN power consumption gains of a homogeneous and heterogeneous cellular network deployment with different N values.

tion. The benefits that can be derived from heterogeneous cellular networks include mitigating the possible occurrence of capacity bottleneck in the AN and BH network and connections, improving SE, and reducing the wage bill of network operators.

The performance gains of a heterogeneous cellular network (as in Figure 2.2a) relative to a homogeneous network (as illustrated in Figure 2.2b) are briefly discussed below to provide useful insights on how HetNets can meet the growing UE traffic and network power consumption. In the simulation, each PBS/MBS equally shares its available transmit power to all of its subchannels. The bandwidth of each subchannel is 180 kHz. N represents the number of users in the network. The channel gain considered includes pathloss, log-normal shadowing and multipath fading. The user association employed here is the LTE-A reference signal received power (RSRP) scheme [1]. In RSRP users get associated with the BS from which it receives the strongest signal.

In Figure 2.4, the average total DL AN throughput is depicted for a homogeneous cellular network and a heterogeneous cellular network. Energy saving as high as 44.24% (typically for low number of UEs) and 27.06% (typically for high number of UEs) is achieved in the HetNet deployment. This is because whenever a UE gets associated with a PBS (i.e. UE receives best signal power from a PBS), less energy

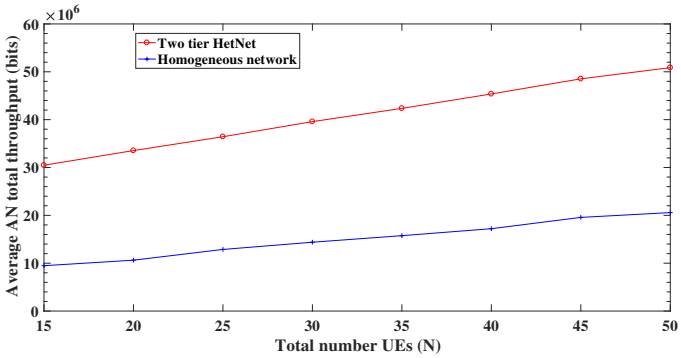

Figure 2.5: Comparison of the average AN throughput gains of a homogeneous and heterogeneous cellular network deployment with different N values.

is consumed as compared to the amount of energy a MBS would have consumed. Similarly, significant throughput improvement is achieved in the HetNet deployment for different N values. The average network EE of the two deployment strategies is shown in Figure 2.6. Better AN EE is achieved in the heterogeneous network deployment than in the homogeneous network. However, questions that arise from these results include; (i) is this user association scheme the best way of associating UEs so as to maximize AN throughput while minimizing power consumption, (ii) will this large AN total throughput cause a bottleneck problem in backhauling traffic to the CN, (iii) what about interference in HetNet deployment, and (iv) will the "sweet spot" frequency spectrum be able to support this potential increase in AN throughput for the HetNet deployment?

Moving on to future cellular HetNets, the successful integration of the different BSs and realistic simulations becomes more complex due to the extremely distinct characteristics of each tier of BS. In the next sub-chapter, the different technical aspects of HetNets technology, the challenges and future technology directions are discussed.

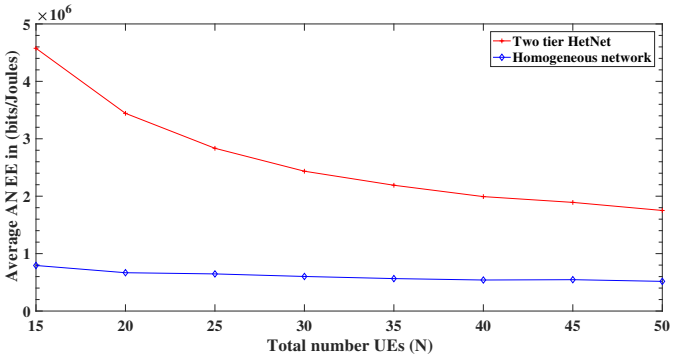

Figure 2.6: Average total downlink energy efficiency for different N values.

2.3 Technical Challenges in Heterogeneous Networks

In this section, some of the new challenges that arise in the deployment of HetNets are discussed. It focuses on both technical and economic issues.

2.3.1 User Association

User association can be defined as a mechanism through which a UE selects a single BS based on certain criteria from which it will receive network services. The different criteria that user association schemes can use include:

- Energy efficiency: UEs are associated to BSs such that the total network throughput is maximized while the total power consumption is minimized.
- Channel conditions: which can be signal quality at the receiver or the pathloss that the UE experiences.
- Backhaul: this criterion may consider the BH link length or number of hops, its capacity, and/or power consumption.

- Power consumption: this criterion focuses on minimizing power consumption in the network.
- Bandwidth: this criterion tries to maximize the transmitted data rate per spectrum resource unit (spectrum efficiency).
- Load balancing: this criterion focuses on the equal distribution of UE traffic to the different tiers of BSs.
- Interference: this criterion will try to minimize the interference that UEs in the network suffer.
- Bias: this criterion favors LPNs by actively pushing UEs to LPNs using a positive *bias value.*

The BS selection decision can be coordinated by a single entity within the whole network (centrally coordinated) or distributed, where each UE chooses a serving BS by itself. In general, finding the truly optimal BS-UE association is a combinatorial optimization problem and the complexity grows exponentially with the scale of the network. LTE technology, which constitutes a major step towards 5G standardization, uses a centralized user association scheme in which UEs send measurement reports to the radio admission control entity when configurable conditions are met. In particular, each UE measures the received signal strength from BSs and submit a report on the BSs and their respective received signal strength. With the goal of maximizing radio resources usage, a UE gets associated to the specific BS that provides the maximum received signal strength. This method of user association scheme is referred to as RSRP. However, simulation results and field trials have demonstrated that such an approach does not increase the overall throughput as has been anticipated in HetNets since LPNs typically have few active users [3]. In HetNets, RSRP scheme can lead to

a serious load imbalance since the majority of UEs get associated to the MBS due to the MBS's relatively stronger downlink transmit power [4]. As such, this rudimentary user association scheme may result in an inefficient use of LPNs' resources since most LPNs will have only few or no UEs associated to them. To cope with this problem, range expansion (RE) was proposed in 3GPP Release 10, where UE's power received from a LPN is artificially increased by adding a positive bias to it in order to ensure that more UEs get associated to it. Despite a potentially significant signal-to-noise ratio (SNR) hit for UEs, the issue of how much biasing is "optimal" still remains debatable. Also, RE presents lower SE than RSRP as a UE may be connected to a BS that does not provide the highest SNR which can consequently affect the overall power consumption in the network. These conventional user association schemes consider only the AN and do not guarantee efficient network (AN and BH) energy consumption. To that end, innovative backhual-aware user association schemes are needed to address the unique features of future 5G networks.

2.3.2 Backhauling

As discussed in the introduction, the proliferation of mobile data applications and traffic calls for a revolution in the design approaches for the realization of future 5G systems. Making reference to today's 4G wireless networks, 5G networks will need to provide support for the following [5]:

- 1000 times higher mobile data volume per area.
- 10 to 100 times higher number of connected devices.
- 10 to 100 times higher user data rate.
- 10 times longer battery life for low power massive machine-to-machine communications.

- Five times reduced end to end delay.

As a promising approach to attaining the above listed ambitious goals of 5G, HetNets are considered as one of the candidate technologies for 5G. While LPNs in HetNets can greatly maximize network total throughput, coverage, and EE, one of the numerous significant challenges to overcome lies in providing a scalable, affordable, and flexible mobile BH to connect the high capacity LPNs to the CN. Mobile BH in cellular networks is a term commonly used to describe connectivity between BSs and radio controllers. The dense deployment of LPNs overlaid the MBS in HetNets exacerbates this problem since (i) LPNs are mostly located in hard-to-reach areas and (ii) reliable BH connectivity must come at a lower cost. Moreover, providing direct high speed BH connection to the CN for each LPN becomes highly impractical. To that end, numerous researchers have offered a comprehensive study on the current and future cellular BH network requirements and candidate technologies [6] [7] [8].

Fiber connections have long been considered as the best BH solution due to their ability to provide abundant capacity and high scalability. However, this solution is highly impractical and prohibitive in HetNets due to the high deployment cost and challenge of laying fiber to each LPN, especially in such an unplanned, dense LPN deployment [5]. Wireless BH may be seen as a better alternative BH solution in HetNets. But other factors need to be considered before implementing wireless BH solutions. These factors include spectrum availability, propagation environment, line-of-sight (LOS) availability as well as capacity requirements. Although the sub-6 GHz band has higher tolerance to non line-of-sight (NLOS) propagation, it does not have sufficient bandwidth to support BH links requirement in 5G. Likewise, the traditional LOS microwave point-to-point links would not work in 5G due to its limited capacity and the possible occurrence of interference due to the large number of LPNs. A comparison of the different possible BH solutions in HetNets is summarized in

Table 2.1: Backhauling candidate solutions in heterogeneous cellular networks [5].

Backhaul candidate	**Cost**	**Reliability**	**Capacity**	**Deployment**	**Typical link distance**
Fiber	Medium	Very high	Very high	Difficult	>10 km
Licensed sub 6 GHz	Low	High	Low	Easy	<5 km
Unlicensed sub 6 GHz	Low	High	Low	Easy	<5 km
Unlicensed 6-42 GHz	Low	Medium	Medium	Easy	<5 km
Beyond 42 GHz mmWave	Low	Medium	High	Easy	<1 km

Table 2.1.

In HetNets, it is expected that the LPNs will be as close as 50 m apart. Hence, a LPN may connect to the CN through another LPN or an aggregation gateway as in LTE-A [6]. Multi-hop BH transmission is considered to enable BSs, beyond LoS communication to the CN, to send their BH traffic through relay BSs. Contrary to existing works that employ single BH link routes between neighboring BSs, it is more desirable to have multiple BH link routes between BSs. This is necessary to make BH traffic flow robust, to link failures and channel fading effects. Such multi-hop and multi-routes BH network topology requires proper BH network dimensioning and flow assignment to optimize energy consumption, with the consequent reduction of CAPEX and OPEX. Since most user association schemes do not consider BH link availability, BH network can become a performance limiting factor in 5G. Hence, the problem of jointly optimizing AN and BH network resources needs thorough studies. The ideal BH solution is likely a mixture of both wireless and wired BH technologies, in which some BSs (specifically the LPNs) may form a cluster to aggregate and forward BH traffic to the CN while other BSs may serve as relay nodes. The efficient design of such BH network in future cellular networks that incorporates considerations of important factors like network capacity, deployment density, required data rate, infrastructure cost, interference, operating carrier frequency, and the availability of radio spectrum remains a challenging task.

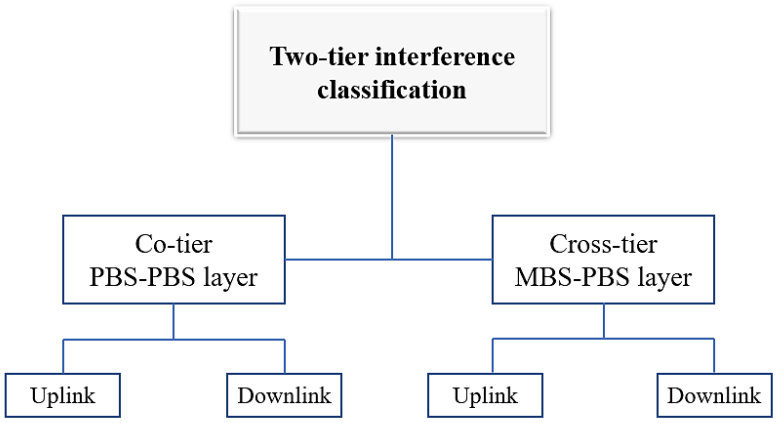

Figure 2.7: Interference classification in two-tier HetNets.

2.3.3 Interference

Besides backhauling and user association, another substantial challenge in the deployment of HetNets is the issue of cross-tier (inter-tier) or co-tier (intra-tier) interference. In traditional single-tier cellular networks, interference can be mitigated using well planned frequency reuse schemes. However, such frequency reuse schemes will reduce spatial reuse as subchannels used in one cell cannot be reused in neighboring cells. The roll outs of PBSs and FBSs overlaid MBSs will create new cell boundaries, in which users may suffer from strong inter-cell interference particularly when they all share the same frequency band. This could also possibly degrade the overall network performance. Figure 2.7 shows the various types of interference in a two-tier HetNet. Uplink co-tier interference can be caused by nearby, co-located UEs or a rise in the noise level to other neighboring PBSs. PBSs transmission interfering with neighboring PBSs' UEs result in downlink co-tier interference. A PBS UE acting as a source of interference to a MBS or vice-versa refers to uplink cross-tier interference and downlink cross-tier interference occurs when a PBS transmits too close to a MBS UE.

Aside from the large number of new cell boundaries, the sources of the interference

issue in HetNets include [9] [10]:

Unplanned deployment–LPNs are typically deployed according to UEs traffic distribution. Since UE traffic distribution cannot be predicted, the traditional network planning and optimization procedures become inefficient because neither the number of UEs nor the location of LPNs can be controlled by network operators. To that end, each BS should be able to configure and optimize its resources (transmit power and bandwidth allocation) so as to avoid the possible occurrence of interference in nearby cells. This motivates the search for novel decentralized interference avoidance schemes.

FBSs closed subscriber group (CSG) access–In CSG-based FBSs, only subscribed femto UEs (FUEs) have access to the resources of the FBS. Thus non-subscribers would not always be connected to closest BS. Such scenario may cause cross-tier interference. As depicted in Figure 2.8a, a MBS user (MUE), who is not subscribed to the FBS, transmits at a high power on its UL to its far serving MBS. This has led to the occurrence of strong interference in the UL of the nearby FUE. In Figure 2.8b, a FUE interferes with the DL reception of a nearby MUE. In summary, CSG access FBSs can potentially generate high interference to nearby MBS and PBS UEs and vice versa. As the deployment of MBSs, PBSs and FBSs are expected to be high, the corresponding associated interference may significantly increase as well. This calls for further studies.

Transmit power difference between BSs–The imbalance in the pathloss of UEs from the different tiers of BSs and in the transmit power of BSs belonging to different tiers can cause strong interference in HetNets. It has been highlighted earlier that the RSRP user association scheme usually leads to an overload of UEs for the MBSs due to the uneven traffic distribution. UEs associated with the MBSs in the DL can severely interfere with the UL of UEs associated with LPNs in the vicinity of

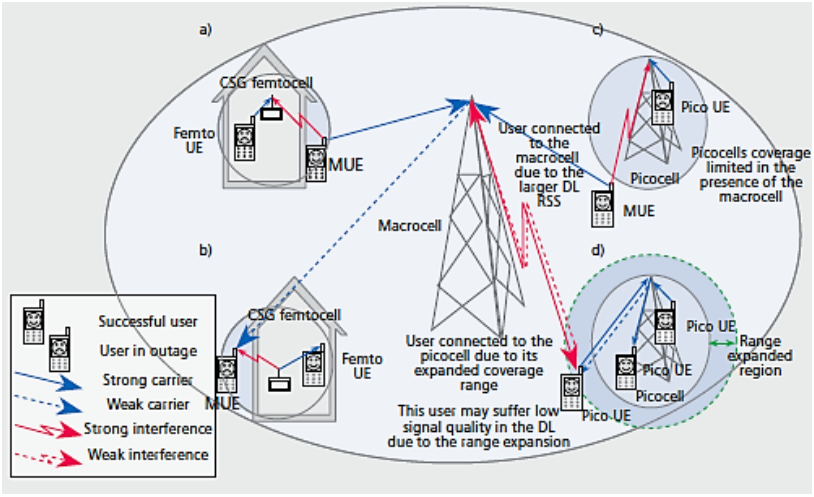

Figure 2.8: Various possible UL and DL cross-tier interference scenarios in HetNets [9].

the MUEs. Figure 2.8c shows how a UE associated to a MBS (as a result of RSRP user association scheme) creates a strong UL interference to a nearby PUE. Similarly, the MUE will receive a strong DL interference.

Figure 2.8d illustrates how RE mitigates the PUE UL interference encountered in Figure 2.8c. With RE, the MUE in Figure 2.8c gets associated to the PBS, and hence transmits less UL power, thereby mitigating the cross-tier interference in the UL. However, this can also reduce the DL signal quality of UEs in the expanded region or cause a higher DL transmit power to that UE from the PBS.

2.3.4 Energy efficiency maximization

Energy efficiency (units: bits-per-Joule) is defined as the amount of information (bits) that can be reliably transmitted per Joule of consumed energy. It has been identified as one of the key performance indicators for 5G networks. Maximizing overall network EE may be defined as maximizing the successfully sent data rate while minimizing the total energy consumption [11]. In cases where by the demanded data rates of UEs are fixed, EE maximization translates to satisfying the UE traffic demands, while

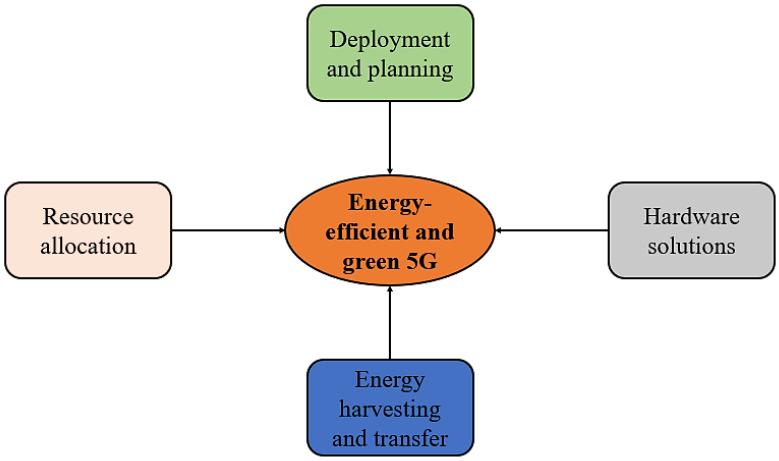

Figure 2.9: Approaches for increasing the energy efficiency of future wireless networks.

minimizing the total energy consumption. Maximizing EE does not only help achieve cost reduction, but also green environmental targets. A general consensus in the wireless academic industry is achieving a 1000× data rate increase for the same or lower power consumption as today's networks [12] [13].

The total energy consumption is the sum of the AN and BH links energy consumption. Since BH networks will form a critical part in the design of future cellular networks, their energy consumption cannot be neglected. Generally, the total transmit power of a BS is equally distributed among its subchannels. The more UEs in the network, the higher the number of subchannels needed to meet the demands of the UEs and the higher the AN energy consumption. Also, the AN energy consumption becomes higher when more UEs are associated with the MBS, since the MBS transmits higher power than the LPNs. Controlling the transmission power of BSs according to UE demand rates and channel conditions can help minimize energy consumption and CO_2 emission.

Energy consumption in a BH link is a scalar function of the aggregated throughput that flows through the link. An aggregated throughput can be defined as the sum of

the throughput of all UEs associated to all LPNs that backhaul their traffic through this BH link. It has beeg reported that user association schemes in HetNets can significantly influence the energy consumption of the BH network, a claim which will be investigated as part of this dissertation [11]. Another way of improving the EE of BH network is by performing BH load balancing.

Figure 2.9 illustrates the four main approaches for increasing the EE of future wireless networks. Two of the approaches, key to this dissertation, are explained as follows. Details on the remaining two can be found in [13] [12].

1. *Resource allocation:* This includes the design of resource allocation (including power and bandwidth) strategies for either the AN or BH network or both aimed at optimizing the network EE. Different energy efficient resource allocation schemes have been investigated in [14] [15] [16] [17]. They all come to the conclusion that large energy savings can be attained at the cost of moderate reduction in achievable data rates, as most of these resource allocation schemes only guarantee the minimum achievable data rate. However, this conclusion slightly differs from the true meaning of EE maximization, as the total throughput of the network is not maximized.

2. *Network deployment and planning:* This technique includes the deployment of BSs in a network so as to maximize the covered area per consumed energy, rather than just maximizing the covered area. One way of achieving this is by reducing the number of BSs for a coverage target or designing adaptive BS sleep/wake algorithms depending on the network traffic conditions [18] [19] [20].

Summarizing the discussion in this subsection, it can be agreed upon that EE is highly dependent on user association, power and flow control in both AN and BH links, as well as the data rate that users enjoy. Hence, future energy efficient algorithms

Table 2.2: mmWave frequency band designation [21].

Band	Frequency range
Q	33-50 GHz
U	40-60 GHz
V	50-75 GHz
E	60-90 GHz
W	75-110 GHz
F	90-170 GHz
D	110-170 GHz
G	140-220 GHz

must make provisions for optimizing all these components that help to maximize the network EE.

2.4 Millimeter Wave Frequency Communication

Recently, millimeter wave (mmWave) frequency communications have drawn a great deal of interest from researchers in academia, industry, and global standardization bodies. This is due to the large available bandwidth as well as ability to support multi gigabit data rates required for future cellular networks. mmWave frequency communication can be classified as communication links occupying the electromagnetic spectrum within the range 30 GHz to 300 GHz. This frequency range corresponds to wavelengths from 10 mm to 1mm. The mmWave frequency band designations are summarized in Table 2.2.

With the rapid increase in the deployment of BSs and the exponential growth in cellular traffic, it is necessary to deliver dedicated peak data rates of 1 Gbps to 10 Gbps for BH links. In HetNets, another key enabling technology of 5G, BH links between LPNs are required to have peak data rates of up to 1 Gbps while BH links between an aggregation point and the MBS are expected to have a peak rate of 10 Gbps. Due to the large amount of bandwidth available in the mmWave band, and

knowing that the capacity of an AWGN channel increases linearly with the channel bandwidth, mmWave frequency communication can provide these data rates under good channel conditions [22] [23]. Presently, the available bandwidth for cellular networks (2G, 3G, 4G and LTE-Ad spectrum) is globally smaller than 780 MHz and each major wireless provider has only a total of about 200 MHz spectrum [24]. This bandwidth is not enough to provide data rates of Gbps in future mobile networks. As shown in Figure 1.3, a large chunk of bandwidth is available in the mmWave bands for future mobile networks. In October 2003, the FCC announced the availability of the 71-76 GHz, 81-86 GHz, and 92-95 GHz frequency bands for ultra-high speed data transmission including point-to-point WLAN, mobile BH, and broadband internet access [23]. Moreover, this provides a sustainable way of enhancing network capacity as compared to the more conventional way of increasing transmit power to increase network capacity, since transmit power is limited in practice. More particularly, the application of mmWave frequencies in the 60 GHz band and within the 70-80 GHz band in mobile backhaul have gained prominence in the wireless industry [6]. As an example, the use of the newly unlicensed 60 GHz band for high throughput wireless local area networks and personal area networks was studied in [25]. Although data rates in excess of 1 Gbps were recorded, the links were generally limited to short range or point-to-point LOS settings.

2.4.1 Characteristics of Millimeter Waves

Unlike lower frequency signals that can propagate for many miles and penetrate more easily through buildings, mmWave signals are known to travel only a few miles or less and are not capable of penetrating solid materials well. This has limited its usage to strictly LOS communications and only for short distances, with a maximum practical reach of about 1 km. As such, the design and planning of mmWave communica-

tions must take into account the propagation characteristics of radio signals at this frequency range.

Nonetheless, two recent trends in cellular wireless communications have encouraged a thorough investigation on the viability of mmWave cellular communications. Firtsly, the advancement in complementary metal-oxide semiconductor (CMOS) radio frequency (RF) technology and digital processing have enabled the production of low cost mmWave chips for commercial mobile devices usage and highly integrated transmitters and receivers [26] [27]. Again, the very small wavelengths of mmWaves would enable large antenna arrays to be fabricated in a small area of less than one or two cm^2. This will provide path diversity from human and non-human obstructions. Secondly, the coverage area of BSs in cellular networks is evolving towards smaller radii. Particularly, in dense urban areas, cell sizes are often less than 100 m to 200 m in radius and it is expected that LPNs will eventually be as little as 50 m apart, possibly within the range of mmWave signals [28].

The discussions above shows that the high frequencies and propagation characteristics of mmWaves are not necessarily disadvantageous, but rather make them suitable for a variety of applications that include the transmission of large amounts of data in cellular communications while offering other benefits like:

1. Unlicensed or "light licensing" operation: Unlike the sub-3 GHz frequency bands, no license from regulatory bodies like the Federal Communications Commission (FCC) is required.

2. Promises highly secure operation: This is due to the short wavelength and narrow beamwidth characteristics of mmWaves. Additionally, transmission at such high frequencies carries minimal risk of interference as it heavily relies on highly directive narrow beamwidth antennas at each end of a link, with no

penetration through or reflection from obstacles such as buildings and vegetation [6] [29].

3. High level of frequency reuse enabled: mmWave communications can allow densely packed communication links, thus enabling more efficient spectrum utilization. In this way, the communication needs of multiple cells located in a close proximity can be satisfied.

4. Mature technology: The mmWave frequency band has long been used for secure communications, notably for the military use.

Since mmWave communication technology constitute a major portion of the HetNet system model in this dissertation, it is important to understand the characteristics of mmWaves and its radio channel. In what follows, the characteristics of mmWave propagation including free space path loss ($FSPL_{(dB)}$) and the effects of various physical factors,called millimeter wave propagation loss factors ($PL_{(dB)}$) are reviewed.

Millimeter wave propagation loss factors

Propagation loss for signal transmission in microwave communication systems is primarily characterized by free-space loss. However, signal transmission in mmWave frequency bands suffer from additional loss factors such as atmospheric gaseous (oxygen and water vapor) attenuation and rain attenuation. In this dissertation, attenuation is defined in decibels (dB) loss per kilometer of propagation. Also, reflective surfaces in mmWave communication appear rougher due to the high frequencies and the corresponding shorter wavelengths. These result in diffused reflection.

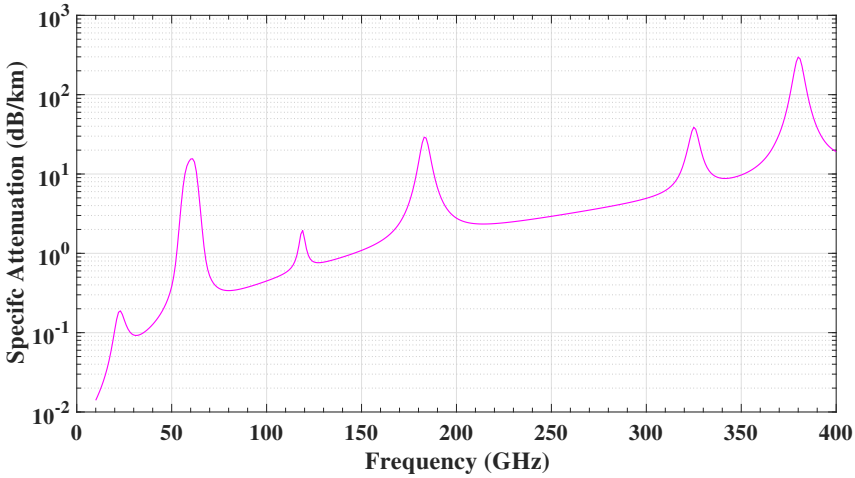

Figure 2.10: Specific attenuation due to atmospheric gases.

Table 2.3: Environmental conditions for mmWave channel.

Total air pressure (hPa)	**1013**
Temperature (K)	288.15
Water vapor concentration $\left(g/m^3\right)$	7.5

Attenuation due to atmospheric gases

Atmospheric attenuation refers to transmission losses that occur when mmWaves propagating in the atmosphere are absorbed by molecules of oxygen, water vapor, and other gaseous atmospheric constituents. These losses can be greater at specific frequencies depending on the mechanical resonant frequencies of the gas molecules. Figure 2.10 shows a plot of the attenuation due to atmospheric gases across the different frequencies in the mmWave band. The parameters used in the calculation of the attenuation for the different frequency components are summarized in Table 2.3.

Several peaks, denoting the absorption of radio signals by oxygen and water vapor, can be noticed in Figure 2.10. This absorption of radio signals, at these mmWave frequencies, leads to high attenuation, thereby limiting their propagation to short distances. In between the absorption peaks are spectral windows where absorption

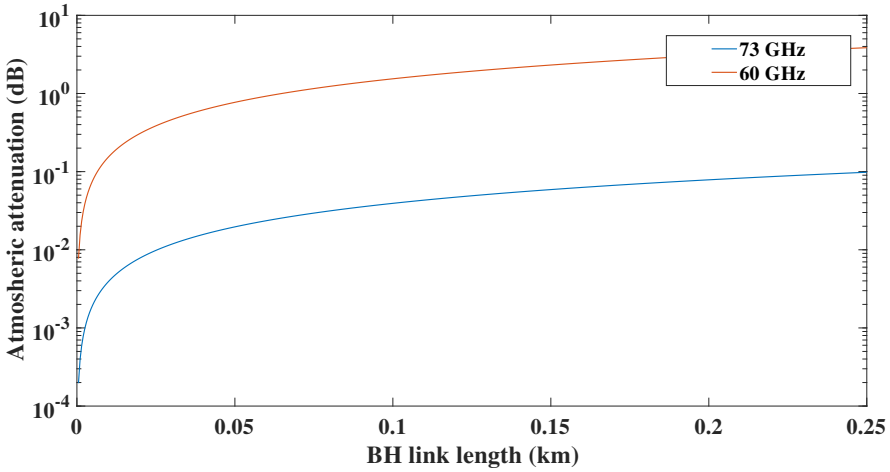

Figure 2.11: Atmospheric attenuation versus BH link length.

reduces significantly. These windows include 35 GHz, 94 GHz, 140 GHz and 220 GHz. It can also be observed that the 60 GHz suffers from a higher atmospheric attenuation, 15 dB/km, than the 0.3 dB/km of the 70-80 GHz frequency band. More precisely, for frequencies below 100 GHz, the highest atmospheric attenuation occurs at the 60 GHz frequency. Because of this, the working range for a communication link using the 60 GHz should not exceed 1 km. Another link could be employed on that same frequency (60 GHz), if separated from the first link by an appropriate distance [21]. A plot of the atmospheric attenuation versus distance is shown in Figure 2.11. It can be observed that the 60 GHz experiences the highest attenuation due to its high oxygen absorption. This absorption gets higher with an increase in the BH link. But for BH link lengths below 200 m, an attenuation of about only 3 dB is recorded for the 60 GHz, making it a good candidate for short backhauling.

Attenuation due to rain

mmWave signals are roughly of the same size as raindrops. Hence, raindrops can easily have significant scattering effects on the mmWave signals. Figure 2.12 shows the

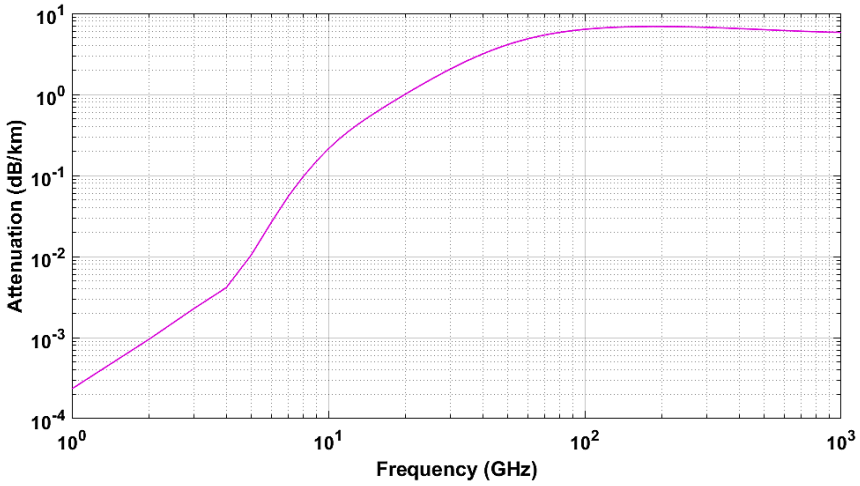

Figure 2.12: Attenuation due to rainfall (amount of rainfall is 10mm/hr).

attenuation per km for mmWave frequencies as a function of a rain rate of 10mm/hr. The rain rate in any location in the United States and Canada can be found in a map of rain rate climate regions and a chart of associated rainfall statistics in [21].

Figure 2.12 shows that higher frequencies experience higher rain attenuation. As such, the 70-80 GHz range is more likely to suffer from higher rainfall attenuation than the 60 GHz. Since the atmospheric gas attenuation effect on the 70-80 GHz is minimal, its typical transmission distance equates to a link distance of up to a few kilometers depending on the rainfall rate of that area. A plot of rain attenuation versus BH link length for the 60 GHz and 73 GHz mmWave frequency is shown in Figure 2.13. Because the 60 GHz is shorter in reach, it is well suited for BH connectivity of two LPNs belonging to the same tier (eg. PBS to PBS), as the higher attenuation effects at longer distances can help minimize possible interference. The 60 GHz can be used in multi hop BH connections. The 70-80 GHz is a better fit for BH connections between LPN aggregation points and the MBS. Based on the discussions of Figure 2.10 and Figure 2.12, as well as key information provided in Table 2.4, the 60 GHz frequency will be used for BH connection between two LPNs and the 73 GHz will be

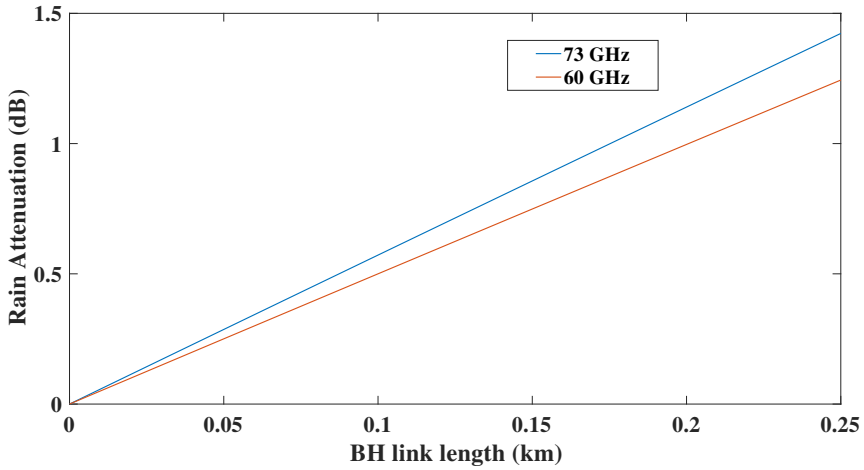

Figure 2.13: Rain attenuation versus BH link length

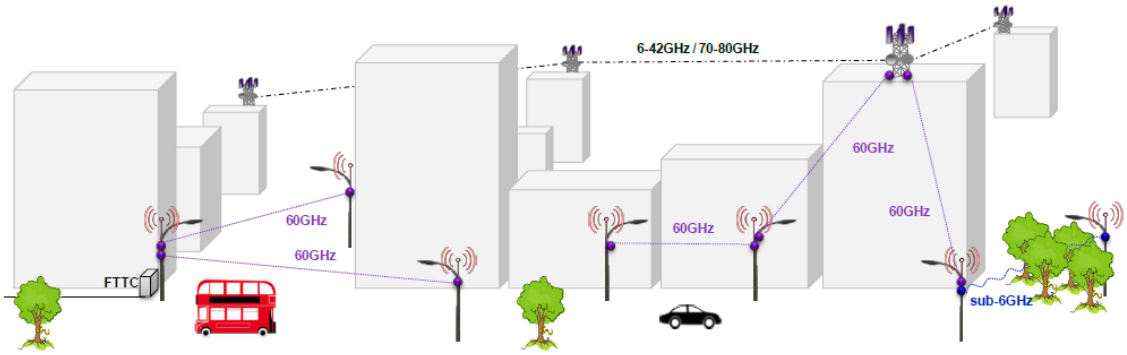

Figure 2.14: An illustration of the 60 GHz and 70-80 GHz technologies for backhauling in a two-tier HetNet [6].

used for BH connection between LPNs aggregation point and the MBS. The smaller equipment size and lower production cost of the 60 GH technology also favor their large scale deployment for the numerous LPNs expected to be deployed in future HetNets. The use of the 60 GHz and the 70-80 GH frequency band for backhauling in a two-tier HetNet is illustrated in Figure 2.14.

Table 2.4: Comparison of key aspects of 60 GHz and 70-80 GHz mmWave bands [30] [31] [6] [32].

Aspect	**57-66 (V band)**	**70-80 GHz (E band) 71-76 GHz and 81-86 GHz**
BH link frequency	60 GHz	73 GHz and/or 83 GHz
Capacity	up to 1 Gbps	up to 10 Gbps
Coverage	up to 1km hop length	up to 3 km hop length
Spectrum availability	up to 9 GHz contiguous	2 x 5 GHz
Antenna gain (dBi)	GTx=GRx=37 (max)	GTx=GRx=43 (min)
Licensing	mostly unlicensed	mostly light licensed
Physical size of equipment	Ranges from 10-20 cm in width and length.	Ranges from 25-35cm in width and length.
Relative equipment cost	lower	higher
Installation	line-of-sight	line-of-sight
Main use case(s)	Capacity/urban: wireless technology for SC BHs	Capacity/urban: SCs aggregation point connection to MBS

Free space pathloss

$FSPL$ predicts the received signal strength when the transmitter and receiver have a clear, unobstructed LOS path between them. The frequency and distance dependence of the loss between any two isotropic antennas is given as

$$FSPL = \left(\frac{4\pi R}{\lambda}\right)^2, \tag{2.1}$$

where R is the LOS transmission distance between the transmitting and receiving antennas, and λ is the operating wavelength. In dB form, the $FSPL$ in (2.1) becomes:

$$FSPL_{(dB)} = 92.4 + 20\log_{10}\left(f_{(GHz)}\right) + 20\log_{10}\left(R_{(km)}\right), \tag{2.2}$$

where R is still the LOS separation distance between the transmit and receive antennas (but in km) and f is the frequency in (GHz). Because mmWave signals have much shorter wavelength than the conventional microwave communication signals operating

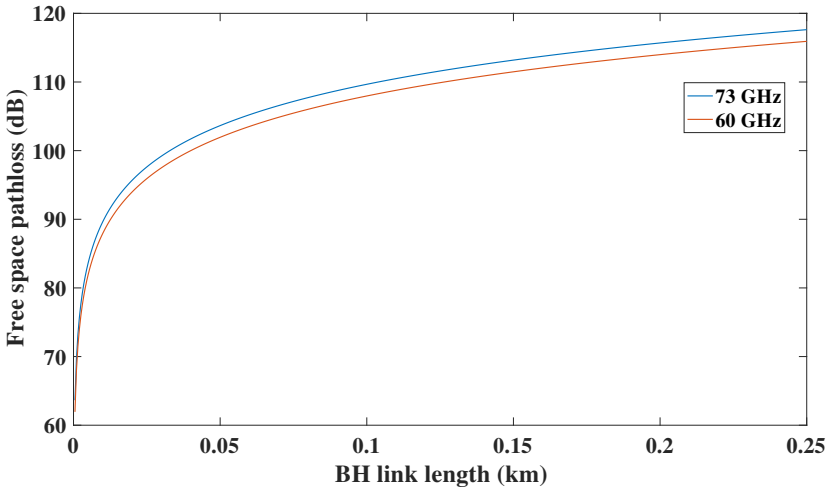

Figure 2.15: Free space pathloss versus BH link length.

at carrier frequency below 6 GHz, the pathloss of mmWave signals is higher than that of microwave signals, given that all other conditions like antenna gains remain the same. Although the pathloss of mmWave signals is generally high, it is feasible to employ them for communication links over distances that are common in urban mobile networks, such as a few hundreds of meters or even a few kilometers [24] [23]. Since BSs in dense HetNets will be some few meters apart, BH links are expected to be on the order of up to 500 m. A plot of the $FSPL$ for the two mmWave frequencies considered in this dissertation is shown in Figure 2.15. It can be observed that these effects are insignificant for such short BH link lengths.

The total path loss ($TPL_{(dB)}$) can be expressed as

$$TPL_{(dB)} = FSPL_{(dB)} + PL_{d(dB)}. \tag{2.3}$$

It can also be observed from Figure 2.16 that the total pathloss for the 60 GHz frequency increases at a faster rate after 0.1 km than the 73 GHz frequency. As such, the use of the 60 GHz frequency for PBS-PBS backhauling can help avoid the

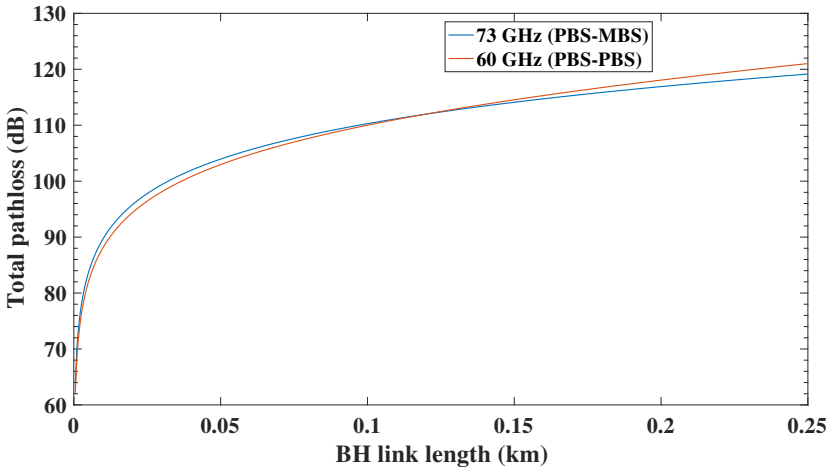

Figure 2.16: Total pathloss versus BH link length.

occurence of interference at nearby links since attenuation increases with distance at a higher rate.

2.5 Energy Efficiency

In this section, recent work on EE in wireless communication is presented. The section begins with optimization schemes that maximizes EE in only the AN, and then continues with optimization schemes that maximizes EE in only the BH network. The very few schemes that considers EE maximization in both the AN and BH network are summarized next. Motivated by the literature gaps in the summarized existing work, the chapter concludes with our research contribution.

2.5.1 Energy Efficiency in the Access Network

There are numerous works on energy efficient user association and power control for the AN [33-44]. Based on how energy consumption is minimized in the AN, these existing works can be divided into three groups. We focus on the first two.

Firstly, the authors jointly consider the problem of user association and power control [33] [34] [35] [36] [37] [38] [39] [40]. This problem comes with extraordinary challenges due to its non-convex and combinatorial nature. In [33], the authors design a joint user association and power control algorithm for the uplink of a HetNet. In their algorithm, each UE gets associated to a number of BSs that guarantee min-imimizing UE effective interference. In [34], the authors studied an integrated BS assignment, diversity, and power control and proposed a signal-to-interference-and-noise ratio (SINR) feedback-based algorithm. Under range expansion association, a power control scheme that minimizes the interference experienced by UEs in the cell range expansion (CRE) region from the MBS is proposed in [35]. Their algorithm offloads UEs from the MBSs in the downlink and associate them to PBSs. While this improves the performance of UEs in the CRE, it results in an inefficient usage of MBS resources. A joint user association and power control algorithm that minimizes the required power to satisfy the fixed rate demands of UEs was proposed in [36].

It is important to mention that all of the above mentioned papers do not let EE be the objective of the optimization problem. Because the algorithms considered by the authors only satisfy the fixed demand rates of UEs, they simply minimize the overall power consumption satisfying the QoS requirements of UEs. With the objective of maximizing EE, a joint user association and power control algorithm that also maximizes system throughput has been studied in [37]. The proposed algorithm was derived from the classical Benders' Decomposition method. A user association and power control algorithm that maximizes the uplink EE is studied in [38]. The resulting optimization problem was a non-convex and mixed-integer optimization problem. To get a tractable solution, the original problem was decomposed into subproblems and iteratively solved using the sum-of-ratios programming, the parametric Dinkelbach algorithm and convex optimization. A sub-optimal heuristic algorithm that maximizes

the EE for users by performing joint subcarrier and power allocation is proposed in [39] using sum-of-ratios optimization and the generalized fractional programming. Energy efficient user association and power control scheme that maximizes the AN EE is studied in [40]. Because the resulting optimization problem had a fractional and mixed-integer form, the authors proposed a three-layer iterative algorithm using the bisection method, dual decomposition method and a power update function.

Secondly, some authors employ beamforming approaches during user association to maximize EE. The joint problem of user association and weighted sum rate maximization in the uplink of a MIMO HetNet is studied in [41]. The problem of energy-efficient joint power allocation and beamforming for coordinated multicell multiuser downlink system is studied in [42]. However, as revealed in [43], the joint optimization of user association and beamforming may not be advisable since the former takes place at a larger time scale and the latter takes place at a smaller time scale. Thus, while the user association utilizes a slow fading channel, the beamforming exploits a fast fading channel.

The authors in the third group often perform user association and power control through the on/off control of BSs [44].

2.5.2 Energy Efficiency in the Backhaul Network

There are only few existing works in the literature that study how to achieve high EE in the BH network. Due to the expected large number of BH links and the fact that the exponential growth in AN traffic will increase BH traffic, subsequently leading to higher energy consumption, improving EE in the BH network should be of utmost importance. The role of BH in future outdoor HetNets is studied in [45]. The authors investigate how BH energy consumption impact the overall (AN and BH) network consumption and from their results determine if BH could become an energy bottle-

neck for the network. Among the different BH technologies considered are mmWave frequency bands, microwave frequency bands and the sub-6 GHz band. Similarly, the impact of BH on the energy consumption of wireless AN, taking into account the current and projected data traffic requirements is studied in [46]. From their studies, BH can amount to up to 50% of the power consumption in a wireless network. It was also shown that hybrid BH architectures (fiber and microwave) perform relatively well than the case when only one BH architecture is used.

2.5.3 Energy Efficiency in the Access Network and Backhaul Network

It can be observed from the works presented in Section 2.5.1 and Section 2.5.2 that current approaches overlook the BH capacity constraints and energy impact and as such the overall network EE cannot be determined. In [47], the problem of user association aimed at the joint EE and SE maximization for both the AN and BH was studied. With the objective of minimizing the total (AN and BH) transmit power, a user association algorithm that also optimizes SE without compromising UE QoS was proposed. A context-aware energy efficient algorithm that takes as input the available context-aware information (such as UEs' measurements and requirements, the HetNet architecture knowledge, and the available spectrum resources of each BS), to associate UEs to BSs aiming to minimize network energy consumption has been proposed in [11]. An optimization model that minimizes the total (AN and BH) power consumption in a HetNet for given UE throughput demand is studied in [48].

2.6 Conclusion and Summary of Research Contribution

From the previous discussion, the following observations can be noted:

1. Most existing EE maximization schemes do not guarantee the actual network EE because they only minimize network energy consumption while satisfying the fixed traffic demands of UEs. This is somehow different from the true meaning of EE, which is maximizing network capacity while minimizing the total energy consumption.

2. Most existing EE maximization schemes neglect the capacity and energy constraints of BH links. But BH network will form a key component in HetNets and such their EE cannot be neglected.

3. Because of the multiple-hop nature that BH networks in HetNets will assume, it becomes necessary to optimize the traffic assignment on the numerous BH links while satisfying BH links capacity and energy constraints.

4. None of the above mentioned referenced papers jointly optimize power, BH flow assignment and UE throughput demands to maximize overall network (AN and BH) EE.

5. None of the above mentioned referenced papers consider a user association scheme that jointly performs power allocation and BH flow assignment. It is important to study user association scheme that associates UEs to BSs such that the AN and BH energy consumption is minimized and the numerous BH links are effectively utilized.

Motivated by these observations, we make the following contributions:

1. We develop a fixed-rate joint energy efficient, power allocation and BH flow control optimization model, and show how it can can be solved to global optimum.

2. We develop a variable-rate joint energy efficient, power and BH flow control, and throughput demand maximization optimization model, and proposed a bisection method based algorithm that yields the global optimum solution.

3. We develop an energy efficient user association scheme that jointly performs power allocation and BH flow assignment without compromising the QoS requirements of UEs. Because the original problem is non-convex and in mixed-integer form, we show how it can be tailored into an equivalent form that allows the application of a classical mathematical programming approach called column generation. We use column generation and convex optimization to derive the optimum solution with a lower complexity.

Bibliography

[1] A. Damnjanovic, J. Montojo, Y. Wei, T. Ji, T. Luo, M. Vajapeyam, T. Yoo, O. Song, and D. Malladi, "A survey on 3gpp heterogeneous networks," *IEEE Wireless Commun.*, vol. 18, no. 3, pp. 10–21, Jun. 2011.

[2] T. Nakamura, S. Nagata, A. Benjebbour, Y. Kishiyama, T. Hai, S. Xiaodong, Y. Ning, and L. Nan, "Trends in small cell enhancements in lte advanced," *IEEE Commun. Mag.*, vol. 51, no. 2, pp. 98–105, Feb. 2013.

[3] J. G. Andrews, H. Claussen, M. Dohler, S. Rangan, and M. C. Reed, "Femtocells: Past, present, and future," *IEEE J. Sel. Areas Commun.*, vol. 30, no. 3, pp. 497–508, Apr. 2012.

[4] J. G. Andrews, S. Singh, Q. Ye, X. Lin, and H. S. Dhillon, "An overview of load balancing in hetnets: old myths and open problems," *IEEE Wireless Commun.*, vol. 21, no. 2, pp. 18–25, Apr. 2014.

[5] L. Wei, R. Q. Hu, Y. Qian, and G. Wu, "Key elements to enable millimeter wave communications for 5g wireless systems," *IEEE Wireless Commun.*, vol. 21, no. 6, pp. 136–143, Dec. 2014.

[6] S. C. Forum, "Backhaul technologies for small cells: Use cases, requirements and solutions, rel. 1,049.01.01," Feb. 2013.

[7] O. Tipmongkolsilp, S. Zaghloul, and A. Jukan, "The evolution of cellular backhaul technologies: Current issues and future trends," *IEEE Commun. Surveys Tuts.*, vol. 13, no. 1, pp. 97–113, 1st Quart. 2011.

[8] N. Wang, E. Hossain, and V. K. Bhargava, "Backhauling 5g small cells: A radio resource management perspective," *IEEE Wireless Commun.*, vol. 22, no. 5, pp. 41–49, Oct. 2015.

[9] D. Lopez-Perez, I. Guvenc, G. de la Roche, M. Kountouris, T. Q. S. Quek, and J. Zhang, "Enhanced intercell interference coordination challenges in heterogeneous networks," *IEEE Wireless Commun.*, vol. 18, no. 3, pp. 22–30, Jun. 2011.

[10] I. Hwang, B. Song, and S. S. Soliman, "A holistic view on hyper-dense heterogeneous and small cell networks," *IEEE Commun. Mag.*, vol. 51, no. 6, pp. 20–27, Jun. 2013.

[11] A. Mesodiakaki, F. Adelantado, L. Alonso, and C. Verikoukis, "Energy-efficient user association in cognitive heterogeneous networks," *IEEE Commun. Mag.*, vol. 52, no. 7, pp. 22–29, Jul. 2014.

[12] S. Buzzi, C. L. I, T. E. Klein, H. V. Poor, C. Yang, and A. Zappone, "A survey of energy-efficient techniques for 5g networks and challenges ahead," *IEEE J. Sel. Areas Commun.*, vol. 34, no. 4, pp. 697–709, Apr. 2016.

[13] J. G. Andrews, S. Buzzi, W. Choi, S. V. Hanly, A. Lozano, A. C. K. Soong, and J. C. Zhang, "What will 5g be?" *IEEE J. Sel. Areas Commun.*, vol. 32, no. 6, pp. 1065–1082, Jun. 2014.

[14] C. U. Saraydar, N. B. Mandayam, and D. J. Goodman, "Efficient power control via pricing in wireless data networks," *IEEE Trans. Commun.*, vol. 50, no. 2, pp. 291–303, Feb. 2002.

[15] F. Meshkati, H. V. Poor, S. C. Schwartz, and R. V. Balan, "Energy-efficient resource allocation in wireless networks with quality-of-service constraints," *IEEE Trans. Commun.*, vol. 57, no. 11, pp. 3406–3414, Nov. 2009.

[16] S. Buzzi and H. V. Poor, "Joint receiver and transmitter optimization for energy-efficient cdma communications," *IEEE J. Sel. Areas Commun.*, vol. 26, no. 3, pp. 459–472, Apr. 2008.

[17] S. Buzzi, G. Colavolpe, D. Saturnino, and A. Zappone, "Potential games for energy-efficient power control and subcarrier allocation in uplink multicell ofdma systems," *IEEE J. Sel. Topics Signal Process.*, vol. 6, no. 2, pp. 89–103, Apr. 2012.

[18] E. Oh and B. Krishnamachari, "Energy savings through dynamic base station switching in cellular wireless access networks," in *Proc. IEEE GLOBECOM*, Dec. 2010, pp. 1–5.

[19] Z. Niu, Y. Wu, J. Gong, and Z. Yang, "Cell zooming for cost-efficient green cellular networks," *IEEE Commun. Mag.*, vol. 48, no. 11, pp. 74–79, Nov. 2010.

[20] A. Conte, A. Feki, L. Chiaraviglio, D. Ciullo, M. Meo, and M. A. Marsan, "Cell wilting and blossoming for energy efficiency," *IEEE Wireless Commun.*, vol. 18, no. 5, pp. 50–57, Oct. 2011.

[21] M. Marcus and B. Pattan, "Millimeter wave propagation; spectrum management implications," *IEEE Microw. Mag.*, vol. 6, no. 2, pp. 54–62, Jun. 2005.

[22] T. S. Rappaport, Y. Xing, G. R. MacCartney, A. F. Molisch, E. Mellios, and J. Zhang, "Overview of millimeter wave communications for fifth-generation (5g) wireless networks x2014;with a focus on propagation models," *IEEE Trans. Antennas Propag.*, vol. 65, no. 12, pp. 6213–6230, Dec. 2017.

[23] M. Xiao, S. Mumtaz, Y. Huang, L. Dai, Y. Li, M. Matthaiou, G. K. Karagiannidis, E. Björnson, K. Yang, C. L. I, and A. Ghosh, "Millimeter wave communications for future mobile networks," *IEEE J. Sel. Areas Commun.*, vol. 35, no. 9, pp. 1909–1935, Sep. 2017.

[24] T. S. Rappaport, S. Sun, R. May.zus, H. Zhao, Y. Azar, K. Wang, G. N. Wong, J. K. Schulz, M. Samimi, and F. Gutierrez, "Millimeter wave mobile communications for 5g cellular: It will work!" *IEEE Access*, vol. 1, pp. 335–349, 2013.

[25] R. C. Daniels, J. N. Murdock, T. S. Rappaport, and R. W. Heath, "60 ghz wireless: Up close and personal," *IEEE Microw. Mag.*, vol. 11, no. 7, pp. 44–50, Dec. 2010.

[26] T. S. Rappaport, J. N. Murdock, and F. Gutierrez, "State of the art in 60-ghz integrated circuits and systems for wireless communications," *Proc. IEEE*, vol. 99, no. 8, pp. 1390–1436, Aug. 2011.

[27] C. H. Doan, S. Emami, D. A. Sobel, A. M. Niknejad, and R. W. Brodersen, "Design considerations for 60 ghz cmos radios," *IEEE Commun. Mag.*, vol. 42, no. 12, pp. 132–140, Dec. 2004.

[28] S. Rangan, T. S. Rappaport, and E. Erkip, "Millimeter-wave cellular wireless networks: Potentials and challenges," *Proc. IEEE*, vol. 102, no. 3, pp. 366–385, Mar. 2014.

[29] F. 15-1166, "Federal communications commission," Oct. 2015.

[30] S.-K. Y. *et. al.*, *60 GHz Technology for Gbps WLAN and WPAN: From Theory to Practice*. http://goo.gl/aqkPI: Wiley, 2010.

[31] A. H. Nuttall, *Millimeter-Wave Radius in Backaul Networks*. Communication Infrastructure Corporation, 2008.

[32] A. Mesodiakaki, A. Kassler, E. Zola, M. Ferndahl, and T. Cai, "Energy efficient line-of-sight millimeter wave small cell backhaul: 60, 70, 80 or 140 ghz?" in *2016 IEEE 17th International Symposium on A World of Wireless, Mobile and Multimedia Networks (WoWMoM)*, Jun. 2016, pp. 1–9.

[33] V. N. Ha and L. B. Le, "Distributed base station association and power control for heterogeneous cellular networks," *IEEE Trans. Veh. Technol.*, vol. 63, no. 1, pp. 282–296, Jan. 2014.

[34] J. T. Wang, "Sinr feedback-based integrated base-station assignment, diversity, and power control for wireless networks," *IEEE Trans. Veh. Technol.*, vol. 59, no. 1, pp. 473–484, Jan. 2010.

[35] S. N. S. Kshatriya, S. R. Yerrapareddy, N. Akhtar, and J. K. Milleth, "A novel power control scheme for macro-pico heterogeneous networks with biased association," in *Proc. IEEE ICC,*, Jun. 2013, pp. 1117–1122.

[36] S. Wang and Y. Sun, "Enhancing performance of heterogeneous cloud radio access networks with efficient user association," in *Proc. IEEE ICC,*, May 2017, pp. 1–6.

[37] L. P. Qian, Y. J. A. Zhang, Y. Wu, and J. Chen, "Joint base station association and power control via benders' decomposition," *IEEE Trans. Wireless Commun.*, vol. 12, no. 4, pp. 1651–1665, Apr. 2013.

[38] M. Wang, H. Gao, and T. Lv, "Energy-efficient user association and power control in the heterogeneous network," *IEEE Access*, vol. 5, pp. 5059–5068, 2017.

[39] L. Xu, G. Yu, and Y. Jiang, "Energy-efficient resource allocation in single-cell ofdma systems: Multi-objective approach," *IEEE Trans. Wireless Commun.*, vol. 14, no. 10, pp. 5848–5858, Oct. 2015.

[40] T. Zhou, Y. Huang, and L. Yang, "Energy-efficient user association in downlink heterogeneous cellular networks," *IET Communications*, vol. 10, no. 13, pp. 1553–1561, Sep. 2016.

[41] M. Hong and Z. Q. Luo, "Distributed linear precoder optimization and base station selection for an uplink heterogeneous network," *IEEE Transactions on Signal Processing*, vol. 61, no. 12, pp. 3214–3228, Jun. 2013.

[42] S. He, Y. Huang, S. Jin, and L. Yang, "Coordinated beamforming for energy efficient transmission in multicell multiuser systems," *IEEE Trans. Commun.*, vol. 61, no. 12, pp. 4961–4971, Dec. 2013.

[43] K. Shen and W. Yu, "Distributed pricing-based user association for downlink heterogeneous cellular networks," *IEEE J. Sel. Areas Commun.*, vol. 32, no. 6, pp. 1100–1113, Jun. 2014.

[44] K. Son, H. Kim, Y. Yi, and B. Krishnamachari, "Base station operation and user association mechanisms for energy-delay tradeoffs in green cellular networks," *IEEE J. Sel. Areas Commun.*, vol. 29, no. 8, pp. 1525–1536, Sep. 2011.

[45] A. Mesodiakaki, F. Adelantado, A. Antonopoulos, E. Kartsakli, L. Alonso, and C. Verikoukis, "Energy impact of outdoor small cell backhaul in green heterogeneous networks," in *2014 IEEE 19th International Workshop on Computer Aided Modeling and Design of Communication Links and Networks (CAMAD)*, Dec. 2014, pp. 11–15.

[46] S. Tombaz, P. Monti, F. Farias, M. Fiorani, L. Wosinska, and J. Zander, "Is backhaul becoming a bottleneck for green wireless access networks?" in *Proc. IEEE ICC,*, Jun. 2014, pp. 4029–4035.

[47] A. Mesodiakaki, F. Adelantado, L. Alonso, M. D. Renzo, and C. Verikoukis, "Energy- and spectrum-efficient user association in millimeter-wave backhaul small-cell networks," *IEEE Trans. Veh. Technol.*, vol. 66, no. 2, pp. 1810–1821, Feb. 2017.

[48] E. Zola, A. J. Kassler, and W. Kim, "Joint user association and energy aware routing for green small cell mmwave backhaul networks," in *2017 IEEE Wireless Communications and Networking Conference (WCNC)*, Mar. 2017, pp. 1–6.

Chapter 3

Energy Efficient Joint Power and Flow Control in Millimeter Wave Backhaul Heterogeneous Networks

3.1 Abstract

In this chapter*, a variable-demand rate energy efficient joint power allocation and backhaul links flow assignment algorithm in a millimeter wave backhaul heterogeneous network is proposed. Most EE algorithms in cellular networks consider satisfying the fixed-demand rates (i.e. minimum rate that guarantees users quality-of-service (QoS)) of users. While such formulations have the advantage of simplifying the resulting optimization problem (mostly a convex optimization problem as will be shown later in this chapter), their EE gains might not always be the best. This is because the original EE optimization problem translates to a convex power minimization problem for

*The work in this chapter has been presented in "Sylvester B. Aboagye, Ahmed Ibrahim and Telex M. N. Ngatched, "Energy efficient power and flow control in millimeter wave backhaul heterogeneous networks," submitted for presentation at *IEEE Global Telecommunications Conference (GLOBECOM 2018), Dec. 2018*"

the given fixed users demands (as shown in joint EE power and flow control (JEEPF) formulation). However, wireless devices often support multiple data rates so why not increase data rates for users with good channel conditions, which in effect will increase the total throughput that can be carried by the network. Specifically, users can receive higher throughput than what they demanded depending on the channel condition of their link but never receive throughput that violates users QoS. It is shown in this chapter how this little change (fixed-demand rate to variable-demand rate) causes a drastic difference in the EE problem formulation, leading to a non-convex joint EE, power allocation, flow control and throughput (JEEPFT) optimization problem. Using the relationship between fractional and parameteric programming, the original non-convex JEEPFT problem is reformulated into a quasiconvex optimization problem for which a bisection method based approach is proposed. Our simulation results show the superiority of JEEPFT over the JEEPF and other simple benchmark schemes.

Index Terms–Energy efficiency; throughput demand; heterogeneous networks; mmWave communication; quasiconvex.

3.2 Introduction

The exponential growth in mobile data traffic is a well established fact, and this groundbreaking trend is expected to continue in the years to come. Future cellular networks should be able to support this galloping demand for data traffic since the performance of current Third Generation Partnership Project (3GPP) Long Term Evolution (LTE) and LTE-Advanced standards do not meet the requirements of 5G. Energy efficiency (EE) has been identified as one of the critical and urgent design

issues in future networks. The proper allocation of the various network resources, in terms of power control in the AN and BH links as well as flow assignment in the BH network, is paramount to improving the EE of wireless networks. Especially, when multi-hop relaying in multi-routes mmWave BH networks cannot be avoided due to the use of highly directional beams and the high pathloss that mmWave signals suffer. Generally, these different network resources (power, flow and throughput) are coupled together such that optimizing them separately may not lead to the optimal solution.

Most power control schemes are effectively designed to satisfy the minimum throughput demands (fixed-demand rates) of UEs. Thus, for each UE's channel condition, the minimum power required to guarantee the throughput demand is allocated to the UE. If a channel is subjected to fading, its capacity will vary with the changes in the propagation medium. Particularly, it is correct to say that the channel capacity "inherits" the stochastic properties of the fading processes. Adapting to the channel condition of UEs allows the channel to be used more efficiently since the transmit power and rate of UEs can be allocated to make use of favorable channel conditions. Some UEs in the network can enjoy higher rates than the throughput demanded as long as their channel conditions can support higher transmit rates at "reasonable" transmit power. Nonetheless, very few studies have proposed power control schemes that support variable transmission rates in an energy efficient manner. The use of adaptive techniques have been investigated for capacity maximization over Rayleigh fading channels [1], in high-speed modems [2], satellite links [3] and for combined power control and transmission rate selection in wireless networks [4] [5].

EE maximization in HetNets has been separately studied for the access network (AN) [6] [7] [8] and BH [9] [10] [11] [12], and both [13] [14] [15]. However, none of the aforementioned approaches (i) takes EE as the objective function but rather minimizes power consumption, and (ii) considers an EE maximization algorithm that

jointly assigns optimal flows on BH links, minimizes power consumption in the AN and BH, and maximizes AN throughput. Also, most authors assume a single BH link connection between BSs, making the BH network less resilient to link failures and channel fading effects.

This chapter of the dissertation presents a novel approach relative to the above mentioned adaptive techniques in that, the demand rates (transmission rates) and the required transmit power of UEs as well as BH links power allocation and flow control are jointly optimized to maximize the overall network EE, while satisfying the AN and BH network power constraints as well as the capacity constraints of BH links.

In this chapter, we present a fixed-demand rate EE maximization optimization technique and a variable-demand rate EE maximization optimization technique for a mmWave BH two-tier HetNet. Specifically, the contributions of this chapter are summarized as follows:

1. We consider a two-tier (i.e., macro base station (MBS) and pico base station (PBS)) HetNet with multiple mmWave line-of-sight (LOS) BH links, and present two EE maximization optimization frameworks:

    - Joint EE, power, and flow control (JEEPF): For a given strict UEs' throughput demands, we jointly determine the optimal power allocation and assign network flows on the multiple BH links. This is formulated as a convex optimization problem that can be solved to optimality.
    - Joint EE, power, flow control, and throughput (JEEPFT): Given the lower and upper bound of UE throughput demands, we formulate a problem that jointly maximizes UE demands, determines the optimal power allocation, and assigns flows on the BH links. We show that this is a non-linear, sum-of-ratio programming problem which can be reformulated as a quasiconvex

optimization problem. We propose an algorithm based on the bisection method for solving the quasiconvex problem.

2. Simulation results show that JEEPFT outperforms JEEPF and non-optimal benchmark schemes.

The rest of the chapter is organized as follows. We describe our system model in Section 3.3. In Section 3.4, we introduce the problem formulation, present the solution approach in Section 3.5 and develop the algorithms in Section 3.6. Section 3.7 presents the simulation results. Finally, Section 3.8 gives some useful insights and concludes the chapter.

3.3 System Model

3.3.1 Network Deployment

We consider the downlink of a two-tier orthogonal frequency-division multiple access (OFDMA) network composed of a set of N BSs, represented by BS_n where $n \in \{0, 1, ..., N-1\}$ and 0 is the MBS (source node) index as was shown in Figure 2.3. The $N-1$ PBSs act as destination and/or relay nodes. We assume that the destination nodes are labelled $d = 1, 2, \ldots, D$, where $N - 1 = D$. The PBSs are organized into clusters, each with a cluster head. We make the assumption that the MBS and PBSs operate on a different carrier frequency, with the channel bandwidth F_m for MBS and F_s for each PBS, and by that avoid any cross–tier interference. These resource blocks are subdivided into downlink OFDMA sub-channels. The PBSs in each cluster reuse the same sub-channels. In order to avoid co-tier interference among the PBSs, the coverage area of PBSs do not overlap. Again, we assume that neighboring MBSs are located far away from each other such that inter-cell interference is avoided. The z_s

sub-channels from the F_s resource block and k_m sub-channels from the F_m resource block are represented by the set $z = \{1, 2, ..., z_s\}$ and $k = \{1, 2, ..., k_m\}$, respectively. The bandwidth of each MBS sub-channel is $\Delta B^m = \frac{F_m}{k_m}$ and that of a PBS is $\Delta B^s = \frac{F_s}{z_s}$. We assume that the total available maximum transmit power (MTP) of each BS is equally distributed to all of its sub-channels.

The network serves a total of J UEs represented by the set $\mathcal{UE} = \{1, 2, ..., J\}$. We use j to represent the index of $\mathcal{UE}$. We assume that each UE has already been associated to exactly one BS and is allocated enough sub-channels. We let $\mathcal{U}_0$ and $\mathcal{U}_d$ represent the set of UEs associated with the MBS and PBS d, respectively. For the J UEs in the network, $\mathcal{UE} = \left[\bigcup_{d=1}^{D} \mathcal{U}_d\right] \cup \mathcal{U}_0$. Each UE has a throughput demand that needs to be satisfied. We label the demand of a UE $j \in \mathcal{U}_0$ as y_j and that of UE $j \in \mathcal{U}_d$ as $y_j^{(d)}$. For each PBS d, we define a source-sink vector $\mathbf{s^{(d)}} \in \mathbb{R}^{N-1}$, whose nth ($n \neq d$) entry $s_n^{(d)}$ represents the non-negative amount of flow into the network at the MBS and destined for PBS d. Since we consider a single source node (i.e. MBS), $s_n^{(d)} = 0, \forall n \neq 0$. According to the flow conservation law, the sink flow at PBS d can be given by $s_d^{(d)} = -s_0^{(d)}$. From the throughput demands of UEs associated with PBS d, we can calculate the total demand at PBS d as $s_d^{(d)} = \sum_{j \in \mathcal{U}_d} y_j^{(d)}$. The total demand for UEs associated with the MBS is given as $s_0 = \sum_{j \in \mathcal{U}_0} y_j$.

$$
\begin{aligned}
y_j^{(d)} &= \Delta B^s \log_2 \left(1 + \frac{\left|h_j^d\right|^2 P_j^{(d)}}{\sigma^2}\right), \ \forall j \in \mathcal{U}_d, \\
y_j &= \Delta B^m \log_2 \left(1 + \frac{|h_j|^2 P_j}{\sigma^2}\right), \ \forall j \in \mathcal{U}_0.
\end{aligned}
\tag{3.1}
$$

In (3.1), $P_j^{(d)}$ is the transmit power of PBS d to UE $j \in \mathcal{U}_d$ and P_j is the transmit power of the MBS to UE $j \in \mathcal{U}_0$. $\left|h_j^d\right|^2$ and $|h_j|^2$ represent the magnitude of the channel gain for UE $j \in \mathcal{U}_d$ and UE $j \in \mathcal{U}_0$, respectively. σ^2 is the variance of the additive white Gaussian noise channel (AWGN).

3.3.2 Flow Constraint

For the directed BH links labelled $l = 1, 2, ..., L$, we define a *node-link incidence* matrix $A \in \mathbb{R}^{N \times L}$ whose entry A_{nl} is associated with node n and link l via

$$A_{nl} = \begin{cases} 1, & \text{if } n \text{ is the start node of link } l \\ -1, & \text{if } n \text{ is the end node of link } l \\ 0, & \text{otherwise.} \end{cases} \tag{3.2}$$

Let $O(n)$ represents the set of outgoing links from node n and $I(n)$ represents the set of incoming links to node n. On each link l, we let $x_l^{(d)} \geq 0$ represents the amount of flow destined for PBS d. $\mathbf{x^{(d)}} \in \mathbb{R}^L$ denotes the flow vector for PBS d. The flow conservation law required at each node n is expressed as

$$\sum_{l \in O(n)} x_l^{(d)} - \sum_{l \in I(n)} x_l^{(d)} = \begin{cases} s_0^{(d)}, n = 0 \\ 0, \forall n \neq 0 \\ -s_n^{(d)}, n = d \end{cases} \tag{3.3}$$

and can be written in matrix-vector form as

$$A\mathbf{x^{(d)}} = \mathbf{s^{(d)}}, \ d = 1, 2, ..., D. \tag{3.4}$$

Due to the capacity constraint on each BH link l, the total amount of traffic flow on link l, denoted as t_l, should be below the link's capacity, c_l, that is

$$t_l = \sum_d x_l^{(d)} \leq c_l. \tag{3.5}$$

3.3.3 mmWave BH link channel model

We consider a mmWave LOS multiple BH links among the PBSs and a single BH link between the cluster head and the MBS. Without loss of generality, we assume that the MBS is connected to the CN via a fiber connection. Each PBS connects to the MBS through the cluster head either directly or through one or more PBS aggregation points. Two mmWave subband frequencies are used in our BH network. We use the 73 GHz (E band) for PBS-MBS single BH links, and 60 GHz (V band) for multiple BH links among the PBSs. The path attenuation suffered by mmWave signals can be categorized into two components: free space path loss ($FSPL_{(dB)}$) and mmWave propagation loss factors ($PL_{(dB)}$). These are given as [16]

$$\begin{aligned} FSPL_{(dB)} &= 92.4 + 20\log_{10}\left(f_{(GHz)}\right) + 20\log_{10}\left(d_{(km)}\right), \\ PL_{d(dB)} &= d_{(km)}\left(\underbrace{L_{vap} + L_{O_2}}_{atmospheric\,gas} + L_R\right)_{(dB/km)}, \end{aligned} \tag{3.6}$$

where d is LOS separation distance in km between the transmitter and receiver, and f is the frequency in GHz. L_{vap}, L_{O_2}, and L_R represent the attenuation in dB/km due to water vapour, oxygen, and rain, respectively. The total path loss (TPL) can be expressed as

$$TPL_{(dB)} = FSPL_{(dB)} + PL_{d(dB)}. \tag{3.7}$$

3.3.4 BH Power Consumption Model

From the literature, there is no standardized power consumption model for mmWave communication. Nevertheless, the use of the linear approximation model for power consumption in mmWave communication networks has received much attention [14] [17]. We focus only on the dynamic power consumption, P_l, which on BH link l is

modelled as

$$P_l = P^{BH}_{\max_l} \frac{t_l}{c_l},\ 0 \leq P_l \leq P^{BH}_{\max_l}, \tag{3.8}$$

where $P^{BH}_{\max_l}$ is the MTP on BH link l. $P^{BH}_{\max_l}$ is calculated as

$$P^{BH}_{\max_l(dBm)} = EIRP_{\max(dBm)} + T_{xloss(dB)} - G_{Tx(dBi)}, \tag{3.9}$$

where $EIRP_{\max(dBm)}$ is the maximum equivalent isotropically radiated power, $T_{xloss(dB)}$ is the transmitter loss, and $G_{Tx(dBi)}$ is the gain of the transmitter. For the chosen mmWave frequency subbands, EIRP is given as [18],

$$\begin{aligned} \text{V band} &: EIRP_{\max(dBM)} = 85_{(dBm)} - 2 \cdot x_{(dB)}, \\ E \text{ band} &: EIRP_{\max(dBM)} = 85_{(dBm)} - 2 \cdot y_{(dB)}, \end{aligned} \tag{3.10}$$

where x is the number of dB that G_{Tx} is less than 51 dBi and y is the number of dB that G_{Tx} is less than 50 dBi. The signal-to-noise power ratio at the receiving end of BH link l $\left(SNR^{BH}_{l(dB)}\right)$ is given as

$$\begin{aligned} SNR^{BH}_{l(dB)} = P_{l(dBm)} - N_{th(dBm)} - NF_{(dB)} - T_{xloss(dB)} \\ -R_{xloss(dB)} + G_{Rx(dBi)} - L_{\text{margin}} - TPL_{(dB)} \end{aligned}, \tag{3.11}$$

where N_{th} is the thermal noise and NF is the noise figure. The parameters $R_{xloss(dB)}$, G_{Rx}, and L_{margin} represent the receiver loss, receiver antenna gain and link margin, respectively.

3.4 Problem Formulation

The solution of the problem under study maximizes network EE while jointly optimizing power consumption in both AN and BH network, BH links flow control and UEs throughput demand. The EE (unit : bits/Joule) is defined as the ratio of total network throughput to the total power consumed in both the AN and the BH network. Mathematically,

$$EE = \frac{f_1(\mathbf{y},\mathbf{t},\mathbf{p})}{f_2(\mathbf{y},\mathbf{t},\mathbf{p})} = \frac{\sum\limits_{j\in\mathcal{U}_d} y_j^{(d)} + \sum\limits_{j\in\mathcal{U}_0} y_j}{\sum\limits_{\forall d}\sum\limits_{j\in\mathcal{U}_d} \underbrace{\frac{\left(2^{\frac{y_j^{(d)}}{\Delta B^s}}-1\right)\sigma^2}{\left|h_j^{(d)}\right|^2}}_{P_j^d} + \sum\limits_{j\in\mathcal{U}_0} \underbrace{\frac{\left(2^{\frac{y_j}{\Delta B^m}}-1\right)\sigma^2}{\left|h_j\right|^2}}_{P_j} + \sum\limits_{l\in O(n)} \underbrace{P^{BH}_{\max_l}\frac{t_l}{c_l}}_{P_l}}. \tag{3.12}$$

3.4.1 Fixed-Rate Joint Energy Efficiency, Power, and Flow Control Optimization

We consider a system in which each UE has a strict throughput demand $\left(y_j^{(d)} \text{ or } y_j\right)$ that must be met. Mathematically, the JEEPF maximization problem can be formulated as a joint optimization over the BH power and flow control variables as in (3.13). Since BH power, P_l, is dependent on the BH flow $\left(\text{i.e. } P_l = P^{BH}_{\max_l}\frac{t_l}{c_l}\right)$, optimizing t_l also

optimizes P_l.

$$\begin{aligned}
&\max_{\mathbf{t}} \ EE \\
&\text{s.t} \\
&C1 : \mathbf{Ax^{(d)}} = \mathbf{s^{(d)}}, \ d = 1, 2, ..., D \\
&C2 : t_l = \sum_d x_l^{(d)}, \ l = 1, 2, ..., L \\
&C3 : t_l \leq c_l, \ l = 1, 2, ..., L \\
&C4 : P_l \leq P_{\max_l}^{BH}, \ l = 1, 2, ..., L \\
&C5 : \mathbf{x^{(d)}} \succeq 0, \ d = 1, 2, ..., D.
\end{aligned} \tag{3.13}$$

For the fixed UE throughput demands, the EE maximization is equivalent to the power minimization problem

$$\begin{aligned}
&\min_{\mathbf{t}} \ f_2(\mathbf{t}) \\
&\text{s.t} \\
&C1 \sim C5.
\end{aligned} \tag{3.14}$$

The problem in (3.14) is of the same form as problem (7) by Lin Xiao *et. al.* [19], and can be solved by exploiting the problem structure via dual-decomposition method.

3.4.2 Variable-Rate Joint Energy Efficiency, Power, and Flow Control Optimization

We consider a system in which the throughput demand for each UE falls within a range. We represent the lower and upper bound of this range as $y_{\min}$ and $y_{\max}$, i.e. $y_{\min} \leq \left(y_j^{(d)}, y_j\right) \leq y_{\max}, \forall j \in \mathcal{UE}$. Thus, there is the freedom of providing higher possible throughput to some UEs while guaranteeing minimum for all depending on channel conditions. Adapting the throughput of UEs to signal fading allows the channel to be used more efficiently since power and rate can be allocated to exploit favorable channel conditions. This is expected to improve the network EE as the

results will confirm. The JEEPFT problem for the variable-rate joint EE, power, and flow control can be formulated as

$$
\begin{aligned}
&\max_{\mathbf{t},\mathbf{y},\mathbf{p}} EE \\
&\text{s.t} \\
&C1: s_d^{(d)} = \sum_{j \in U_d} y_j^{(d)}, \quad d = 1, 2, ..., D \\
&C2: \mathbf{A}\mathbf{x}^{(\mathbf{d})} = \mathbf{s}^{(\mathbf{d})}, \ d = 1, 2, ..., D \\
&C3: t_l = \sum_d x_l^{(d)}, \ l = 1, 2, ..., L \\
&C4: t_l \leq c_l, \ l = 1, 2, ..., L \\
&C5: \sum_{\forall d} \sum_{j \in U_d} \frac{\left(2^{\frac{y_j^{(d)}}{\Delta B^s}} - 1\right)\sigma^2}{\left|h_j^{(d)}\right|^2} + \sum_{l \in O(d)} P^{BH}_{\max_l} \frac{t_l}{c_l} \leq P^{(d)}_{max}, \forall d \\
&C6: \sum_{j \in U_0} \frac{\left(2^{\frac{y_j}{\Delta B^m}} - 1\right)\sigma^2}{|h_j|^2} + \sum_{l \in O(0)} P^{BH}_{\max_l} \frac{t_l}{c_l} \leq P^{0}_{max}, \\
&C7: \mathbf{x}^{(\mathbf{d})} \succeq 0, \ \mathbf{s}^{(\mathbf{d})} \succeq 0, \ d = 1, 2, ..., D \\
&C8: y_j^{(d)} \leq y_{\max}, \ y_j \leq y_{\max}, \\
&C9: y_j^{(d)} \geq y_{\min}, \ y_j \geq y_{\min},
\end{aligned}
\tag{3.15}
$$

where $C5$ and $C6$ are the MTP constraint for the PBSs and MBS, respectively. We can observe that (3.15) has a non-linear, fractional objective function and hence can be classified as a non-convex optimization problem which is generally difficult to solve. To get the global optimal solution, we exploit the relationship between fractional programming and parametric programming to reformulate (3.15) into a quasiconvex optimization problem. An iterative algorithm, that uses the bisection method, is then proposed to obtain the optimal solution.

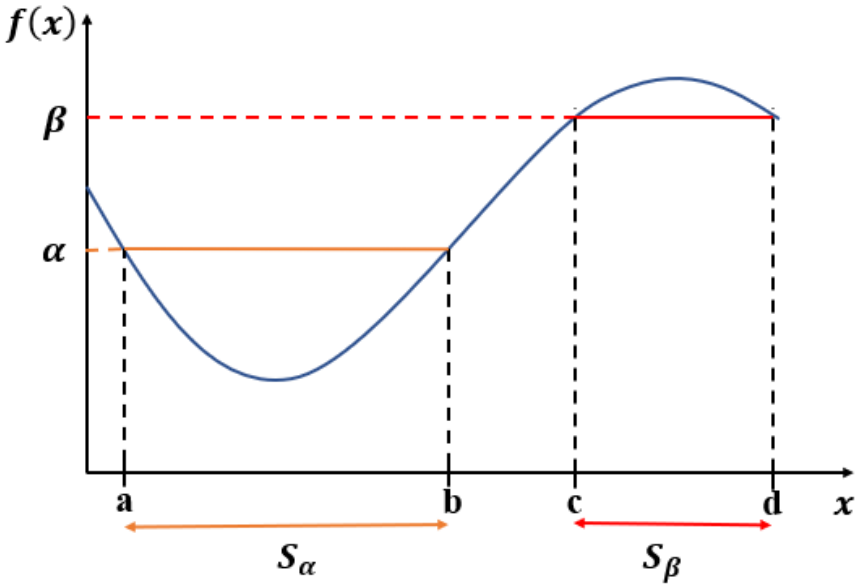

Figure 3.1: A quasiconvex function $f(x)$. For each α, the α–sublevel sets S_α are convex within the interval $[a, b]$. However, this quasiconvex function is not convex. This is because the line segment within the interval $[c, d]$ lies below the function $f(x)$.

3.5 The Quasiconvex Optimization

In this section, the problem formulation in (3.15) is shown to be a quasiconvex optimization problem.

Definition 1. *A function $f : \mathbb{R}^n \to \mathbb{R}$ is called quasiconvex if its domain and all its sublevel sets*

$$S_\alpha = \{x \in \text{dom } f | f(x) \leq \alpha\}, \tag{3.16}$$

for all $\alpha \in \mathbb{R}$, are convex [20]. Convex functions have convex sublevel sets, and hence are also quasiconvex. But the converse is not necessarily true, as illustrated in Figure 3.1. As shown in Figure 3.1, the β–sublevel sets S_β indicates the non-convexity of the function $f(x)$.

By defining η as an EE parameter, (3.15) can be written as

$$\begin{aligned} &\max_{\mathbf{t},\mathbf{y},\mathbf{p}} \ EE = \max_{\mathbf{t},\mathbf{y},\mathbf{p}} \ \frac{f_1(\mathbf{y},\mathbf{t},\mathbf{p})}{f_2(\mathbf{y},\mathbf{t},\mathbf{p})} = \eta \\ &\text{s.t} \\ &C1 \sim C9. \end{aligned} \tag{3.17}$$

Considering the constraints on UEs' throughput demands, the following inequalities are easily obtained

$$\begin{cases} Jy_{\min} \leq f_1(y,t,p) \leq Jy_{\max} \\ \left(0 + \sum\limits_{\forall j} P_j^{\min}\right) \leq f_2(y,t,p) \leq \left(\sum\limits_{\forall l} P_{\max_l}^{BH} + \sum\limits_{\forall j} P_j^{\max}\right) \end{cases}, \tag{3.18}$$

where $P_j^{\min}$ and $P_j^{\max}$ correspond to the transmit power to guarantee $y_{\min}$ and $y_{\max}$, respectively. By employing (3.18), we obtain bounds on η as

$$\frac{Jy_{\min}}{\left(\sum\limits_{\forall l} P_{\max_l}^{BH} + \sum\limits_{\forall j} P_j^{\max}\right)} \leq \eta \leq \frac{Jy_{\max}}{\left(0 + \sum\limits_{\forall j} P_j^{\min}\right)}. \tag{3.19}$$

The maximization of EE is equivalent to minimizing the inverse of EE ($\overline{EE} = \frac{f_2(\mathbf{y},\mathbf{t},\mathbf{p})}{f_1(\mathbf{y},\mathbf{t},\mathbf{p})}$) as

$$\begin{aligned} &\min_{\mathbf{t},\mathbf{y},\mathbf{p}} \ \overline{EE} \\ &\text{s.t.} \\ &C1 \sim C9. \end{aligned} \tag{3.20}$$

It can be observed from (3.20) that $\overline{EE}$ is the ratio of a convex function and an affine function. Furthermore, the inequality constraint functions are all convex while the equality constraint functions are affine. As shown in [19, Sec. 3.4.5], any function of the form $f(x) = \frac{p(x)}{q(x)}$, where p is a convex function and q is a concave function,

with $p(x) \geq 0$ and $q(x) > 0$, on a convex set C, is a quasiconvex function. Hence, the minimization problem in (3.20) is a quasiconvex optimization problem whose global optimum can be achieved by solving a sequence of convex feasibility problems.

Theorem 1. *Any function that conforms to the general form in (3.20) is a quasiconvex function.*

Proof. We denote α as $\overline{EE}$ parameter, and represent its lower bound, l_b, and upper bound, u_b, as

$$\frac{\left(0 + \sum\limits_{\forall j} P_j^{\min}\right)}{Jy_{\max}} \leq \alpha \leq \frac{\left(\sum\limits_{\forall l} P_{\max_l}^{BH} + \sum\limits_{\forall j} P_j^{\max}\right)}{Jy_{\min}} \tag{3.21}$$

For any α, the α-sublevel set of $\overline{EE}$ is

$$\begin{aligned} S_\alpha &= \left\{(y,t,p) \,\middle|\, \tfrac{f_2(y,t,p)}{f_1(y,t,p)} \leq \alpha, y \geq 0, t \geq 0, p \geq 0\ .\right\} \\ &= \{(y,t,p)\,|f_2(y,t,p) - \alpha f_1(y,t,p) \leq 0, f_1(y,t,p) > 0.\} \end{aligned} \tag{3.22}$$

$f_2(y,t,p)$ is a convex function, and $-\alpha f_1(y,t,p)$ is a linear function, and therefore, a convex function. The sum of these two convex functions, denoted as $\phi(y,t,p) = f_2(y,t,p) - \alpha f_1(y,t,p)$, is still a convex function. Any sublevel set of a convex function is a convex set. Hence, S_α is a convex set. This is due to the fact that, S_α is the intersection of two convex sets: the zero sublevel set of $\phi(y,t,p)$ and the half-space defined by $f_1(y,t,p) > 0$. Since $dom(f) = \{(y,t,p)\,|f_1(y,t,p) > 0\}$ and S_α are all convex, it can be concluded that $\frac{f_2(y,t,p)}{f_1(y,t,p)}$ is quasiconvex.

3.5.1 Solution via convex feasibility problems

The global optimum of a quasiconvex optimization problem can be computed via a sequence of convex feasibility problems. The quasiconvex optimization problem in

(3.20) is written as

$$\begin{aligned} &\min_{\mathbf{t},\mathbf{y},\mathbf{p}} \ \alpha \\ &\text{s.t} \\ &C1 \sim C9. \end{aligned} \tag{3.23}$$

For a fixed $\alpha = \widehat{\alpha}$, (3.23) reduces to a convex feasibility problem. Thus, the convex feasibility problem for (3.20) is

$$\begin{aligned} &\text{find} \ \ \mathbf{y}, \mathbf{t}, \mathbf{p} \\ &\text{s.t} \\ &f_2(\mathbf{y}, \mathbf{t}, \mathbf{p}) - \widehat{\alpha} f_1(\mathbf{y}, \mathbf{t}, \mathbf{p}) \leq 0 \\ &C1 \sim C9. \end{aligned} \tag{3.24}$$

Let α^* be the optimal value of problem (3.23). If (3.24) is feasible, then $\alpha^* \leq \widehat{\alpha}$, and any feasible point $(\mathbf{y}, \mathbf{t}, \mathbf{p})$ is feasible for the quasiconvex problem (3.23) and satisfies $\frac{f_2(\mathbf{y},\mathbf{t},\mathbf{p})}{f_1(\mathbf{y},\mathbf{t},\mathbf{p})} \leq \widehat{\alpha}$. On the contrary, we can conclude that $\alpha^* \geq \widehat{\alpha}$ if (3.24) is infeasible. Thus, we can determine if the optimal value α^* of (3.23) is less than or greater than any given value of α by solving (3.24).

3.6 Proposed JEEPFT Algorithm for the variable-rate EE optimization problem

Based on this idea, we propose an effective, iterative algorithm that solves the quasiconvex optimization problem (3.20) to global optimality. This algorithm uses the bisection method to find α by searching the one-dimensional range, $[l_b, u_b]$, known to contain α^*. In each iteration of the bisection method, we solve the feasibility problem (3.24). The algorithm is summarized in Algorithm 1.

Algorithm 1 JEEPFT optimization algorithm

Given $l_b \leq \alpha^* \leq u_b$, iteration index $i = 1$, and error tolerance $\varepsilon > 0$;
while $(u_b - l_b) > \varepsilon$ **do**
  Set $\widehat{\alpha}_{(i)} = \frac{1}{2}(l_b + u_b)$;
  Solve the feasibility problem (3.24);
  if (3.24) is feasible **then**
    Update $u_b = \widehat{\alpha}_{(i)}$;
  else
    Update $l_b = \widehat{\alpha}_{(i)}$;
  end if
  Update $i = i + 1$;
end while

3.7 Simulation Results and Discussion

In this section, we investigate the performance of JEEPF and JEEPFT through simulations using MATLAB, and compare them with equal power allocation (EPA) and random allocation (RA). In EPA, all BSs equally share their MTP to associated UEs and BH links and each UE and BH link utilizes all the power allocated to them. In order to ensure that the aggregate demand at each BS does not exceed the capacity of the available BH links, we perform model validation for $C1 \sim C5$ in (3.13). With no objective function, the RA algorithm searches for any $\mathbf{t}$, i.e. find $\mathbf{t}$, while satisfying $C1 \sim C5$ in (3.13).

In our simulation, we consider a HetNet with one MBS, three PBSs and four BH links as shown in Figure 3.2. The length of each BH link is between 150-200 m. We consider two UE distributions [21]:

1. *Hotspot (Hs) UEs*: UEs are randomly dropped within a coverage radius range of (5–20 m) for PBSs and (35-50 m) for MBSs.

2. *Random (Rn) UEs*: UEs are randomly distributed within the radius range of the MBS.

The channel gain considered in this chapter includes pathloss, log-normal shadow-

Table 3.1: Simulation parameters for AN

Parameter	**Value**
MBS carrier frequency	2 GHz
PBS carrier frequency	2.6 GHz
$\Delta B^m, \Delta B^s$	180 kHz
MBS MTP	46 dBm
PBS MTP	30 dBm
Distance-dependent path loss (dB)	MBS-UE $128.1 + 37.6\log_{10}(d_{km})$
	PBS-UE $140.7 + 36.7\log_{10}(d_{km})$
Penetration loss	20 dB
Shadowing effect	10 dB
N_{th}	-174 dBm/Hz

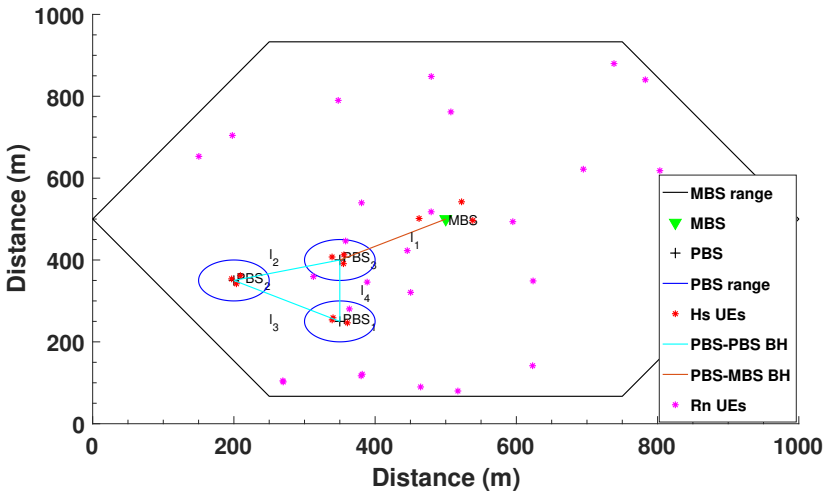

Figure 3.2: Network model simulation scenario.

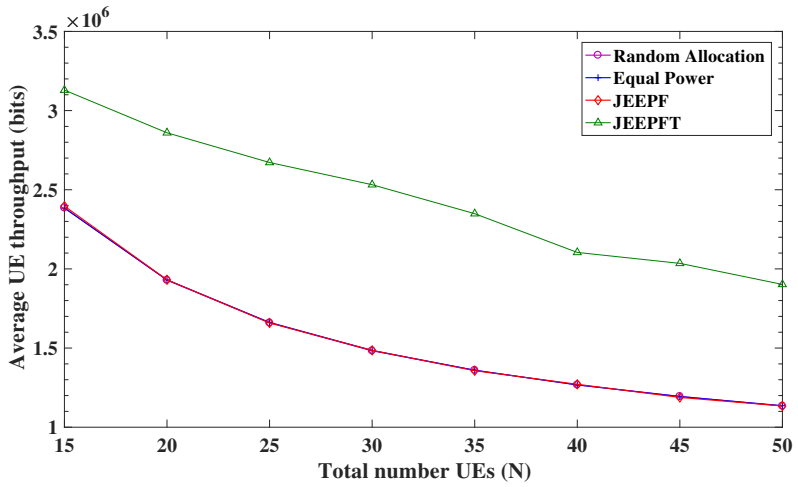

Figure 3.3: Average throughput per UE for different EE algorithms versus total number of UEs, N.

ing and multipath fading. The multipath fading is assumed to follow a Rayleigh distribution; the Rayleigh fading channel gains are modelled as independent and identically distributed unit mean, exponentially distributed random variables. The throughput demand of UEs vary between 0.5–4 Mbps. The bandwidth of each mmWave BH link is 3.5 GHz. We set $R_{xloss} = T_{xloss} = 5$ dB, $G_{TX} = G_{RX} =$ [V band : 36 dBi, E band : 43 dBi], $L_{margin} = 15$ dB and NF = [V band : 4.5 dB, E band : 6 dB]. The rest of the simulation parameters are summarized in Table 4.1. We provide results averaged over 1000 independent simulations. The performance indicators used for our analysis include network EE, average UE and total network throughput, and total network power consumption. Moreover, we also investigate how these indicators behave under different MTP settings.

Figure 3.3 compares the average UE throughput of JEEPF and JEEPFT with that of EPA and RA. It can be observed that the JEEPFT algorithm achieves significantly higher UE throughput than the remaining algorithms. This is because the JEEPFT algorithm has the flexibility of providing higher throughput demand to UEs that have favorable channel conditions. This throughput slightly decreases as N increases

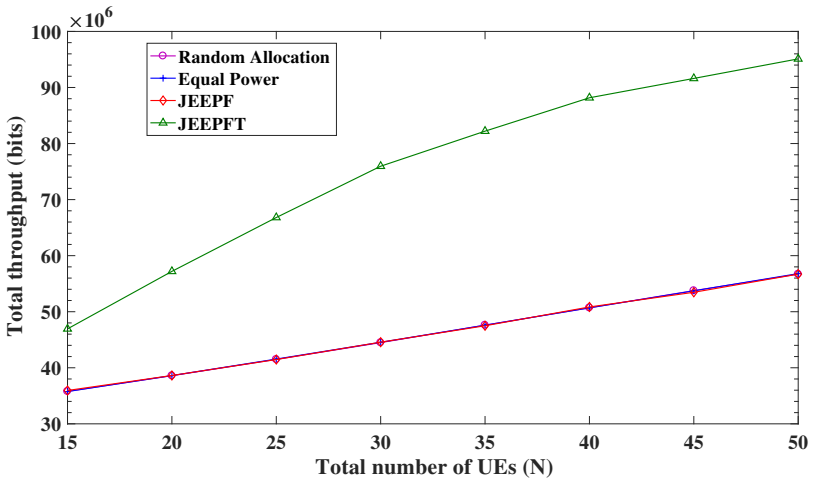

Figure 3.4: Average total throughput for different EE algorithms versus total number of UEs, N.

since the algorithm maximizes the achievable throughput of each UE. The average UE throughput is almost the same for the JEEPF, EPA, and RA algorithms, and it decays exponentially as N increases. This happens because the strict throughput demand of UEs decreases as N increases since the same MTP is shared equally among the UEs. As shown in Figure 3.4, the overall network throughput increases almost linearly as N gets bigger for the JEEPFT algorithm while the remaining three algorithms show little improvement with N for the same MTP. This is because the remaining three algorithms only satisfy the fixed-demand rates that ensure UE QoS requirements are satisfied.

Figure 3.5 compares BH links capacity and their average traffic (link utilization in %) for the RA, JEEPF, and JEEPFT algorithms. It is observed that the JEEPFT algorithm achieves the best load balancing and link utilization, and hence makes efficient use of BH link resources. Also, the high capacity of the BH links reduces the potential possibility of a BH link being a bottleneck to traffic flow to the CN.

Figure 3.6 depicts the average total power consumption for the different EE algorithms. EPA performs worst since each BS utilizes the MTP for both the AN and BH

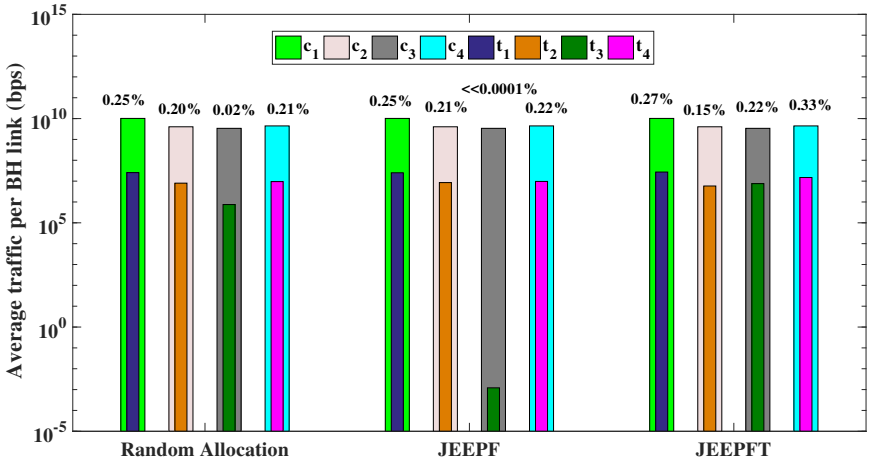

Figure 3.5: Average BH link utilization for different EE algorithms, N=50 UEs.

network. Little energy saving is achieved for the RA because it performs only flow control without maximizing or minimizing any objective function. The JEEPFT and JEEPF algorithms consume the least power, with the JEEPFT performing slightly better than the JEEPF. This is because, while the JEEPF algorithm only minimizes power and perform flow control, the JEEPFT algorithm jointly minimizes power, perform flow control and enjoys the freedom of maximizing UEs' throughput.

In Figure 3.7, we compare the average EE of the different algorithms for different N. It can be observed that the JEEPF and JEEPFT algorithms offer better EE than the RA and EPA algorithms. This is because the JEEPF and the JEEPFT algorithms perform optimal power allocation and flow control. Nevertheless, JEEPFT outperforms the JEEPF due to the difference in their objective function. The JEEPFT has its objective function as maximizing EE. In achieving that, it jointly optimizes UEs' throughput demands and power consumption in both the AN and the BH network. As illustrated by the JEEPFT curve, the weight of the network throughput gain on the EE exceeds that of the increment in power consumption for low N, resulting in a steeper rise in EE as N increases. But as N gets high, the EE remains steady as the

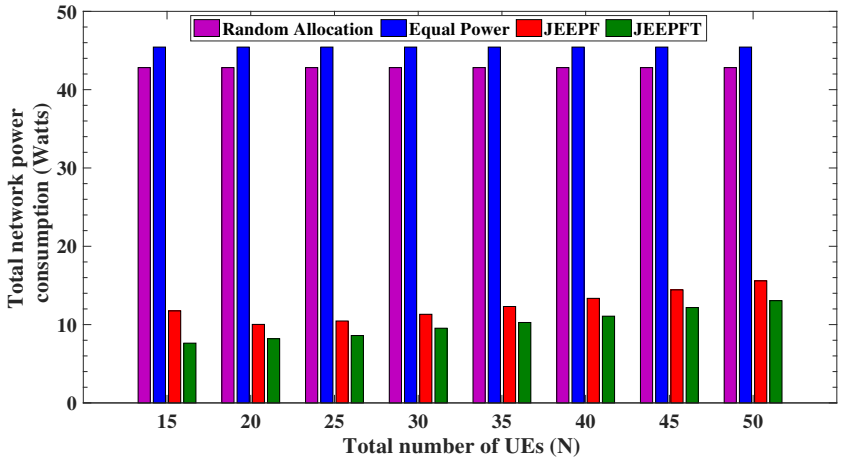

Figure 3.6: Average total network power consumption for different EE algorithms versus total number of UEs, N.

increase in throughput compensates for the rise in power consumption. As N continues to grow, the EE gradually declines as the network throughput gain cannot balance the large power consumption. But in the JEEPF, only the power consumption is optimized while satisfying the strict throughput demand of UEs. This shows that from the perspective of EE, it is better to jointly optimize UEs' throughput demand, power consumption, and flow control on BH links. Figure 3.8 illustrates the EE performance of the JEEPF and the JEEPFT algorithms for different rate constraints. As evident from the plot, better EE performance is attained for wider rate constraints. This is because the feasible range increases and offers the algorithm more freedom to jointly maximize UE throughput demands and minimize their power consumption. But as we lower the upper bound of the demand rate, the feasible region gets narrower, and the EE decreases. Further reducing the upper bound such that $y_{min} = y_{max} = C_{ue}$ (where C_{ue} is the strict UE demand that must be satisfied) leads to the result that both the JEEPF and the JEEPFT algorithms achieve the same EE. Thus, the JEEPFT algorithm with variable UE throughput demands performs better than the JEEPF with strict UE demand.

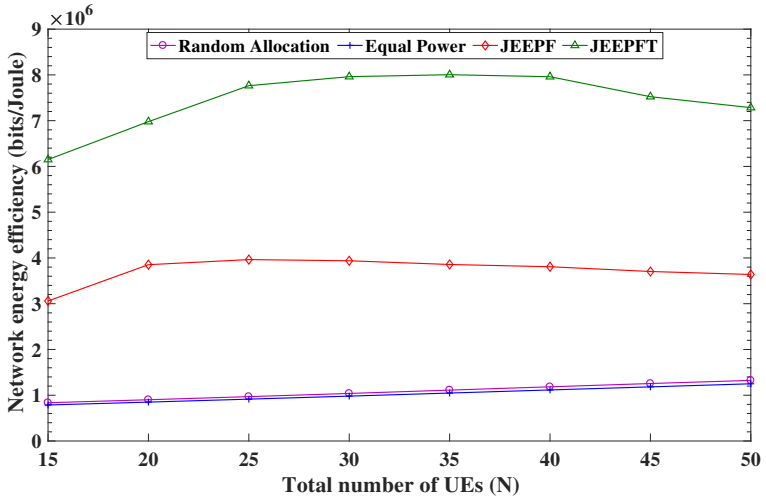

Figure 3.7: EE of different algorithms versus total number of UEs, N.

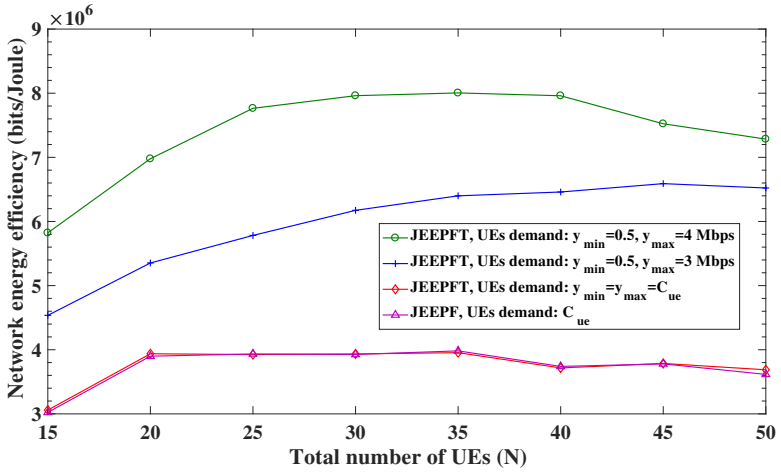

Figure 3.8: EE performance comparison for JEEPF and JEEPFT for different rate constraint.

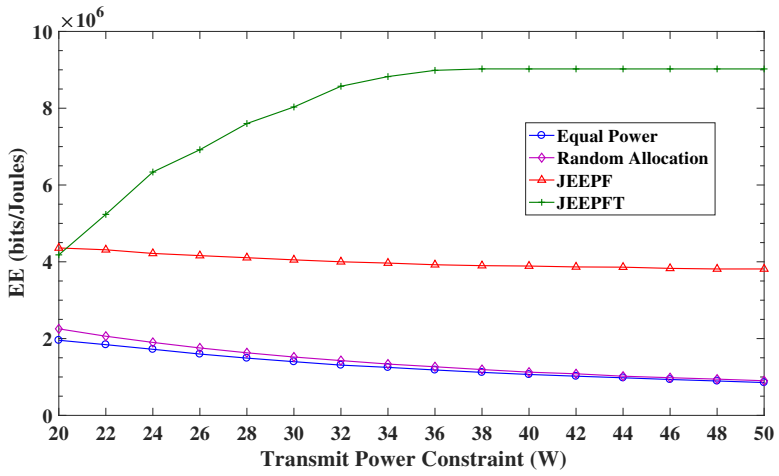

Figure 3.9: Impact of MTP settings on the EE algorithms.

Figure 3.9 shows that the JEEPFT algorithm makes better utilization of power resources than the remaining algorithms. EE grows with an increase in MTP until saturation where further increase in MTP does not affect the EE. Increasing the MTP for the EPA, the RA and the JEEPF does not yield any improvements in the EE. The performance of these algorithms slightly worsens.

We investigate the number of times out of the 1000 independent simulations that each algorithm successfully computes a solution. The metrics that we use are the possible values used to summarize the output of any result in CVX [22]. These metrics are briefly explained below:

1. *Solved*: solver was able to compute the optimal solution.

2. *Infeasible*: problem has been proven to be infeasible through the discovery of an unbounded direction.

3. *Other*: solver deemed the solution as inaccurate (i.e. solution is not within default numerical tolerance) or fails to make sufficient progress towards a solution, even to within a "relaxed" tolerance setting.

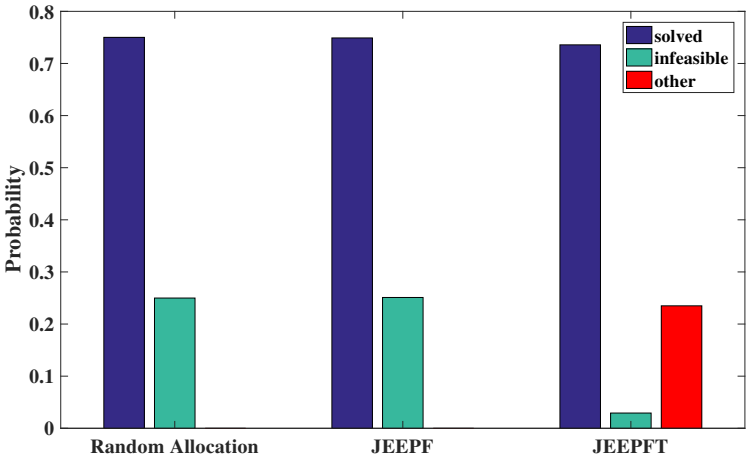

Figure 3.10: Probability of algorithm success.

As shown in Figure 3.10, all three algorithms have the same probability of solving the problem to optimality.

3.8 Conclusion

In this chapter, we investigated the EE maximization problem in mmWave BH HetNet with multiple BH link connections. We developed two EE maximization optimization frameworks: JEEPF and JEEPFT. The JEEPF reduces to a power minimization problem while the JEEPFT is an EE maximization problem. Thus, our JEEPFT formulation captures the joint effect of minimizing power consumption and maximizing UEs' demands on network EE. It was shown that the JEEPF can be formulated as an optimization problem that can be solved to optimality using a dual decomposition approach. We proposed an optimal joint energy-efficient, power allocation and flow control algorithm based on the bisection method for the JEEPFT. Simulation results showed that the proposed JEEPFT algorithm achieves better EE, throughput, power consumption, load balancing and also makes better utilization of power than the other algorithms that do not consider the joint effect of maximizing throughput and min-

imizing power consumption. More generally, we have shown through our work that allocating throughput demands to UEs from a range yields better EE than satisfying the strict demand of UEs. Work is currently underway to develop a low-complexity distributed algorithm for the implementation of the JEEPFT model.

Bibliography

[1] M. S. Alouini and A. J. Goldsmith, "Capacity of rayleigh fading channels under different adaptive transmission and diversity-combining techniques," *IEEE Trans. Veh. Technol.*, vol. 48, no. 4, pp. 1165–1181, Jul. 1999.

[2] J. A. C. Bingham, "Multicarrier modulation for data transmission: an idea whose time has come," *IEEE Commun. Mag.*, vol. 28, no. 5, pp. 5–14, May 1990.

[3] M. Filip and E. Vilar, "Optimum utilization of the channel capacity of a satellite link in the presence of amplitude scintillations and rain attenuation," *IEEE Trans. Commun.*, vol. 38, no. 11, pp. 1958–1965, Nov. 1990.

[4] S.-L. Kim, Z. Rosberg, and J. Zander, "Combined power control and transmission rate selection in cellular networks," in *Gateway to 21st Century Communications Village. VTC 1999-Fall. IEEE VTS 50th Vehicular Technology Conference (Cat. No.99CH36324)*, vol. 3, 1999, pp. 1653–1657 vol.3.

[5] L. C. Yun and D. G. Messerschmitt, "Variable quality of service in cdma systems by statistical power control," in *Communications, 1995. ICC '95 Seattle, 'Gateway to Globalization', 1995 IEEE International Conference on*, vol. 2, Jun. 1995, pp. 713–719 vol.2.

[6] M. Wang, H. Gao, and T. Lv, "Energy-efficient user association and power control in the heterogeneous network," *IEEE Access*, vol. 5, pp. 5059–5068, 2017.

[7] L. Xu, G. Yu, and Y. Jiang, "Energy-efficient resource allocation in single-cell ofdma systems: Multi-objective approach," *IEEE Trans. Wireless Commun.*, vol. 14, no. 10, pp. 5848–5858, Oct. 2015.

[8] T. Zhou, Y. Huang, and L. Yang, "Energy-efficient user association in downlink heterogeneous cellular networks," *IET Communications*, vol. 10, no. 13, pp. 1553–1561, Sep. 2016.

[9] A. Mesodiakaki, F. Adelantado, A. Antonopoulos, E. Kartsakli, L. Alonso, and C. Verikoukis, "Energy impact of outdoor small cell backhaul in green heterogeneous networks," in *2014 IEEE 19th International Workshop on Computer Aided Modeling and Design of Communication Links and Networks (CAMAD)*, Dec. 2014, pp. 11–15.

[10] S. Tombaz, P. Monti, F. Farias, M. Fiorani, L. Wosinska, and J. Zander, "Is backhaul becoming a bottleneck for green wireless access networks?" in *Proc. IEEE ICC,*, Jun. 2014, pp. 4029–4035.

[11] S. Tombaz, Z. Zheng, and J. Zander, "Energy efficiency assessment of wireless access networks utilizing indoor base stations," in *2013 IEEE 24th Annual International Symposium on Personal, Indoor, and Mobile Radio Communications (PIMRC)*, Sep. 2013, pp. 3105–3110.

[12] A. Mesodiakaki, A. Kassler, E. Zola, M. Ferndahl, and T. Cai, "Energy efficient line-of-sight millimeter wave small cell backhaul: 60, 70, 80 or 140 ghz?" in *2016 IEEE 17th International Symposium on A World of Wireless, Mobile and Multimedia Networks (WoWMoM)*, Jun. 2016, pp. 1–9.

[13] A. Mesodiakaki, F. Adelantado, L. Alonso, and C. Verikoukis, "Energy-efficient user association in cognitive heterogeneous networks," *IEEE Commun. Mag.*, vol. 52, no. 7, pp. 22–29, Jul. 2014.

[14] E. Zola, A. J. Kassler, and W. Kim, "Joint user association and energy aware routing for green small cell mmwave backhaul networks," in *2017 IEEE Wireless Communications and Networking Conference (WCNC)*, Mar. 2017, pp. 1–6.

[15] A. Mesodiakaki, F. Adelantado, L. Alonso, M. D. Renzo, and C. Verikoukis, "Energy- and spectrum-efficient user association in millimeter-wave backhaul small-cell networks," *IEEE Trans. Veh. Technol.*, vol. 66, no. 2, pp. 1810–1821, Feb. 2017.

[16] M. Marcus and B. Pattan, "Millimeter wave propagation; spectrum management implications," *IEEE Microw. Mag.*, vol. 6, no. 2, pp. 54–62, Jun. 2005.

[17] G. Auer, V. Giannini, C. Desset, I. Godor, P. Skillermark, M. Olsson, M. A. Imran, D. Sabella, M. J. Gonzalez, O. Blume, and A. Fehske, "How much energy is needed to run a wireless network?" *IEEE Wireless Communications*, vol. 18, no. 5, pp. 40–49, Oct. 2011.

[18] F. 15-1166, "Federal communications commission," Oct. 2015.

[19] L. Xiao, M. Johansson, and S. P. Boyd, "Simultaneous routing and resource allocation via dual decomposition," *IEEE Trans. Commun.*, vol. 52, no. 7, pp. 1136–1144, Jul. 2004.

[20] S. Boyd and L. Vandenberghe, *Convex optimization*. Cambridge, U.K.: Cambridge Univ. Press, Mar. 2004.

[21] "Small cell enhancements for e-utra and e-utran-physical layer aspects, 3gpp tr 36.872, v. 1.0.0, rel. 12," Aug. 2013.

[22] M. Grant and S. Boyd, *CVX: Matlab software for disciplined convex programming, version 1.21*, http://cvxr.com/cvx, Apr. 2011.

Chapter 4

Energy Efficient User Association, Power, and Flow Control in Millimeter Wave Backhaul Heterogeneous Networks

4.1 Abstract

In order to meet the ever increasing wireless traffic requirements, the concept of heterogeneous networks (HetNets) has been proposed and given significant attention by researchers in academia and industry. In HetNets, not all base stations (BSs) will have a direct access to the core network (CN). Some BSs will have to forward their traffic to neighboring BSs thereby forming a multiple-hop backhaul (BH) architecture. Among the goals of 5G technology is energy consumption reduction. In order to reduce the energy consumption in HetNets, it is important to associate user equipment (UEs) to BSs that not only minimizes access network (AN) power consumption, but also the

power consumption in the BH network. Because the BH links are capacity and power constrained, such backhaul-aware user association schemes become more challenging. In this chapter*, we study the problem of joint user association, power control and BH link flow assignment optimization in the downlink (DL) of HetNets. The aim of the optimization problem is to maximize the overall network energy efficiency (EE). The original problem is formulated as a non-convex and mixed-integer optimization problem. To get a tractable solution, we decompose the original joint problem into two separate problems: 1. user association and power control optimization in the AN, and 2. BH link flow assignment and power control optimization problem. While problem 2 is a convex optimization problem and hence can be efficiently solved, problem 1 still remains an integer programming problem in which the number of variables can be very large (for network with large number of BSs and UEs) for any integer programming solver to efficiently solve. To that end, we utilize the column generation method to solve problem 1 by breaking it into a restricted master sub-problem that optimizes over a select subset of BSs and a collection of pricing subproblems that select new BSs to be introduced into the restricted master problem, if that results in a better objective function value. Simulation results indicate that our proposed approach yields significantly higher energy efficiency than the reference approaches.

Index Terms–Energy efficiency; user association; heterogeneous networks; mmWave communication; column generation.

*The work in this chapter has been presented in "Sylvester B. Aboagye, Ahmed Ibrahim and Telex M. N. Ngatched, "Joint user association, power and flow control in millimeter wave backhaul heterogeneous networks: A column generation approach.," submitted to *IEEE Trans. Veh. Technol.*"

4.2 Introduction

Motivated by a new generation of wireless devices and the explosive growth of bandwidth intensive applications, UE data traffic and network load keep skyrocketing, pushing current cellular networks to their break-point. In order to meet these demands and provide a satisfactory UE experience, it is required to increase network capacity and coverage extension. Providing network support to more traffic leads to increased energy consumption. Deploying low power nodes (LPNs) such as micro base stations, pico base stations (PBSs) and femto base stations overlaid the traditional macro base station (MBS) is seen as a potential way of enhancing future cellular network's capacity and coverage in a cost-effective and energy-aware manner. This type of network architecture is generally referred to as heterogeneous networks (HetNets). Research works on the development and deployment of HetNets is still ongoing in the communication industry and research community including standardization bodies like the Third Generation Partnership Project (3GPP) LTE-Advanced [1]. One fundamental objective in the deployment of HetNets for next generation cellular networks is to maximize network energy efficiency (EE).

Although LPNs may have the same access and BH features just like MBSs, they operate with a significantly lower transmit power and can only serve tens of UEs within a coverage radius of up to hundred meters. Specifically, the large difference in the downlink (DL) transmit power of a PBS (≈ 30 dBm) and MBS (≈ 46 dBm) has resulted in some technical challenges in the deployment of HetNets. Prominent among these challenges is the user association problem in HetNets. The conventional approach of associating a UE to a BS is based on the reference signal received power (RSRP) and/or reference signal received quality (RSRQ). In RSRP, UEs are associated to the BS that provides the strongest received signal strength. But as was shown in [2], the closer a LPN gets to a MBS, the smaller its DL coverage area as well as the

area in which it provides the dominant DL received signal strength. Hence, using the RSRP user association scheme in HetNets may not always be the optimal approach as UEs will always be connected to distant high power MBSs other than nearby LPNs, a situation that can also prevent efficient load balancing. This is because while many LPNs will have few active UEs, more of the UEs will be associated to the MBS, and this that can lead to an increase in the AN DL power consumption and an inefficient usage of AN resources. Although this will mean less BH traffic and BH power consumption, the EE and BH links resource utilization of the RSRP user association scheme cannot be guaranteed.

On the contrary, user association schemes that try to connect UEs to nearby BSs would enable better load balancing and resources usage in the AN, and help reduce the total AN power consumption due to relatively lower transmit power of the LPNs. To that end, range expansion (RE) has been proposed to increase LPNs' DL coverage area. RE adds a positive bias (in dB) to the received signal strength from a LPN. As a result, a UE that would have connected to the MBS with the RSRP scheme will now associate with the LPN even though the DL link quality from the MBS may be the better link. RE has the potential of increasing UEs' throughput since UEs get access to a much larger portion of resources while minimizing power consumption in the AN. But its resource utilization rate and overall energy efficiency, both in the AN and BH network cannot be guaranteed. In the AN, UEs do not connect with BSs that provide the highest received signal strength. Also, artificially pushing UEs to LPNs would increase the total BH traffic and consequently BH power consumption. With the dense deployment of LPNs and BH links in future cellular networks, BH network power consumption cannot be neglected. In minimum pathloss user (MPL) association scheme, UEs connect to BSs from which they experience the minimum path loss. In ideal channel conditions, UEs will always be connected to the nearest

BS. While MPL can achieve the best load balancing in the AN, its resource utilization in the AN and BH network might not be the best. Efficient BH link flow assignment and power control algorithm for the massive BH traffic it would generate is needed. To that end, its energy efficiency (in AN and BH network) cannot be guaranteed.

Another challenge in the deployment of HetNets is providing cost-efficient wireless BH solutions. Due to the dense deployment of the LPNs, direct connection of all LPNs to the CN using fiber connections (deemed to be the best BH solution) is highly prohibitive due to its deployment cost. One promising solution involves using high-capacity mmWave frequencies wireless BH connections between the LPNs and the CN. This leads to a mesh multi-hop BH architecture, which requires optimal flow assignment and BH link resources utilization, with the objective of minimizing BH power consumption.

User association problem in HetNets has been extensively studied in literature. A comprehensive survey on the technical challenges and approaches to user association in 5G networks is presented in [3]. The problem of joint power allocation and user association in the DL of a multi-cell massive multiple-input multiple-output (MIMO) was investigated in [4]. The authors considered a single-tier, multi-cell massive MIMO network. The authors proved that the user association and power allocation problem can be solved to optimality with low complexity by linear programming. However, their approach results in instances whereby a UE is associated with more than one BSs. Hence this approach is not suitable in HetNets. The interplay of user association and resource allocation in the AN of a HetNet was studied in [5]. The authors investigated how different channel allocation strategies (i.e. orthogonal deployment, co-channel deployment, and partially shared deployment) and user association affect overall network throughput gains in HetNets. Due to the complexity of the resulting problem, the authors developed techniques that compute upper bounds on the sys-

tem's performance. Similarly, the authors in [6] proposed a contract-based mechanism for user association and inter-cell interference mitigation in the AN of HetNets with the objective of maximizing total network throughput. Taking BH links into account, a backhaul-aware user association and resource allocation in HetNets was studied in [7]. With the same objective of maximizing network throughput, the authors considered the capacity and energy constraints of the BH network in their problem formulation. But in 5G, network operators do not only seek to maximize network throughput, but also minimize energy consumption. An energy efficient user association and power allocation scheme in a mmWave based ultra dense HetNtes was proposed in [8]. An energy efficient user association scheme that maximizes SE and minimizes energy consumption in the AN and BH was proposed in [9]. Using a metaheuristic approach, the authors proposed a heuristic algorithm that aims at a "good" tradeoff between EE and SE.

Different from the studies in the above mentioned references, this chapter of the dissertation, focuses on user association scheme that minimizes power consumption in the AN and BH and performs flow control on multiple mmWave BH links while guaranteeing UE QoS, BH power and capacity constraints. The proposed approach associates each UE to only one BS. Optimal user association, power allocation and flow control solutions are obtained using the column generation method. To the best of the authors' knowledge this is the first work of such kind.

In this chapter, the effects of BS-UE association on AN and BH network energy efficiency is investigated. As discussed above, associating more UEs with LPNs can result in better usage of AN resources and reduce AN power consumption. But this can also lead to high BH network power consumption. Associating more UEs to the MBS can help reduce the total BH network power consumption, but result in a poor usage of AN resources since most LPNs will be idle. Associating UEs to BSs so as to

(i) maximize network energy efficiency, (ii) make efficient usage of network resources, and (iii) assign flows on BH links subject to the throughput demands, channel conditions, and BS power constraints becomes an optimization problem. Specifically, the following contributions are provided:

- The user association problem and BH link flow control in mmWave BH HetNet is studied aiming at maximizing overall network energy efficiency and resource utilization, without compromising UEs QoS requirements.

- The aforementioned problem is formulated as a joint user association, power and BH flow assignment problem, which is shown to be NP-hard. In order to make this problem tractable, the original NP-hard optimization problem is decoupled into two separate sub problems: (i) energy efficient user association scheme in the AN network and (ii) energy efficient power and flow control in the BH network.

- The user association problem, a non-convex problem is tailored to show that classical column generation approach can be used, and thereby is first solved to optimality using the column generation method. Using the solution of the user association problem, the BH power and flow control problem which is a convex problem is then solved to optimality.

- Simulation results are used to provide insights on how different user association schemes (i) affect power consumption in the AN and BH, (ii) make use of the MBS and LPNs' AN resources in terms of load balancing, and (iii) combine with flow control to improve on the EE gains.

The remainder of this chapter is organized as follows. We describe our system model in Section 4.3. In Section 4.4, we introduce the energy efficiency maximization problem

formulation and introduce the solution approach in Section 4.5. In Section 4.6, we develop our column generation approach for the user association and AN power control problem and present a solution technique for the BH power and flow control in Section 4.7. Simulation results are provided in Section 4.8 and we conclude in Section 4.9.

4.3 System Model

We consider the downlink of an OFDMA communication system composed of one MBS (labelled $n = 0$) overlaid with $N - 1$ PBS, that have identical transmit power, antenna gain and BH link capacity as shown in Figure 2.3.

- The set of N BSs are represented by BS_n where $n \in \{0, 1, ..., N-1\}$ and 0 is the MBS (source node) index, as shown in Figure 2.3. The PBSs are organized into clusters, each with a cluster head.

- The $N - 1$ PBSs act as destination and/or relay nodes and are labelled as $d = 1, 2, \ldots, D$, where $N - 1 = D$.

- The MBS and PBSs operate on a different carrier frequency, with the channel bandwidth F_m for MBS and F_s for each PBS, and by that avoid any cross–tier interference. These resource blocks are subdivided into sub-channels. The PBSs in each cluster reuse the same sub-channels. To avoid co-tier interference among the PBSs, the coverage area of PBSs do not overlap. Again, we assume that neighboring MBSs are located far away from each other such that inter-cell interference is avoided.

- The z_s sub-channels from the F_s resource block and k_m sub-channels from the F_m resource block are represented by the set $z = \{1, 2, ..., z_s\}$ and $k = \{1, 2, ..., k_m\}$,

respectively. The bandwidth of each MBS sub-channel is $\Delta B^m = \frac{F_m}{k_m}$ and that of a PBS is $\Delta B^s = \frac{F_s}{z_s}$.

- The total available maximum transmit power (MTP) of each BS is equally distributed to all of its sub-channels.
- The network serves a total of J UEs represented by the set $\mathcal{UE} = \{1, 2, ..., J\}$. We use j to represent the index of $\mathcal{UE}$.
- Each UE j can associate with only one BS.

Each UE has a particular throughput demand that needs to be satisfied. The demand of a UE j is labelled as y_j. For each PBS d, we define a source-sink vector $\mathbf{s^{(d)}} \in \mathbb{R}^{N-1}$, whose nth ($n \neq d$) entry $s_n^{(d)}$ represents the non-negative amount of flow into the network at the MBS and destined for PBS d. Since we consider a single source node (i.e. MBS), $s_n^{(d)} = 0, \forall n \neq 0$. According to the flow conservation law, the sink flow at PBS d can be given by $s_d^{(d)} = -s_0^{(d)}$. From the number of UEs associated to a PBS d, the total throughput demands of that PBS from the MBS (source node) can be calculated as $s_d^{(d)} = \sum_{j \in \mathcal{UE}} a_j^d y_j$, where a_j^d represents the user association variable of UE j to PBS d. Similarly, the total demand of the MBS is given as $s_0 = \sum_{j \in \mathcal{UE}} a_j^0 y_j$. The throughput demand of a particular UE j is given as

$$y_j = \begin{cases} \Delta B^s \log_2 \left(1 + \frac{\left|h_j^d\right|^2 P_{d,j}}{\sigma^2}\right), \text{ if } a_j^d = 1, \\ \Delta B^m \log_2 \left(1 + \frac{|h_j|^2 P_{0,j}}{\sigma^2}\right), \text{ otherwise.} \end{cases} \tag{4.1}$$

In (4.1), $P_{d,j}$ is the transmit power of PBS d to UE j and $P_{0,j}$ is the transmit power of the MBS to UE j. $\left|h_j^d\right|^2$ and $|h_j|^2$ represent the magnitude of the channel gain for UE a UE associated to PBS d and MBS, respectively. σ^2 is the variance of the additive white Gaussian noise channel (AWGN). For the specific throughput demands

of each UE, it is desired to associate UEs to BSs that will satisfy their demands with the minimum power consumption, by considering channel conditions, BSs transmit power constraints as well as BH links capacity.

4.3.1 Flow Constraint

For the directed BH links labelled $l = 1, 2, ..., L$, we define a *node-link incidence* matrix $A \in \mathbb{R}^{N \times L}$ whose entry A_{nl} is associated with node n and link l via

$$A_{nl} = \begin{cases} 1, & \text{if } n \text{ is the start node of link } l \\ -1, & \text{if } n \text{ is the end node of link } l \\ 0, & \text{otherwise.} \end{cases} \tag{4.2}$$

Let $O(n)$ represents the set of outgoing links from node n and $I(n)$ represents the set of incoming links to node n. On each link l, we let $x_l^{(d)} \geq 0$ represents the amount of flow destined for PBS d. $\mathbf{x^{(d)}} \in \mathbb{R}^L$ denotes the flow vector for PBS d. The flow conservation law required at each node n is expressed as

$$\sum_{l \in O(n)} x_l^{(d)} - \sum_{l \in I(n)} x_l^{(d)} = \begin{cases} s_0^{(d)}, n = 0 \\ 0, \forall n \neq 0 \\ -s_n^{(d)}, n = d \end{cases} \tag{4.3}$$

and can be written in matrix-vector form as

$$A\mathbf{x^{(d)}} = \mathbf{s^{(d)}}, \ d = 1, 2, ..., D. \tag{4.4}$$

Due to the capacity constraint on each BH link l, the total amount of traffic flow on link l, denoted as t_l, should be below the link's capacity, c_l, as in

$$t_l = \sum_d x_l^{(d)} \leq c_l. \tag{4.5}$$

4.3.2 mmWave BH link channel model

We consider a mmWave LOS multiple BH links among the PBSs and a single BH link between the cluster head and the MBS. Without loss of generality, we assume that the MBS is connected to the CN via a fiber connection. Each PBS connects to the MBS through the cluster head either directly or through one or more PBS aggregation points. Two mmWave sub-band frequencies are used in our BH network. We use the 73 GHz (E band) for PBS-MBS single BH links, and 60 GHz (V band) for multiple BH links among the PBSs. The path attenuation suffered by mmWave signals can be categorized into two components: free space path loss ($FSPL_{(dB)}$) and mmWave propagation loss factors ($PL_{(dB)}$). These are given as [10]

$$\begin{aligned} FSPL_{(dB)} &= 92.4 + 20\log_{10}\left(f_{(GHz)}\right) + 20\log_{10}\left(d_{(km)}\right), \\ PL_{d(dB)} &= d_{(km)}\left(\underbrace{L_{vap} + L_{O_2}}_{atmospheric\,gas} + L_R\right)_{(dB/km)}, \end{aligned} \tag{4.6}$$

where d is the LOS separation distance in km between the transmitter and receiver, and f is the frequency in GHz. L_{vap}, L_{O_2}, and L_R represent the attenuation in dB/km due to water vapour, oxygen, and rain, respectively. The total path loss (TPL) can be expressed as

$$TPL_{(dB)} = FSPL_{(dB)} + PL_{d(dB)}. \tag{4.7}$$

4.3.3 BH Power Consumption Model

From the literature, there is no standardized power consumption model for mmWave communication. Nevertheless, the use of the linear approximation model for power consumption in mmWave communication networks has received much attention [11] [12]. We focus only on the dynamic power consumption, P_l, which on BH link l is modelled as

$$P_l = P^{BH}_{\max_l} \frac{t_l}{c_l},\ 0 \leq P_l \leq P^{BH}_{\max_l}, \tag{4.8}$$

where $P^{BH}_{\max_l}$ is the MTP on BH link l. $P^{BH}_{\max_l}$ is calculated as

$$P^{BH}_{\max_l(dBm)} = EIRP_{\max(dBm)} + T_{xloss(dB)} - G_{Tx(dBi)}, \tag{4.9}$$

where $EIRP_{\max(dBm)}$ is the maximum equivalent isotropically radiated power, $T_{xloss(dB)}$ is the transmitter loss, and $G_{Tx(dBi)}$ is the gain of the transmitter. For the chosen mmWave frequency subbands, EIRP is given as [13]

$$\begin{aligned} \text{V band} &: EIRP_{\max(dBM)} = 85_{(dBm)} - 2 \cdot x_{(dB)}, \\ E \text{ band} &: EIRP_{\max(dBM)} = 85_{(dBm)} - 2 \cdot y_{(dB)}, \end{aligned} \tag{4.10}$$

where x is the number of dB that G_{Tx} is less than 51 dBi and y is the number of dB that G_{Tx} is less than 50 dBi. The signal-to-noise power ratio at the receiving end of BH link l $\left(SNR^{BH}_{l(dB)}\right)$ is given as

$$\begin{aligned} SNR^{BH}_{l(dB)} = P_{l(dBm)} - N_{th(dBm)} - NF_{(dB)} - T_{xloss(dB)} \\ -R_{xloss(dB)} + G_{Rx(dBi)} - L_{\text{margin}} - TPL_{(dB)} \end{aligned}, \tag{4.11}$$

where N_{th} is the thermal noise and NF is the noise figure. The parameters $R_{xloss(dB)}$, G_{Rx}, and L_{margin} represent the receiver loss, receiver antenna gain and link margin, respectively.

4.4 Problem Formulation

An energy-efficient scheme that (i) performs user association, (ii) minimizes power consumption in both the AN and BH network, and (iii) assigns fows on the BH links, while satisfying the throughput demand of UEs is considered in this section. The optimization problem of maximizing network EE over user association, power control and BH link flow assignment variables can be jointly formulated as in (4.12). In (4.12), a_j^0 is a binary variable that equals 1 when UE j associates with the MBS and 0 otherwise. Similarly, a_j^d equals 1 when UE j associates with PBS d and 0 otherwise.

$$\max_{\mathbf{a},\mathbf{p},\mathbf{t}} \frac{\sum_{j\in J} y_j}{\sum_{\forall j} a_j^0 \left(\frac{y_j}{\frac{2^{\frac{\Delta B^m}{}}-1}{\left|h_j^0\right|^2}}\right)\sigma^2 + \sum_{\forall d}\sum_{\forall j} a_j^d \left(\frac{y_j}{\frac{2^{\frac{\Delta B^s}{}}-1}{\left|h_j^d\right|^2}}\right)\sigma^2 + \sum_{l\in O(n)} P^{BH}_{\max_l} \frac{t_l}{c_l}}$$

s.t.

$$\begin{aligned}
&C1: a_j^0 + \sum_{\forall d} a_j^d = 1, \forall j \\
&C2: s_n^{(d)} = \sum_{\forall j} y_j a_j^d, \forall d \\
&C3: \mathbf{A}\mathbf{x}^{(\mathbf{d})} = \mathbf{s}^{(\mathbf{d})}, \forall d \\
&C4: t_l = \sum_{d} x_l^{(d)}, \forall l \\
&C5: t_l \leq c_l, \forall l \\
&C6: \sum_{\forall j} a_j^0 \left(\frac{y_j}{\frac{2^{\frac{\Delta B^m}{}}-1}{\left|h_j^0\right|^2}}\right)\sigma^2 \leq P^{AN}_{\max^0}, \\
&C7: \sum_{\forall j} a_j^d \left(\frac{y_j}{\frac{2^{\frac{\Delta B^m}{}}-1}{\left|h_j^{(d)}\right|^2}}\right)\sigma^2 \leq P^{AN}_{\max^{(d)}}, \forall d \\
&C8: \sum_{l\in O(d)} P^{BH}_{\max_l} \frac{t_l}{c_l} \leq P^{BH}_{\max^{(d)}}, \forall d \\
&C9: \sum_{l\in O(0)} P^{BH}_{\max_l} \frac{t_l}{c_l} \leq P^{BH}_{\max^{(0)}}, \\
&C10: \mathbf{x}^{(\mathbf{d})} \succeq 0, \forall d \\
&C11: a_j^0 \in \{0,1\}, a_j^d \in \{0,1\}, \forall j \in J, \forall d \in D.
\end{aligned} \tag{4.12}$$

In (4.12), $C1$ ensures that each UE associates with only one BS. $C2$ to $C5$ ensure that UEs are associated to BSs such that the capacity constraints on the BH links are not violated. $C6$ to $C9$ ensure that BSs do not consume more than the available MTP in the AN and BH network. $C10$ ensures the non-negativity of flow assignment on BH links while $C11$ indicates the binary nature of the user association variables.

For the given UE throughput demands, the EE maximization in (4.12) becomes a power minimization problem as shown in (4.13).

$$\min_{\mathbf{a},\mathbf{p},\mathbf{t}} \sum_{\forall j} a_j^0 \left(\frac{2^{\frac{y_j}{\Delta B^m}}-1}{\left|h_j^0\right|^2} \right) \sigma^2 + \sum_{\forall d} \sum_{\forall j} a_j^d \left(\frac{2^{\frac{y_j}{\Delta B^s}}-1}{\left|h_j^d\right|^2} \right) \sigma^2 + \sum_{l \in O(n)} P_{\max_l}^{BH} \frac{t_l}{c_l}$$
$$\text{s.t.} \tag{4.13}$$
$$C1 \sim C11.$$

The optimization problem in (4.13) contains binary variables $\left(a_j^0, a_j^d\right)$ and continuous variables (p, t). Moreover, the coupling of the user association variable in the AN and the flow control variable in the BH network in $C2$ and $C3$ adds to the complexity of the problem. The problem in (4.13) is therefore non-convex and falls into the class of mixed-integer linear programming (MILP) problem, which is generally NP-hard. It is difficult to get the optimal solution. To that end, the original problem in (4.13) is reformulated into a user association problem and BH flow control problem with the same objective of minimizing power consumption in the AN and BH network. This is achieved by decoupling the user association variable and the flow control variable in $C2$ and $C3$, into AN power minimization problem and BH network power minimization problem. Firstly, the user association and power control problem in the AN is solved to optimality, and then using the solution, the BH flow control and power minimization problem is solved.

4.5 Equivalent Separate User Association and BH Flow Control Optimization Problem

The separate power minimization problems for the AN and BH network are presented in (4.14) and (4.15) respectively.

$$
\begin{aligned}
&\min_{\mathbf{a},\mathbf{p}} \ \sum_{\forall j} a_j^0 \left(\frac{2^{\frac{y_j}{\Delta B^m}}-1}{\left|h_j^0\right|^2} \right) \sigma^2 + \sum_{\forall d} \sum_{\forall j} a_j^d \left(\frac{2^{\frac{y_j}{\Delta B^s}}-1}{\left|h_j^d\right|^2} \right) \sigma^2 \\
&\text{s.t.} \\
&C1 : a_j^0 + \sum_{\forall d} a_j^d = 1, \forall j \\
&C6 : \sum_{\forall j} a_j^0 \left(\frac{2^{\frac{y_j}{\Delta B^m}}-1}{\left|h_j^0\right|^2} \right) \sigma^2 \leq P^{AN}_{\max^0}, \\
&C7 : \sum_{\forall j} a_j^d \left(\frac{2^{\frac{y_j}{\Delta B^m}}-1}{\left|h_j^{(d)}\right|^2} \right) \sigma^2 \leq P^{AN}_{\max^d}, \forall d \\
&C11 : a_j^0 \in \{0,1\}, a_j^d \in \{0,1\}, \forall j \in J, \forall d \in D.
\end{aligned}
\tag{4.14}
$$

$$
\begin{aligned}
&\min_{\mathbf{p},\mathbf{t}} \ \sum_{\forall j} a_j^0 \left(\frac{2^{\frac{y_j}{\Delta B^m}}-1}{\left|h_j^0\right|^2} \right) \sigma^2 + \sum_{\forall d} \sum_{\forall j} a_j^d \left(\frac{2^{\frac{y_j}{\Delta B^s}}-1}{\left|h_j^d\right|^2} \right) \sigma^2 + \sum_{l \in O(n)} P^{BH}_{\max_l} \frac{t_l}{c_l} \\
&\text{s.t.} \\
&C2 : s_n^{(d)} = \sum_{\forall j} y_j a_j^d, \forall d \\
&C3 : \mathbf{A}\mathbf{x}^{(\mathbf{d})} = \mathbf{s}^{(\mathbf{d})}, \forall d \\
&C4 : t_l = \sum_{d} x_l^{(d)}, \forall l \\
&C5 : t_l \leq c_l, \forall l \\
&C8 : \sum_{l \in O(d)} P^{BH}_{\max_l} \frac{t_l}{c_l} \leq P^{BH}_{\max^{(d)}}, \forall d \\
&C9 : \sum_{l \in O(0)} P^{BH}_{\max_l} \frac{t_l}{c_l} \leq P^{BH}_{\max^{(0)}}, \\
&C10 : \mathbf{x}^{(\mathbf{d})} \succeq 0, \forall d
\end{aligned}
\tag{4.15}
$$

The problem in (4.14) is first solved for the optimal user association and power allocation in the AN. The problem in (4.15) is then solved using the solution from (4.14).

4.5.1 Optimal user association and AN power allocation

The AN power minimization problem in (4.14) can be re-written in the form

$$
\begin{aligned}
&\min_{\mathbf{a},\mathbf{p}} \ \sum_{\forall j} a_j^{n=0}\left(\frac{2^{\frac{y_j}{\Delta B^m}}-1}{\left|h_j^0\right|^2}\right)\sigma^2+\sum_{\forall j} a_j^{n=1}\left(\frac{2^{\frac{y_j}{\Delta B^m}}-1}{\left|h_j^1\right|^2}\right)\sigma^2+\ldots+\sum_{\forall j} a_j^{n=N}\left(\frac{2^{\frac{y_j}{\Delta B^m}}-1}{\left|h_j^N\right|^2}\right)\sigma^2\\
&\text{s.t}\\
&C1: a_j^{n=0}+a_j^{n=1}+\ldots+a_j^{n=N}=1,\forall j\\
&C6/C7: \sum_{\forall j} a_j^{n=0}\left(\frac{2^{\frac{y_j}{\Delta B^m}}-1}{\left|h_j^0\right|^2}\right)\sigma^2\leq P_{\max^0}^{AN}\\
&\qquad\quad \sum_{\forall j} a_j^{n=1}\left(\frac{2^{\frac{y_j}{\Delta B^m}}-1}{\left|h_j^1\right|^2}\right)\sigma^2\leq P_{\max^1}^{AN}\\
&\qquad\quad \vdots\\
&\qquad\quad \sum_{\forall j} a_j^{n=N}\left(\frac{2^{\frac{y_j}{\Delta B^m}}-1}{\left|h_j^N\right|^2}\right)\sigma^2\leq P_{\max^N}^{AN}\\
&C11: a_j^n\in\{0,1\},\forall j\in J,\forall n\in N,
\end{aligned}
\tag{4.16}
$$

where the objective function minimizes the total AN transmit power at each BS. The sum of the minimum DL transmit power for each UE associated to a BS n will yield the minimum total AN transmit power for that BS n. And the sum of the minimum AN transmit power for each BS n will yield the minimum AN total power consumption in the network. $C1$ still ensures that each user is associated to only one BS. The remaining constraints ensures that each BS does not transmit more than its available maximum transmit power.

One obvious approach to solving (4.16) will be the generation of all the transmit power for all the UEs from each BS and then putting them in a UE-Tx power $\mathbf{P_{matrix}}$

matrix of size $N \times J$ as in (4.17). For the first row entries of $\mathbf{P_{matrix}}$, determine the minimum entry, $\arg\min_{n} p_{n,j=1}$, and associate UE $j = 1$ to the BS n in the arg function. After associating UE $j = 1$ to the BS n from the arg function, ensure $C6$ and $C7$ are satisfied. Then move to the second row entries to determine BS n for UE $j = 2$ and again ensure $C6$ and $C7$ are obeyed. This process continues and more UEs get associated to a BS n until $C6$ and $C7$ are violated for a particular BS n. In that case, the column corresponding to that BS is updated and all its entries are replaced with a very large value. This will obviously prevent UEs from being associated to that particular BS whose column entries were replaced by a large value. The process continues until all UEs are associated to BSs that minimizes their transmit power.

$$P_{matrix} = \begin{bmatrix} p_{n=0,j=1} & p_{n=1,j=1} & \cdots & p_{n=N,j=1} \\ p_{n=0,j=2} & p_{n=1,j=2} & \cdots & p_{n=N,j=2} \\ \vdots & \vdots & \ddots & \vdots \\ p_{n=0,j=J} & p_{n=N,j=J} & \cdots & p_{n=N,j=J} \end{bmatrix}, \tag{4.17}$$

which is compactly written as

$$\mathbf{P}_{matrix} = \begin{bmatrix} \mathbf{p}\,(n=0) & \mathbf{p}\,(n=1) & \ldots & \mathbf{p}\,(n=N) \end{bmatrix}. \tag{4.18}$$

This approach for user association and power allocation will result in a feasible solution but not the optimal solution. This is because, this greedy algorithm does not guarantee that the user association approach will give the optimal user association with respect to minimizing the total AN power consumption. The best combination of BS-UE association cannot be determined from this approach. An optimal user association and power allocation solution is also a feasible solution that minimizes the total power consumption. Aside not giving the optimal solution, this BS-UE association solution approach is inconvenient for several other reasons. Firstly, the

generation of the $\mathbf{P_{matrix}}$ and another matrix for the power constraints is non-trivial even for small number of UEs and BS, and prohibitive as the number of UEs and BSs increases. In 5G, it is expected the number of BSs and UEs will be very high and as such this approach will not be an efficient one. Secondly, even if an explicit enumeration is possible, the resulting mathematical problem would most likely, be intractable and/or computationally infeasible to solve directly due to the large number of variables that would be involved. Moreover, most of the entries in $\mathbf{P_{matrix}}$ will not contribute to the optimal solution in anyway. Even with an integer programming solver, there will be too much columns for the solver to handle, and the same holds for the corresponding linear programming (LP) relaxations.

To overcome this difficulty, a column generation based BS-UE association is proposed. The column generation approach will provide an optimal BS-UE association solution, and has the added advantage that a prior generation of all the transmit power for all the UEs from each BS will not be required as it is understood that not all of them will contribute to the objective function. Unlike the simplex algorithm, the pricing problem of the column generation method does not have to search within all the feasible regions in order to update the basis of the master problem. This can reduce the computational time of the algorithm.

4.6 Column Generation approach to BS-UE Association and Power Control Problem

In this section, it is shown that the user association and power control problem can be approached using a classical technique from mathematical programming known as column generation [14]. To start with, we relax the integer constraint of the user association variables to continuous variables. We name the relaxed version of problem

4.16 as the LP-relaxation. Applying column generation to the LP-relaxation provides a decomposition of the user association and power control problem into a master and subproblems. The master problem, called *full master problem*, is the relaxed version of the original problem in (4.16). The two subproblems are called the *restricted master problem* and *pricing problem*. The *restricted master problem* starts by working on an initial subsets of the variables of the *full master problem*. The benefit here is that columns are left out because there are too many to handle efficiently, and most of them will not be used in the optimal solution. The *pricing problem* uses the optimal dual solution to the *restricted master problem* to identify a new variable with the most negative reduced cost, relative to the objective function of the *restricted master problem*. This new variable gets added to the initial subset of the *restricted master problem*, and it is re-optimized. The process repeats until no variable has a negative reduced cost. To get the integer solution, we solve the *restricted master problem* with an integer programming (IP) solver after the column generation terminates. The process of column generation is shown in Figure 4.1.

4.6.1 Full master problem

The LP-relaxed user association and power control problem can be written as

$$\begin{aligned} &\min_{\mathbf{a}} \sum_{n=0}^{N} \mathbf{a}_n \mathbf{p}\,(n) \\ &\text{s.t} \\ &\sum_{n=0}^{N} a_n^j = 1, a_n^j \geq 0, n = 0, \ldots N, \\ &\mathbf{a}_n \mathbf{p}\,(n) \leq P_{\max^n}^{AN}, n = 0, \ldots N, \end{aligned} \tag{4.19}$$

where,

$$\mathbf{a}_n = \begin{bmatrix} a_n^{j=1} & a_n^{j=2} & \ldots & a_n^{j=J} \end{bmatrix} \tag{4.20}$$

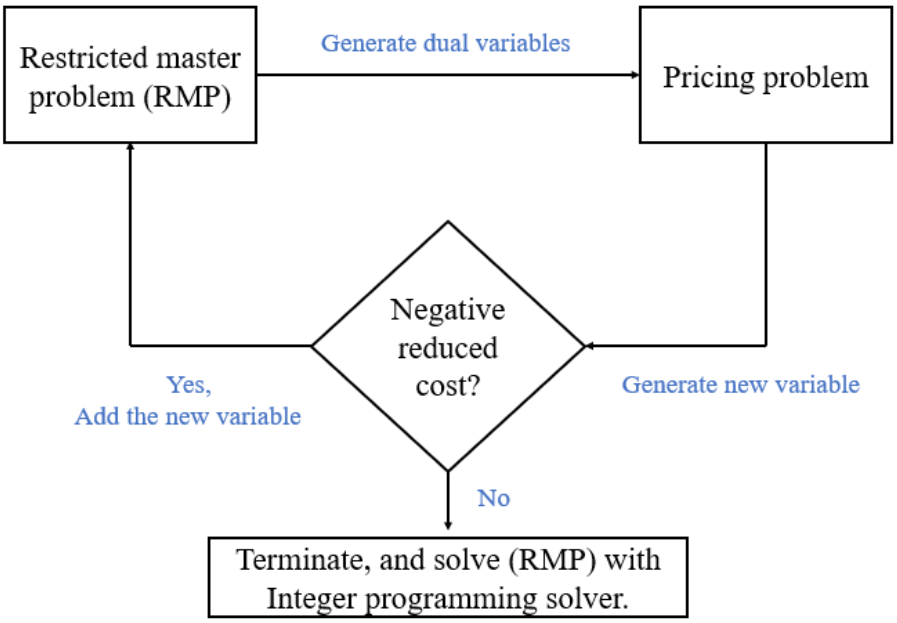

Figure 4.1: Flow chat of the column generation process.

and $\mathbf{p}(n)$ is the required $BS_n - UE$ transmit power vector for all UEs in the network guaranteed to satisfy UEs demand. It is important to notice that the *full master problem* minimizes over all the BSs in the network.

4.6.2 Restricted master problem

Instead of considering all the BSs in the network, labelled $n \in [0, 1, \ldots, N]$, for $\mathbf{p}(n)$ in (4.19), it is desirable to only consider a subset of the BSs for n in the BS-UE transmit power matrix in (4.17). Thus, only consider $\{\mathbf{p}(n)|n \in \mathcal{N}\}$, where $\mathcal{N} \subseteq \{0, 1, \ldots, N\}$. Implementing this constraint on the *full master problem* gives the *restricted master problem*.

$$
\begin{aligned}
&\min_{\mathbf{a}} \sum_{n\in\mathcal{N}} a_n \mathbf{p}\,(n) \\
&\text{s.t} \\
&\sum_{n\in\mathcal{N}} a_n^j = 1, a_n^j \geq 0, n \in \mathcal{N}, \\
&\mathbf{a}_n \mathbf{p}\,(n) \leq P_{\max^n}^{AN}, n \in \mathcal{N}.
\end{aligned}
\tag{4.21}
$$

In the *restricted master problem*, the BS-UE transmit power matrix will have the same number of rows as in (4.17) but much fewer columns. Because (4.21) optimizes over only a subset of BSs in the network, it can be solved to optimality in polynomial time [15], and its dual optimal can be obtained. The optimal solution of the *restricted master problem* provides an upper bound to the optimal of the *full master problem*. This upper bound is decreased when more BSs are included in the *restricted master problem*. Thus, the *pricing problem* is used to determine the new variable, BS n, that has the potential to reduce the objective function of the *restricted master problem* the most. The process continues until we get the optimal solution of the original problem.

The idea behind introducing more BSs into $\mathcal{N}$ (*pricing problem*) is using Lagrange duality. By introducing a Lagrange multiplier λ for the power constraint, the corresponding Lagrangian of the *restricted master problem* is

$$
\begin{aligned}
L\,(a,\lambda) &= \sum_{n\in\mathcal{N}} \mathbf{a}_n \mathbf{p}\,(n) + \sum_{n\in\mathcal{N}} {\lambda_n}^T \left(\mathbf{a}_n \mathbf{p}\,(n) - P_{\max^n}^{AN}\right) \\
&= \sum_{n\in\mathcal{N}} \mathbf{a}_n \mathbf{p}\,(n) + \sum_{n\in\mathcal{N}} {\lambda_n}^T \left(\mathbf{a}_n \mathbf{p}\,(n) - P_{\max^n}^{AN}\right),
\end{aligned}
\tag{4.22}
$$

where

$$
\lambda_n = \left[\begin{array}{cccc} \lambda_n^{j=1} & \lambda_n^{j=2} & \ldots & \lambda_n^{j=J} \end{array} \right], \tag{4.23}
$$

and the dual function is

$$g(\lambda) = \inf_{a} L(a, \lambda) = -\sum_{n \in \mathcal{N}} {\lambda_n}^T P^{AN}_{\max^n} + \inf_{a} \left(\sum_{n \in \mathcal{N}} \mathbf{a}_n \mathbf{p}(n) + \sum_{n \in \mathcal{N}} {\lambda_n}^T \mathbf{a}_n \mathbf{p}(n) \right). \tag{4.24}$$

The Lagrange dual of the *restricted master problem* can be given as

$$\begin{aligned} &\max_{\lambda} \; -\sum_{n \in \mathcal{N}} {\lambda_n}^T P^{AN}_{\max^n} \\ &\text{s.t} \\ &\sum_{n \in \mathcal{N}} \mathbf{a}_n \mathbf{p}(n) + \sum_{n \in \mathcal{N}} {\lambda_n}^T \mathbf{a}_n \mathbf{p}(n) = 0, \\ &\lambda_n \succeq 0. \end{aligned} \tag{4.25}$$

In our implementation, the *restrited master problem* is solved to optimality using a primal-dual interior point method.

4.6.3 Pricing problem

After solving the *restricted master problem*, it is important to identify if new columns need to enter the basis, or possibly verify optimality, by examining whether any of the BSs, $n \in BS_n \backslash \mathcal{N}$, has a negative reduced cost. The reduced cost of a BS $n \in BS_n \backslash \mathcal{N}$ is calculated as:

$$c_n = 1 - \lambda_n \mathbf{s}(n), \tag{4.26}$$

where λ_n are the optimal dual variables corresponding to the *restricted master problem*, and $\mathbf{s}(n)$ is a binary variable indicating whether or not BS n is included in $\mathcal{N}$. Since it is desired to find BSs with the most negative reduced cost, the objective function of the *pricing problem* is:

$$\min_{n \in BS_n \backslash \mathcal{N}} \; c_n, \tag{4.27}$$

or equivalently

$$\max_{n \in BS_n \setminus \mathcal{N}} \lambda_n \mathbf{s}(n). \tag{4.28}$$

Let β_n^* and γ_n^* denote the optimal solution of (4.27) and (4.28), respectively. Since the most negative reduced cost is desired, the process of column generation terminates when $\beta_n^* \geq 0$ or $\gamma_n^* \leq 0$.

To get the integer solution for the user association variables, we solve the *restricted master problem* in (4.21) with an IP solver after the column generation procedure terminates.

4.7 Optimal BH Flow Control and Power Allocation

Having found the optimal user association variables using the column generation approach, the BH flow control and power allocation optimization problem becomes a convex optimization problem. This is because it has a convex objective function, and convex inequality constraints. Hence, it can be solved globally and efficiently by recently developed interior-point methods (see [16] and [17]).

It is important to notice that, solving the user association and power control problem as well as the BH flow and power control problem iteratively would not yield any improvement in the optimal solution. By close inspection of the constraint sets in both problems, it can be concluded that the optimal solution to the user association, power allocation and BH flow control is obtained by solving each subproblem only once. This was also confirmed through simulations.

4.8 Simulation Results and Discussion

4.8.1 Scenario

The extensive simulations done in this section were carried out using MATLAB. We considered a MBS sector area, as shown in Figure 4.2, that overlaps with a single cluster of PBSs. The BH links are LOS multipath mmWave links, each with a channel bandwidth of 50 MHz [18]. We use the 73 GHz band for PBS-MBS single BH links, and the 60 GHz band for the multiple BH links among PBSs. The length of each BH link is between 150-200 m. We consider two UE distributions [19]:

1. *Hotspot (Hs) UEs*: UEs are randomly dropped within a coverage radius range of (5–20 m) for PBSs and (35-50 m) for MBSs.

2. *Random (Rn) UEs*: UEs are randomly distributed within the radius range of the MBS.

In each realization, three UEs are always considered as HS UEs, whiles the remaining are randomly deployed. Thus, UE positions may vary per each realization. The channel gain considered in this chapter includes pathloss, log-normal shadowing and multipath fading. The multipath fading is assumed to follow a Rayleigh distribution; the Rayleigh fading channel gains are modelled as independent and identically distributed unit mean, exponentially distributed random variables. The throughput demand of UEs are preknown before running the algorithm (i.e. fixed). The bandwidth of each mmWave BH link is 3.5 GHz. We set $R_{xloss} = T_{xloss} =$ 5 dB, $G_{TX} = G_{RX} = [\text{V band}: 36 \text{ dBi}, \text{E band}: 43 \text{ dBi}]$, $L_{m\arg in} = 15$ dB and NF $= [\text{V band}: 4.5 \text{ dB}, \text{E band}: 6 \text{ dB}]$. The rest of the simulation parameters are summarized in Table 4.1. We provide results averaged over 1000 independent simulations.

Table 4.1: Simulation parameters for AN

Parameter	**Value**
MBS carrier frequency	2 GHz
PBS carrier frequency	2.6 GHz
$\Delta B^m, \Delta B^s$	180 kHz
MBS MTP	46 dBm
PBS MTP	30 dBm
Distance-dependent path loss (dB)	MBS-UE $128.1 + 37.6\log_{10}(d_{km})$
	PBS-UE $140.7 + 36.7\log_{10}(d_{km})$
Penetration loss	20 dB
Shadowing effect	10 dB
N_{th}	-174 dBm/Hz

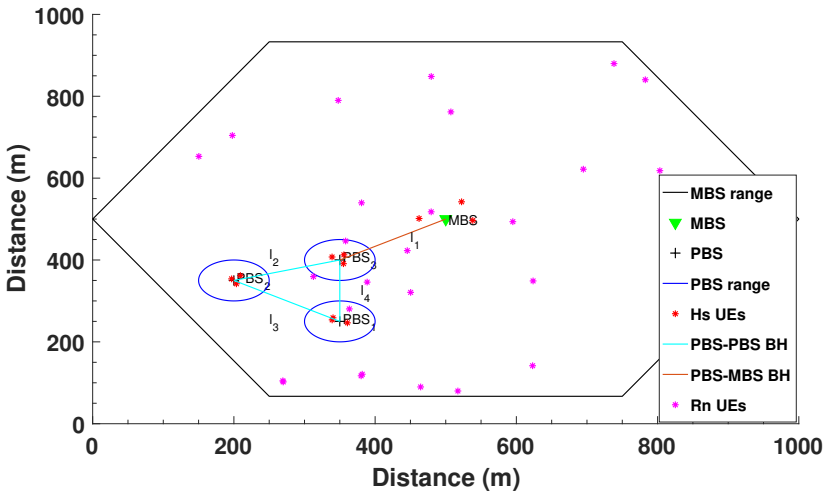

Figure 4.2: Network model simulation scenario.

The throughput demands of UEs are fixed. Each UE has a DL throughput demand of 1 Mbps. The following reference algorithms will be considered:

- RSRP: In RSRP, the average received power of each UE is measured. UEs get associated to the BS from which they receive the strongest signal power [20]. Thus UE j is associated with BS n^*, where

$$n^* = \arg\max_n \ \mathrm{SNR}_j^n. \tag{4.29}$$

- RE: The RSRP of LPNs is relatively smaller as compared to that of MBS. In RE, a *bias* (measured in dB) is added to the RSRP of LPNs. This is done to force more UEs to associate with LNPs [1]. Thus UE j is associated with BS n^*, where

$$n^* = \arg\max_n \ \left(\mathrm{SNR}_j^n + bias_n\right). \tag{4.30}$$

- MPL: In MPL, a UE is associated with a BS from which it experiences the MPL [5]. Thus UE j is associated with BS n^*, where

$$n^* = \arg\min_n \ \left(\mathrm{PL}_j^n\right). \tag{4.31}$$

4.8.2 Results and discussions

The number of UEs, N, considered in the simulation has been appropriately chosen to avoid system overloading. All the algorithms satisfy the fixed throughput demands of UEs. Thus, UEs QoS are guaranteed. To that end, all the algorithms achieve the same DL total throughput for any particular N. As a result, the total network EE will depend only on the total power consumption in the both the AN and BH network.

The simulation results of the proposed approach for solving the energy efficient

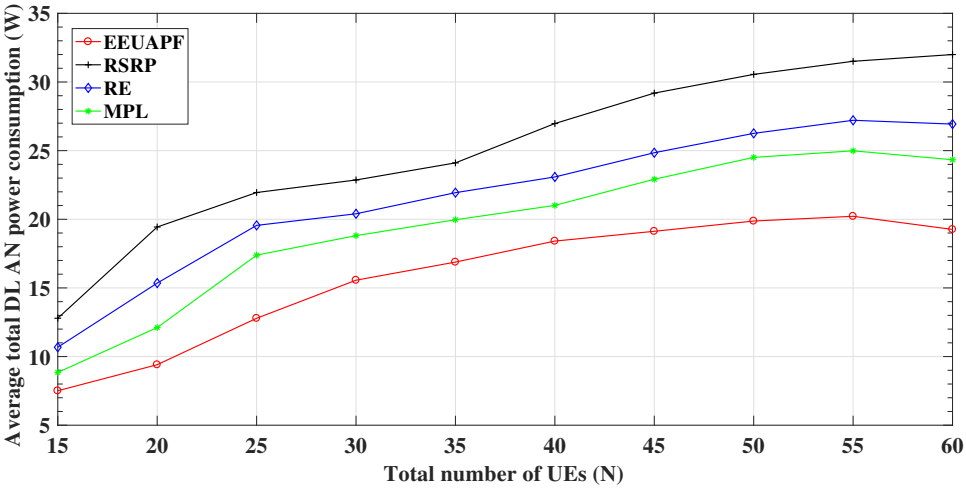

Figure 4.3: Average AN downlink power consumption for different N values.

user association, power and flow control optimization problem is compared with state-of-the-art user association schemes, which is each followed by our proposed joint BH power and flow assignment optimization. Since our proposed approach is in two stages: (i) energy efficient user association and (ii) energy efficient joint power and flow control on the BH links, the reference algorithms considered will also have two sequential stages. The first stage will consist of the user association scheme, and the second stage will consist of the joint BH power and flow control optimization. This will ensure a fair comparison of our proposed scheme and the reference algorithms.

The average total AN DL power consumption is shown for the reference algorithms and our proposed column generation based approach, labelled energy efficient user association, power and flow control (EEUAPF), in Figure 4.3. As noticed, the EEUAPF consumes the least DL power consumption for all N. This is because EEUAPF exploits all possibilities and associate UEs to BSs that minimize the AN power consumption in the DL. The MPL algorithm performs better than the RSRP and RE because it always associate UEs to the closest Bs, regardless of their received signal power. But associating UEs to the closest BS does not always guarantee

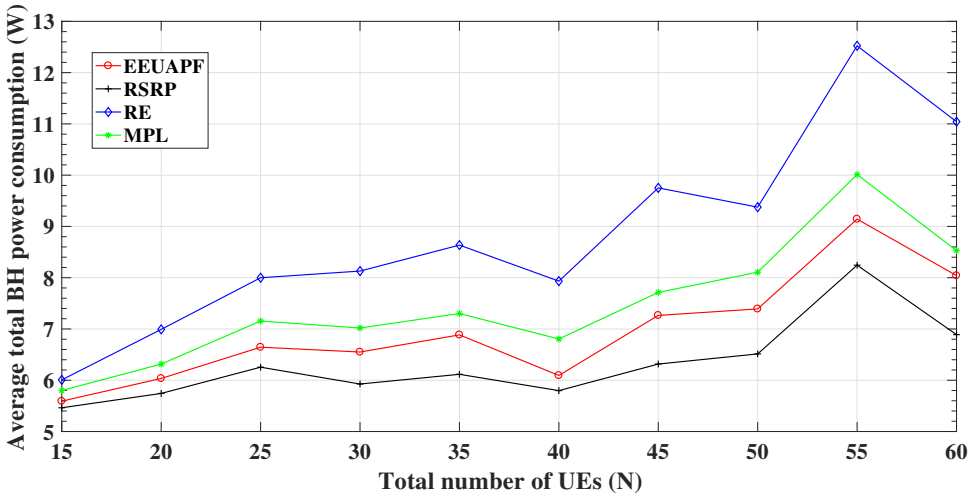

Figure 4.4: Average BH power consumption for different N values.

minimimum power consumption. This is because the channel considered is not an ideal channel (i.e. there is fading), and the closest BS would not always provide the most favorable channel condition for UEs. As a result, MPL performs worse than the EEUAPF. Comparing the two worst algorithms, RE performs slightly better since it mostly associates UEs to the PBSs. PBSs transmit significantly less power than the MBS, but UEs do not connect to BSs that provide the highest SNR due to the bias used. This can result in more power consumption in guaranteeing UEs throughput demands. The RSRP performs the worst since most of UEs associate with the MBS, and thereby consuming significant amount of power.

The average BH power consumption for the four approaches versus the number of UEs, N, is depicted in Figure 4.4. It is observed that the RSRP algorithm achieves the least BH power consumption. This stems from the fact that most of the UEs get associated to the MBS with the RSRP algorithm leading to only few BH traffic. The RSRP has the smallest BH traffic. RE has the highest BH power consumption because most UEs get associated to the nearest PBS resulting in the most highly loaded BH links. Because RE has the highest BH traffic, its BH network consumes the

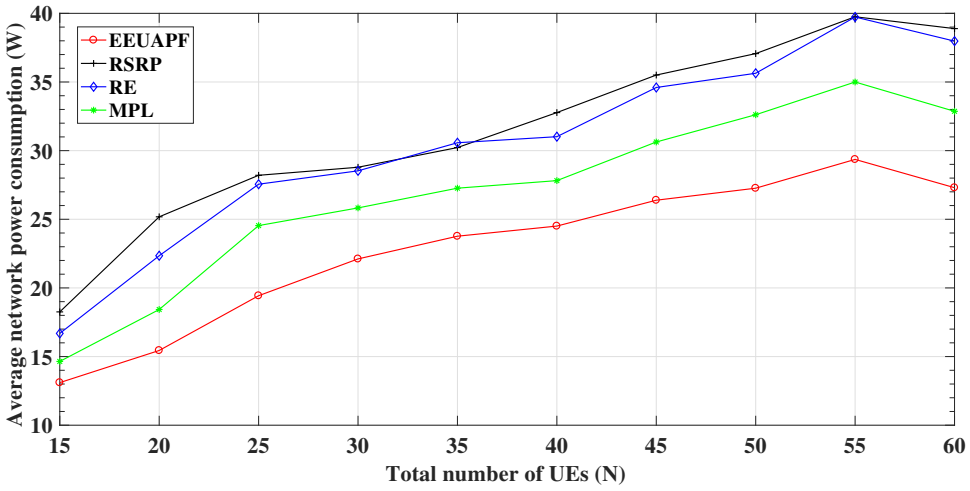

Figure 4.5: Average total downlink power consumption for different N values.

highest BH power consumption. Our EEUAPF approach performed better than RE and MPL, but worse than the RSRP algorithm in terms of BH power consumption. With the optimal user association solution, EEUAPF determined the optimal BH flow assignment that minimizes the overall BH power consumption. One insight from Figure 4.4 is that, BH power consumption is highly dependent on the user association scheme employed in the AN.

The total network DL power consumption is the summation of the power consumed in the AN and that of the BH network. For the four algorithms considered in this chapter, their overall average total DL power consumption for different N is shown in Figure 4.5. It can be noticed that the EEUAPF has the lowest total DL power consumption. Although, the RSRP algorithm performed better than EEUAPF in the BH power consumption, the weight of its power consumption in the AN significantly outweighed that of EEUAPF in the AN, and impacted RSRP's overall network power consumption. RSRP has the highest total DL power consumption because of its power consumption in the AN. RE follows the RSRP (in descending order of total DL power consumption) since it consumes the highest BH power.

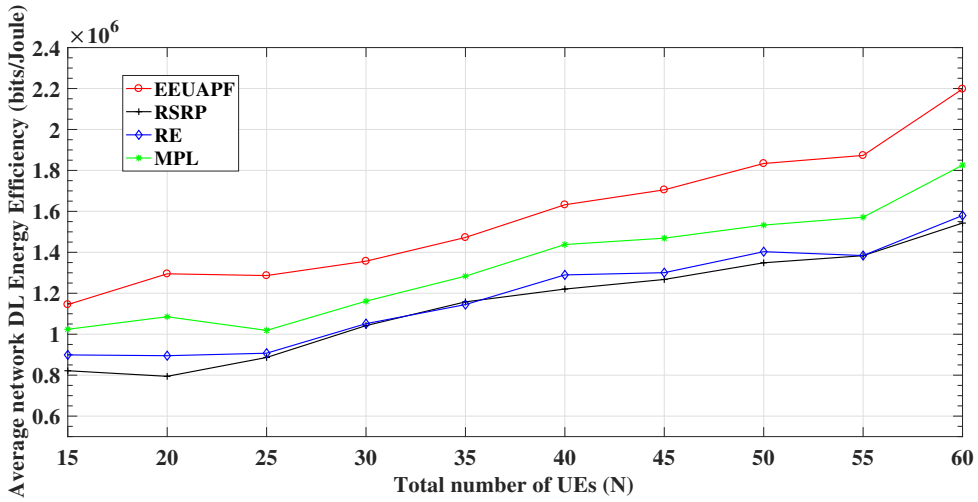

Figure 4.6: Average total downlink energy efficiency for different N values.

The total DL energy efficiency for all the algorithms is depicted in Figure 4.6. It can be seen that EEUAPF significantly outperforms the rest of the algorithms. This is due to the fact that, it presents the "best" combination of user association and power control in the AN as well as flow control and power consumption in the BH network. "Best" in the sense that, it optimizes user association with respect to minimizing AN and BH power consumption, and also optimizes BH flow assignment with respect to minimizing power consumption in the BH network. The EE of all the four algorithms improve as the number of UEs N increases. RSRP has the lowest EE among the four algorithms because its user association procedure negatively affects its AN power consumption, and this consequently affects its EE. Similarly, the EE performance of RE is lower than that of the MPL and EEUAPF because its user association procedure negatively affects its BH power consumption.

It is shown in Figure 4.7 that solving the user association and power control problem in the AN as well as the BH flow assignment and power control problem iteratively would not yield any improvement in the initial solution obtained. To solve the problem in (4.14) and (4.15) iteratively, first solve the AN optimization problem

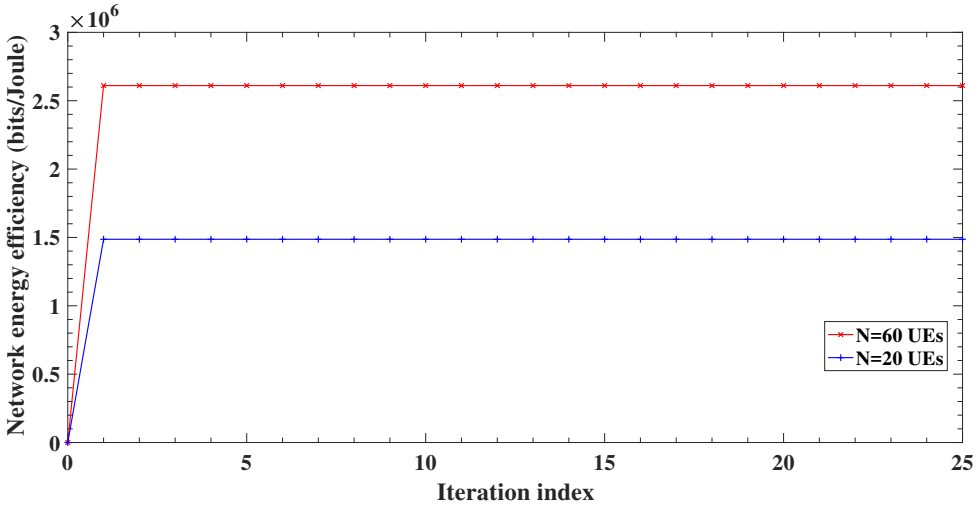

Figure 4.7: Average total downlink energy efficiency for different iteration index.

in (4.14) for the initial user association variables $\mathbf{a}$. Use the initial user association variables solution from (4.14) in $C2$ of the BH flow assignment and power control problem (4.15) and solve (4.15) for the initial BH flow assignment. For iteration index 1, add $C2$ and $C3$ of (4.15) to the constraints set of the user association and power control problem in the AN optimization problem in (4.14) using the initial user association variables and BH flow assignment variables solutions. Reoptimize (4.14) for new user association variables. With the updated user association variables from iteration index 1, solve (4.15) again for the BH flow assignment varaibles. Repeat this procedure until the maximum iteration index is reached. It is realized from Figure 4.7 that, solving (4.14) and (4.15) once, without iterating between them, yields the optimal solution.

4.9 Conclusion

In this chapter, we studied the joint optimization problem of user association, power control and BH link flow assignment in a mmWave BH HetNet with multiple BH link connections. The objective of this optimization problem was to maximize the network

total DL energy efficiency. The original formulated joint optimization problem was shown to be NP-hard. To reduce the complexity of the joint user association, power control and BH flow assignment problem, we separated it into two problems, namely; (i) user association and power control optimization in the AN as well as (ii) BH link flow assignment and power control optimization problem. These two problems were solved separately. Problem (i) is first solved, and its solution is used in problem (ii). While the BH link flow assignment and power control optimization problem was a convex optimization problem, the user association and power control optimization in the AN was shown to be an integer programming problem, which is still NP-hard. We therefore developed a specialized solution method based on Lagrange duality and column generation, and demonstrated the effectiveness of this approach by some simulations. This is considered as the main contribution in this chapter. From our simulations, we can draw the conclusion that user association in the AN significantly determines the power consumption in the AN and BH network. Hence it is important to determine the user association scheme that maximizes network EE. Our proposed user association scheme, that takes into account AN and BH power constraints, BH links capacity and UE QoS constraints, and also performs power control and BH link flow assignment, achieves the best EE gains as compared to some existing user association schemes.

Bibliography

[1] A. Damnjanovic, J. Montojo, Y. Wei, T. Ji, T. Luo, M. Vajapeyam, T. Yoo, O. Song, and D. Malladi, "A survey on 3gpp heterogeneous networks," *IEEE Wireless Commun.*, vol. 18, no. 3, pp. 10–21, Jun. 2011.

[2] D. Lopez-Perez, X. Chu, and [U+FFFD] Guvenc, "On the expanded region of

picocells in heterogeneous networks," *IEEE J. Sel. Topics Signal Process.*, vol. 6, no. 3, pp. 281–294, Jun. 2012.

[3] D. Liu, L. Wang, Y. Chen, M. Elkashlan, K. K. Wong, R. Schober, and L. Hanzo, "User association in 5g networks: A survey and an outlook," *IEEE Commun. Surveys Tuts.*, vol. 18, no. 2, pp. 1018–1044, 2nd Quart. 2016.

[4] T. V. Chien, E. Björnson, and E. G. Larsson, "Joint power allocation and user association optimization for massive mimo systems," *IEEE Trans. Wireless Commun.*, vol. 15, no. 9, pp. 6384–6399, Sep. 2016.

[5] D. Fooladivanda and C. Rosenberg, "Joint resource allocation and user association for heterogeneous wireless cellular networks," *IEEE Trans. Wireless Commun.*, vol. 12, no. 1, pp. 248–257, Jan. 2013.

[6] A. Asheralieva and Y. Miyanaga, "Optimal contract design for joint user association and intercell interference mitigation in heterogeneous lte-a networks with asymmetric information," *IEEE Trans. Veh. Technol.*, vol. 66, no. 6, pp. 5284–5300, Jun. 2017.

[7] Q. Han, B. Yang, G. Miao, C. Chen, X. Wang, and X. Guan, "Backhaul-aware user association and resource allocation for energy-constrained hetnets," *IEEE Trans. Veh. Technol.*, vol. 66, no. 1, pp. 580–593, Jan. 2017.

[8] H. Zhang, S. Huang, C. Jiang, K. Long, V. C. M. Leung, and H. V. Poor, "Energy efficient user association and power allocation in millimeter-wave-based ultra dense networks with energy harvesting base stations," *IEEE J. Sel. Areas Commun.*, vol. 35, no. 9, pp. 1936–1947, Sep. 2017.

[9] A. Mesodiakaki, F. Adelantado, L. Alonso, M. D. Renzo, and C. Verikoukis, "Energy- and spectrum-efficient user association in millimeter-wave backhaul

small-cell networks," *IEEE Trans. Veh. Technol.*, vol. 66, no. 2, pp. 1810–1821, Feb. 2017.

[10] M. Marcus and B. Pattan, "Millimeter wave propagation; spectrum management implications," *IEEE Microw. Mag.*, vol. 6, no. 2, pp. 54–62, Jun. 2005.

[11] E. Zola, A. J. Kassler, and W. Kim, "Joint user association and energy aware routing for green small cell mmwave backhaul networks," in *2017 IEEE Wireless Communications and Networking Conference (WCNC)*, Mar. 2017, pp. 1–6.

[12] G. Auer, V. Giannini, C. Desset, I. Godor, P. Skillermark, M. Olsson, M. A. Imran, D. Sabella, M. J. Gonzalez, O. Blume, and A. Fehske, "How much energy is needed to run a wireless network?" *IEEE Wireless Communications*, vol. 18, no. 5, pp. 40–49, Oct. 2011.

[13] F. 15-1166, "Federal communications commission," Oct. 2015.

[14] P. Bjorklund, P. Varbrand, and D. Yuan, "Resource optimization of spatial tdma in ad hoc radio networks: a column generation approach," in *IEEE INFOCOM 2003. Twenty-second Annual Joint Conference of the IEEE Computer and Communications Societies (IEEE Cat. No.03CH37428)*, vol. 2, Mar. 2003, pp. 818–824 vol.2.

[15] D. Bertsimas and J. N. Tsitsiklis, *Introduction to Linear Optimization*. vol.6. Belmont, MA, USA: Athena Scientific, 1997.

[16] S. Boyd and L. Vandenberghe, *Convex optimization*. Cambridge, U.K.: Cambridge Univ. Press, Mar. 2004.

[17] Y. Nesterov and A. Nemirovskii, "Interior-point polynomial algorithms in convex programming," in *SIAM Studies in Applied Mathematics*, SIAM 1994.

[18] K.-C. Huang and Z. Wang, *Millimeter Wave Communication Systems*. Wiley, Mar. 2011.

[19] "Small cell enhancements for e-utra and e-utran-physical layer aspects, 3gpp tr 36.872, v. 1.0.0, rel. 12," Aug. 2013.

[20] H. S. Dhillon, R. K. Ganti, F. Baccelli, and J. G. Andrews, "Modeling and analysis of k-tier downlink heterogeneous cellular networks," *IEEE J. Sel. Areas Commun.*, vol. 30, no. 3, pp. 550–560, Apr. 2012.

Chapter 5

Conclusions and Future Work

This chapter completes the dissertation by summarizing the contributions. Potential research lines for future consideration are also provided. In particular, Section 5.1 presents concluding remarks from each chapter while Section 5.2 lists the open research extensions relating to our contributions.

5.1 Conclusion

In order for network operators to cope with the ever-increasing data rate demands of UEs, drastic expansion of network infrastructures as well as rapid rise of energy demands are expected. As a result, it becomes imperative for operators to achieve a sustainable capacity growth with a limited electricity bill. Also, resulting from the network infrastructure expansion, the efficient assignment of flows on BH links taking into account BH capacity and energy constraints is another urgent problem for operators. The aforementioned goals translates into the joint maximization of energy efficiency, user association and BH flow assignment optimization. This is a major fundamental design objective for future cellular networks and was the main aim of this dissertation.

Chapter 1 presented the motivation, objectives and the outline of this dissertation.

In Chapter 2, we introduced the concepts of homogeneous and heterogeneous networks and demonstrated the potential significant improvement in network capacity and reduction in energy consumption that can be achieved from heterogeneous networks. We showed how suitable mmWave frequency bands can be used for backhauling in HetNets so as to avoid the incident of BH capacity bottleneck.

In Chapter 3, two energy efficiency maximization optimization frameworks were proposed. Firstly, for a given strict UE throughput demands, a joint energy efficient, power and flow control (JEEPF) scheme was proposed. It was shown that JEEPF is a convex optimization problem and therefore the optimal power and BH flow control can be efficietly obtained using convex optimization. Secondly, a novel joint energy efficient, power allocation, flow control and throughput (JEEPFT) optimzation algorithm, which: i) maximizes the throughput demands of UE (i.e. network capacity maximization), ii) minimizes energy consumption in the AN and BH, iii) optimizes flow assignment on the BH links and iv) maximizes the overall network energy efficiency was proposed. This optimization problem had a non-linear fractional objective function, and hence falls into non-convex optimization problem. The non-convex optimization problem was reformulated into a quasiconvex problem, and was solved to optimality using the bisection method. The proposed two optimization frameworks were compared with two other benchmark schemes, and JEEPF and JEEPFT performed better than the benchmark schemes. But JEEPFT outperforms JEEPF. This provide an insight that maximizing energy efficiency achieves better results than minimizing energy consumption for given UE traffic requirements.

In Chapter 4, we propose an energy efficient user association, power, and flow control optimization algorithm. The algorithm aims at associating UEs to BSs such that: i) the overall energy consumption in the network (BH and AN) is minimized, and

ii) BH links capacity constraints are not violated. It was shown that the formulated optimization problem was non-convex and in mixed-integer form. To get a tractable solution, column generation and convex optimization was used to obtain the optimum user association, power allocation and BH flow assignment. Compared to referenced existing user association schemes, the proposed algorithm shows promising energy efficiency enhancement.

5.2 Future Work

A number of open research issues have resulted from this dissertation. They are summarized as follows:

- The use of mmWave frequencies for the BH network was shown to enhance the capacity of BH links due to the large bandwidth available. It would be interesting to investigate the use of mmWave frequencies in the AN. Bearing in mind that mmWave communication only works for very short distances, new challenges like frequent handovers and realistic channel models must be given a detailed look.

- The development of a low complexity distributed algorithm for the implementation of the JEEPFT model using the generalized benders decomposition is currently underway as an extension to Chapter 3.

- The user association problem can be extended to the variable-rate joint energy efficiency, power, and flow control optimization. In this joint optimization problem, UEs will be associated to BSs that i) maximizes their achievable throughput, ii) minimizes the AN and BH energy consumption and iii) optimizes the flow of their BH traffic in the BH network.

- Massive MIMO, another key enabling technology for 5G, can be considered in our system model.

Bibliography